Cannabinoid CB1 Receptor: Role in Primate Prefrontal Circuitry and Schizophrenia

by

Stephen Melford Eggan

Bachelor of Science, Neuroscience and Psychology, University of Pittsburgh, 2001

Submitted to the Graduate Faculty of

Arts and Sciences in partial fulfillment

of the requirements for the degree of

Doctor of Philosophy

University of Pittsburgh

2007

UNIVERSITY OF PITTSBURGH

School of Arts and Sciences

This dissertation was presented

by

Stephen Melford Eggan

It was defended on

July 19, 2007

and approved by

Bradley Alger, Ph.D., Department of Physiology and Psychiatry, University of Maryland

Etienne Sibille, Ph.D., Department of Psychiatry

Charlie Bradberry, Ph.D., Department of Psychiatry

J. Patrick Card, Ph.D., Department of Neuroscience

Susan Sesack, Ph.D., Department of Neuroscience

Dissertation Advisor: Dr. David A. Lewis, M.D., Department of Psychiatry

Cannabinoid CB1 Receptor: Role in Primate Prefrontal Circuitry and Schizophrenia

Stephen Melford Eggan, Ph.D.

University of Pittsburgh, 2007

Schizophrenia is a complex and devastating psychiatric disorder that creates a substantial emotional and economic burden on individuals with the illness, their families, and society. Understanding the causes and identifying the molecular alterations in the brain that underlie the pathophysiology of core clinical features of schizophrenia are central to the development of new therapeutic interventions. In particular, schizophrenia is characterized by impairments in working memory, which are thought to result from a deficit in GABA neurotransmission in the dorsolateral prefrontal cortex (DLPFC). Interestingly, exposure to cannabis has been associated with an increased risk for developing schizophrenia and cannabis use is associated with DLPFC-related working memory impairments similar to those observed in schizophrenia. The effects of cannabis are mediated by the brain cannabinoid 1 (CB1) receptor, which in the rodent, is heavily localized to certain inhibitory axon terminals and, when activated, inhibits GABA release. Here, we have investigated the anatomical distribution of the CB1 receptor in the primate brain and characterized the cellular localization and synaptic targets of the CB1 receptor in the primate DLPFC. In addition, we explored the potential relationship between CB1 receptor signaling and altered GABA neurotransmission in schizophrenia by evaluating CB1 receptor mRNA and protein expression in the DLPFC of subjects with schizophrenia. We found that CB1 receptors are highly expressed in the primate DLPFC and that CB1 receptors are localized in the terminals of the subtype of perisomatic-targeting GABA interneurons that contain the neuropeptide cholecystokinin (CCK). We found that CB1 mRNA and protein are reduced in schizophrenia, which may represent a compensatory mechanism to increase GABA transmission from perisomatic-targeting CCK neurons with impaired GABA synthesis. We conclude that reductions in the expression of the CB1 receptor mRNA and protein in CCK neurons represent a novel neuropathological entity in the DLPFC of individuals with schizophrenia. These findings suggest a novel drug target for the treatment of cognitive dysfunction in schizophrenia.

TABLE OF CONTENTS

LIST OF TABLES

LIST OF FIGURES

PREFACE

I feel very fortunate to have chosen the University of Pittsburgh for my undergraduate education and especially for my graduate training. The Center for Neuroscience at the University of Pittsburgh graduate program has provided me with an extremely rich training environment through its commitment to being multidisciplinary across different fields of neuroscience and to being collaborative between departments within the university and with Carnegie Mellon University through participation in the Center for the Neural Basis of Cognition.

Through the years that I have been at the University of Pittsburgh, both my scientific and personal life has been enriched by knowing and working with many outstand scientists, mentors, students, and staff who have all helped me reach the completion of graduate career.

I must start by thanking my extremely supportive and helpful committee who has guided me throughout my dissertation work. I would especially like to thank to Susan Sesack who has given up her valuable time to chair all of my committees since I began my graduate training. I have had the pleasure of being a student of Susan's as an undergraduate and working with Susan as her teaching assistant during my graduate training. Susan has been a second mentor to me and has helped me in innumerable ways through the years. Pat Card has also guided me since I was an undergraduate and has provided me with excellent advice. I am particularly indebted to Pat because he is the person who steered me to work with my mentor David Lewis. Etienne Sibille and Charlie Bradberry have both provided me with insightful and useful comments and have been wonderful committee members. Finally, I would like to extend my gratitude to Bradley Alger who took the time to participate in this dissertation as my outside examiner.

I am truly indebted to my mentor David Lewis who took me into his lab when I was an undergraduate and knew almost nothing about neuroscience. Dave's teachings and mentorship have helped mold me into the scientist and, to some extent, the person that I am today. Dave has been an incredible supporter over the years and I value his advice and friendship. Dave truly

deserves my most sincere gratitude and appreciation and I hold him in the highest regard and utmost respect. I look forward to many rich collaborative interactions with him both as his postdoctoral trainee and beyond.

I would like to thank the entire CNUP community and the wonderful Lewis lab members for their time, advice, and friendship. I am particularly appreciative to Darlene Melchitzky, Takanori Hashimoto, Ken Fish, and Mary Brady who have played a significant role in my scientific training and in helping to advance my dissertation to its completion.

My close friends Deanne Buffalari, Annie Cohen, Vince McGinty, Harvey Morris, Cathy Dunn, and Jaime Maldonado have shared the experience of going through graduate training and have commiserated with me in my failures and celebrated with me in my successes. I thank them for wonderful memories and lasting friendships. I have also been blessed to have a family whose support, love, and encouragement have been unremitting over the years. I thank them dearly, in particular my parents Gary Eggan and Talletha and Curt Hampton, my brother Jeremy Eggan, and my sister Amelia Eggan. I am especially grateful to my incredible wife Brittanie who has been my biggest supporter in this journey over the last couple of years. Her commitment to helping me succeed has been astonishing and inspiring. I hope that I can provide her with the same support and encouragement as she finishes her training.

Finally, I would like acknowledge the many family members who generously gave consent for brain tissue donation from their deceased loved ones and who patiently participated in our diagnostic interviews.

1.0   GENERAL INTRODUCTION

1.1   OVERVIEW OF SCHIZOPHRENIA

1.1.1   The burden of schizophrenia

Schizophrenia is a complex and devastating psychiatric disorder that affects ~1% of the population worldwide across countries and diverse cultures and is unbiased with respect to ethnic groups or genders (Bromet and Fennig, 1999; Lewis and Lieberman, 2000). The formal clinical onset of schizophrenia (marked by the development of psychotic episodes) typically occurs in late adolescence and early adulthood (Lewis and Lieberman, 2000); in males, the onset of clinical symptoms most frequently begins between 15 and 25 years of age, whereas in females symptoms typically appear between 20 and 30 years of age (Lewis, 2000). Although mild premorbid abnormalities including disturbances in motor, social, or cognitive functions may be apparent early in life that may foretell the development of schizophrenia, these disturbances do not place individuals outside the normal range of functioning and frequently go unnoticed (Yung and McGorry, 1996; McGlashan, 1996; Erlenmeyer-Kimling et al., 2000; Lewis and Lieberman, 2000). The time course of schizophrenia following clinical onset typically involves episodes of remission and relapse of psychotic symptoms and a general deterioration of function during the first 5-10 years of the illness. Later in life clinical deterioration often plateaus and the intensity of positive symptoms diminishes in some individuals; however, profound and persistent functional impairments typically remain (Lewis and Lieberman, 2000).

Based on these characteristics, schizophrenia is characterized by a lifetime of disability and unremitting impairments in social and occupational functioning. Many individuals with schizophrenia will also develop comorbid mood disorders such as depression and anxiety and 5-10% of individuals with schizophrenia will eventually commit suicide (Lewis and Lieberman,

2000). As a result, schizophrenia creates a substantial emotional and financial burden on the families of those affected (Brown et al., 1999). In addition, due to the cost of medical treatment and lost productivity, schizophrenia generates an enormous economic liability for society and is one of the most expensive disorders in medicine. Indeed, in the United States alone the direct and indirect costs of schizophrenia were estimated at $33 billion in 1990 (Rupp and Keith, 1993; Carpenter, Jr. and Buchanan, 1994; Andreasen, 1995).

1.1.2 Etiology of schizophrenia

The etiological factors, or causes, of schizophrenia remain largely unknown, but appear to be multifaceted. Family, twin, and adoption studies demonstrate that the risk of developing schizophrenia is directly associated with the degree of genetic relatedness to an affected individual (Lewis and Lieberman, 2000). For instance, the concordance of schizophrenia among first-degree relatives (parents and siblings) of individuals with schizophrenia ranges from 6-17%, whereas the concordance among monozygotic twins (who share the same genetic makeup) approaches 50% (Kendler, 1983; Tsuang, 2000). In addition, a number of putative susceptibility genes on several different chromosomes have recently been identified (Pulver, 2000; Owen et al., 2004). However, each of these genes alone confers only a small degree of risk for schizophrenia. Therefore, it is likely that multiple interacting genes are necessary to impart significant vulnerability to the illness (Mirnics and Lewis, 2001; Harrison and Weinberger, 2005).

Although heritable influences represent a major etiological component of schizophrenia, the 50% concordance rate of schizophrenia among monozygotic twins indicates that genetic liability alone is not sufficient for the appearance of clinical features and suggests that other non-genetic risk factors play a role in the etiology of schizophrenia. In line with this interpretation, a number of environmental insults across development have been implicated as factors that increase the risk of developing schizophrenia later in life (Lewis and Lieberman, 2000). These environmental factors range from gestational and birth complications to stressful childhood events and frequent cannabis use during adolescence (McDonald and Murray, 2000; Lewis and Lieberman, 2000).

Consequently, the etiology of schizophrenia appears to involve multiple "hits" consisting of genetic susceptibility and environmental risk factors (Bayer et al., 1999; Maynard et al.,

2

2001). The interaction of these genetic and environmental factors during adolescence is believed to alter normal neurodevelopmental processes that occur before the onset of clinical features of the illness. The functional consequences of these disturbances manifest as the clinical syndrome in late adolescence or early adulthood as the affected neural networks become fully mature (Lewis and Lieberman, 2000; Lewis et al., 2004a).

1.1.3 Clinical features of schizophrenia

Schizophrenia is defined as a clinical syndrome comprised of a constellation of clinical symptoms classically divided into 1) positive symptoms, which reflect the *presence* of distinctively abnormal behaviors and 2) negative symptoms, which reflect the *absence* of certain normal social and interpersonal behaviors (Andreasen, 1995; Elvevag and Goldberg, 2000). Positive symptoms (or psychoses) include disturbances in perception, such as hallucinations that can arise in most sensory modalities, but are classically auditory in nature; disturbances in inferential thought, such as delusions that typically manifest as false beliefs of control or danger; and formal thought disorder, which includes the expression of disorganized speech and behavior. Negative symptoms typically include reduced expression of emotions (flat affect), impaired goal-directed behaviors (avolition), and loss of pleasure in activities (anhedonia), as well as social withdrawal and poverty of speech (Andreasen, 1995). In addition to these cardinal signs, schizophrenia is also characterized by a variety of cognitive deficits, which include *impairments* in executive functions, attention, and especially working memory (**see chapter 1.1.4**; Elvevag and Goldberg, 2000).

Each of these symptoms is present in some subjects with schizophrenia; however, none are present in all subjects with the illness. Consequently, schizophrenia cannot be diagnosed by a unitary feature such as the appearance of psychosis, even though these symptoms typically bring individuals to clinical attention. The current DSM-IV (*Diagnosis and Statistical Manual of Mental Disorders*, 1994) diagnosis criteria for schizophrenia requires a deterioration in social and occupational functioning that results from a combination of the characteristic symptoms.

1.1.4 Cognitive impairments: A core feature of schizophrenia

Often, the most remarkable clinical manifestation of schizophrenia is psychosis. However, substantial evidence suggests that disturbances in certain cognitive functions, such as working memory, represent a core feature of the illness (Elvevag and Goldberg, 2000). First, cognitive impairments are perhaps the most prevalent clinical feature among individuals affected with schizophrenia (Keefe et al., 2005). Second, cognitive abnormalities persist throughout the lifetime of individuals with schizophrenia without diminution and have been observed at the onset of the illness, prior to illness onset during adolescence, and as early as childhood (Breier et al., 1991; Heaton et al., 1994; Saykin et al., 1994; Davidson et al., 1999). Third, mild cognitive disturbances are seen in unmedicated, non-affected relatives of individuals with schizophrenia, indicating that cognitive impairments are not due to neuroleptic treatment, are intrinsic to the disease process, and reflect genetic liability (Egan et al., 2001; Sitskoorn et al., 2004). Finally, cognitive dysfunctions have greater detrimental effects on social and occupational abilities than positive symptoms and the degree and severity of cognitive dysfunction is perhaps the best predictor of poor long-term functional outcomes for individuals with schizophrenia (Breier et al., 1991; Green, 1996).

These data converge on the interpretation that disturbances in cognitive functions are the most persistent and debilitating symptoms of schizophrenia. Consequently, these impairments represent a major factor contributing to the burden of schizophrenia by impeding the reintegration of individuals with the illness into society as productive members. Unfortunately, current pharmacological treatments for schizophrenia, while effective at suppressing psychotic symptoms, are for the most part, ineffective at improving cognitive functioning (Lewis and Gonzalez-Burgos, 2006). Therefore, the development of pharmacological agents that successfully improve cognitive functioning is paramount to more effectively treating the illness and has become a major focus of schizophrenia research (Hyman and Fenton, 2003).

1.2 WORKING MEMORY AND GABA: IDENTIFYING A TARGET FOR THERAPUETIC INTERVETION

The development of cognitive enhancing drugs requires the identification of the neuropathological entity (or entities) underlying the pathophysiological processes that give rise to the cognitive impairments associated with schizophrenia (Lewis and Gonzalez-Burgos, 2006). Of the variety of cognitive impairments described in schizophrenia, working memory has been the focus of substantial research because it is one of the most consistently disturbed cognitive functions in individuals with the illness (Weinberger et al., 1986; Callicott et al., 2003).

1.2.1 Working memory, the dorsolateral prefrontal cortex, and schizophrenia

Working memory is defined as the ability to hold onto small bits of information over a period of time in order to guide future behavior. In other words, working memory is the active *maintenance* of internal contextual information that can be modified on-line, allowing it to bias behavior based on goals or instructions. Although working memory is a distributed process that involves multiple brain regions (Goldman-Rakic, 1988), the dorsolateral prefrontal cortex (DLPFC) has been identified as a critical node in working memory by both functional imaging studies in humans and electrophysiological studies in awake behaving monkeys (Funahashi et al., 1989; Funahashi et al., 1993; Weinberger et al., 2001; Miller and Cohen, 2001).

Individuals with schizophrenia, when performing tasks that rely on working memory such as the Wisconsin Card Sort Task and N-back task, perform more poorly and exhibit reduced DLPFC activation (as evident from altered blood flow or glucose utilization) compared to normal controls (Weinberger et al., 1986; Perlstein et al., 2001). These findings have led to the classic hypofrontality hypothesis of schizophrenia (Weinberger et al., 2001). However, recent imaging studies have shown that activity in the DLPFC can be increased under circumstances in which individuals with schizophrenia are either slightly impaired or perform normally on working memory tasks, indicating that the DLPFC in these individuals operates less efficiently (Callicott et al., 2000; Callicott et al., 2003). Together, these data suggest that, whether subjects with schizophrenia show hypofrontality or hyperfrontality, the DLPFC of individuals with schizophrenia functions abnormally during working memory tasks.

1.2.2 Role of DLPFC interneurons in working memory

In primates, working memory function depends critically on the synaptic connectivity and patterns of activity within the DLPFC (reviewed in Goldman-Rakic, 1995; Fuster, 2001). Working memory is thought to be mediated by a reverberating cortical circuit that coordinates the sustained activity of populations of excitatory pyramidal neurons in the DLPFC (Goldman-Rakic, 1995). Reciprocal connections between spatially-segregated populations of DLPFC pyramidal cells may be a substrate for recruiting and maintaining activity of functionally-related populations of prefrontal neurons during working memory tasks (Lewis and Anderson, 1995). Indeed, ultrastructural analyses have revealed that approximately 95% of the excitatory synapses furnished by the long-range, horizontal axon projections of DLPFC pyramidal neurons target dendritic spines of other pyramidal cells (Melchitzky et al., 1998). Furthermore, the functionality of these connections has been confirmed in electrophysiological studies in living slice preparations of monkey DLPFC (Melchitzky et al., 1998).

Although an excitatory reverberating circuit may be necessary to maintain delay activity, inhibitory activity in the DLPFC furnished by GABA neurons plays two critical roles in normal working memory. First, GABA neurons shape and fine tune the firing of pyramidal cells during working memory tasks. Adjacent interneurons and pyramidal cells in the DLPFC fire selectively and robustly during delay periods and demonstrate isodirectional tuning during working memory tasks (Funahashi et al., 1993; Rao et al., 1999) and this inhibitory activity is necessary for the spatial tuning of neuronal responses (Sawaguchi et al., 1988; Sawaguchi et al., 1989). Indeed, iontophoresis of bicuculline, a $GABA_A$ receptor antagonist, into the DLPFC significantly increases neuronal activity at all periods during a working memory task and destroys spatial tuning (Rao et al., 2000). These findings suggest that inhibition serves to determine which DLPFC pyramidal neurons are activated (serves a spatial role) and when they are active (serves a temporal role) during the different phases of working memory tasks (Constantinidis et al., 2002).

Second, networks of chemically and electrically-coupled GABA interneurons are essential for the synchronization of large cell ensembles of neurons (Connors and Long, 2004) and for the pacing of oscillatory patterns required for working memory (Howard et al., 2003). In the human DLPFC, gamma oscillations (30-80 HZ) appear at the onset of, and are maintained during, the delay period of working memory tasks (Tallon-Baudry et al., 1998) and the power of

6

gamma band oscillations increases specifically with, and in proportion to, working memory load (Howard et al., 2003). In individuals with schizophrenia, deficits in cognitive control and working memory are associated with an impairment in phase-locking gamma band activity to stimulus onset and reduced frontal lobe gamma band power (Spencer et al., 2003; Cho et al., 2006).

1.2.3 Altered GABA neurotransmission in the DLPFC: A neuropathological entity underlying working memory impairments

The above data suggest that disturbances in inhibitory neurotransmission could play a prominent role in DLPFC dysfunction in subjects with schizophrenia and could represent a pathological entity underlying working memory disturbances in affected individuals (Lewis et al., 2005). Consistent with this idea, in the DLPFC of subjects with schizophrenia, one of the most replicated findings in postmortem studies is a reduction in the expression of glutamic acid dexcarboxylase (GAD_{67}) mRNA, an enzyme responsible for synthesizing GABA (Akbarian et al., 1995; Guidotti et al., 2000; Volk et al., 2000; Hashimoto et al., 2007; Straub et al., 2007). Analysis of GAD_{67} mRNA expression at the cellular level revealed that the density of GABA neurons with detectable levels of GAD_{67} mRNA is reduced by ~25-35% across layers 2-5 in subjects with schizophrenia (Akbarian et al., 1995; Volk et al., 2000). However, in the remaining GABA neurons with detectable GAD_{67} mRNA, the expression levels per neuron were unchanged in subjects with schizophrenia (Volk et al., 2000). Similarly, the density of neurons expressing detectable levels of mRNA encoding for the GABA membrane transporter (GAT1), a protein responsible for the reuptake of released GABA, is decreased by 21-33% in layers 1-5 and the expression levels of GAT1 mRNA per neuron does not differ in the same subjects with schizophrenia (Volk et al., 2001). These data suggest that both GABA synthesis and re-uptake are reduced in a subset of DLPFC inhibitory interneurons in schizophrenia.

In the cortex, GABA neurons are a heterogeneous group of cells comprised of distinct subclasses that can be distinguished by their morphology, physiological characteristics and the presence of calcium-binding proteins or neuropeptides (Kawaguchi and Kubota, 1997; McBain and Fisahn, 2001; Markram et al., 2004). The subtype(s) of GABA neurons that account for the reduction in GAD_{67} mRNA observed in subjects with schizophrenia is important to know

because the terminals of different classes of interneurons preferentially target different domains of pyramidal cells and play distinct inhibitory roles in controlling pyramidal cell activity (DeFelipe et al., 1989; Thomson et al., 1995; Thomson et al., 1996; Tamas et al., 1997; Xiang et al., 2002).

Convergent evidence suggests that an affected subclass of GABA neurons in the DLPFC of subjects with schizophrenia include parvalbumin (PV)-containing chandelier neurons that provide synapses exclusively onto the axon initial segment (AIS) of pyramidal neurons in distinct vertical arrays termed cartridges (Lewis and Lund, 1990) **(Fig. 1)**. For instance, although the density of neurons with detectable levels of PV mRNA is not altered in subjects with schizophrenia, the level of PV mRNA expression per neuron is significantly reduced in layers 3 and 4, but not in layer 2, 5, or 6 (Hashimoto et al., 2003). The changes in PV mRNA expression correlated with the decrease in the density of neurons containing detectable levels of GAD_{67} mRNA in the same subjects with schizophrenia. These data suggest that GABA synthesis is decreased in PV-expressing neurons that also exhibit reduced PV mRNA expression (Hashimoto et al., 2003). Indeed, in the same subjects with schizophrenia the simultaneous detection of PV and GAD_{67} revealed that ~50% of PV mRNA expressing neurons lacked detectable levels of GAD_{67} mRNA (Hashimoto et al., 2003). In addition, the density of GAT1-immunoreactive (IR) cartridges were significantly reduced by ~50% in layers 3 and 4, whereas the density of GAT1 puncta, representing axon terminals from other GABA neurons, is unaltered (Woo et al., 1998; Pierri et al., 1999). Finally, postsynaptic to GAT1 cartridges, the majority of $GABA_A$ receptors at the AIS contain the α_2 subunit (Nusser et al., 1996; Loup et al., 1998) and the density of AIS immunoreactive for the α_2 subunit is increased more than 100% in subjects with schizophrenia compared to control subjects (Volk et al., 2002) **(Fig. 1)**.

Together, these data suggest that decreased GAD_{67} mRNA expression in chandelier neurons results in deficient inhibitory input to pyramidal neuron AIS. As a result the downregulation of PV and GAT1 mRNAs are interpreted to be compensatory changes in order to augment GABA release at the AIS. Specifically, parvalbumin is reduced in order to increase Ca^{2+} transients and promote GABA release and GAT-1 is decreased in order to prolong inhibitory postsynaptic currents once GABA is released. In addition, postsynaptic $GABA_A$ α_2 subunit at the AIS are upregulated to increase the efficacy of released GABA (Lewis et al.,

2005). However, these compensatory mechanisms are inadequate to boost the amount, and effects, of GABA at this critical synaptic site (Lewis et al., 2005).

These data converge on the idea that a deficit in chandelier cell-mediated inhibition is a neuropathological entity in the DLPFC of subjects with schizophrenia that could be an underlying mechanism that produces altered gamma band power and consequently, impaired working memory in individuals with schizophrenia (Lewis et al., 2005). Therefore, the development of drugs that enhance GABA neurotransmission at the AIS could be effective at treating the cognitive impairments in the illness (Lewis et al., 2005).

These deficits in GABA neurotransmission seem to be relatively specific to parvalbumin neurons because most GABA neurons in the DLPFC express normal levels of GAD_{67} and GAT1 mRNAs (Volk et al., 2000; Volk et al., 2001). For example, gene expression is not altered in the subclass of GABA neurons that target the dendrites of pyramidal cells and contain the calcium binding protein calretinin (Hashimoto et al., 2003; Melchitzky et al., 2005) **(Fig. 1)**. However, reduced expression of GAD_{67} is observed across layer 2-5 in the DLPFC of subjects with schizophrenia and the chandelier subclass accounts only for layer 3 and 4. This suggests that other subclasses of GABA neurons in the superficial layers must be affected and could represent another neuropathological entity in subjects with schizophrenia.
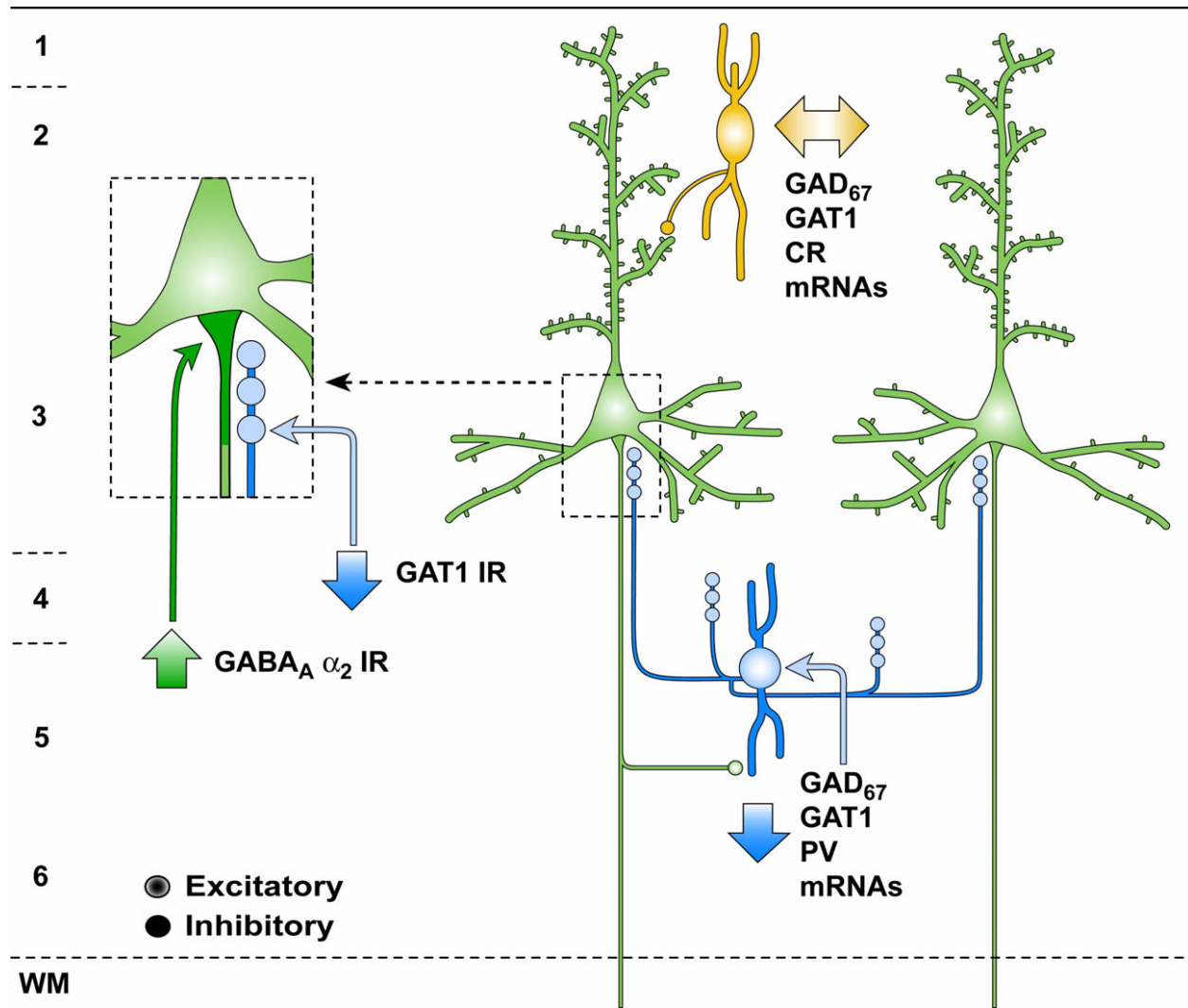
Figure 1. Schematic summary of alterations in GABA circuitry in the dorsolateral prefrontal cortex of individuals with schizophrenia. Reduced levels of gene expression in chandelier neurons (blue) are associated with a decrease in immunoreactivity (IR) for GABA (γ-aminobutyric acid) transporter 1 (GAT1) in the axon cartridges of these neurons and an upregulation of GABAA receptor α2 subunit immunoreactivity in the postsynaptic axon initial segment of pyramidal neurons (green). Gene expression in the calretinin (CR)-expressing subpopulation of GABA neurons (yellow) does not seem to be altered. GAD67, 67 kD isoform of glutamic acid decarboxylase; PV, parvalbumin; 1-6, layers of dorsolateral prefrontal cortex. (from Lewis DA, Hashimoto T, Volk DW: Cortical inhibitory neurons and schizophrenia. Nature Reviews Neuroscience 6:312-324, 2005.)

1.3 CANNABIS USE: COGNITIVE DYSFUNCTION AND ENVIRONMENTAL RISK FACTOR FOR SCHIZOPHRENIA

As mentioned above **(chapter 1.1.2)**, the development of schizophrenia appears to involve an interaction between a genetic predisposition for the illness and exposure to environmental risk factors that trigger alterations in vulnerable circuits and precipitate the clinical onset of the disorder (Bayer et al., 1999; Lewis and Lieberman, 2000; Maynard et al., 2001). Convergent lines of evidence suggest that exposure to cannabis during adolescence is such an environment risk factor. The following sections outline the clinical evidence suggesting a link between cannabis use and the later risk of developing schizophrenia. In **chapter 1.4**, anatomical and physiological data will be reviewed showing that the endocannabinoid system plays a role in modulating GABA neurotransmission in the DLPFC and therefore, alterations in the endocannabinoid system of individuals with schizophrenia could also represent neuropathological entities in the disorder.

1.3.1 Cannabis use is associated with cognitive dysfunction

Chronic cannabis users demonstrate marked impairments in cognitive function, including working memory, that are analogous to those observed in individuals with schizophrenia (Pope, Jr. and Yurgelun-Todd, 1996; Solowij et al., 2002). These impairments are associated with prolonged cannabis use, continue beyond the period of acute intoxication, and worsen with increasing years of use (Pope, Jr. and Yurgelun-Todd, 1996; Solowij et al., 2002). In the absence of intoxication, brain imaging studies have shown that long-term cannabis users exhibit altered patterns of DLPFC activity during both rest (Lundqvist et al., 2001) and working memory tasks compared to control subjects (Block et al., 2002; Kanayama et al., 2004), suggesting that the DLPFC operates less efficiently in these individuals.

In healthy human subjects, acute exposure to cannabis produces impairments in working memory similar to those seen in subjects with schizophrenia (Lichtman et al., 2002; Ilan et al., 2004; D'Souza et al., 2004). For example, exposure to delta-9-tetrahydrocannabinol (Δ^9-THC), the chief psychoactive cannabinoid in cannabis, reduces the number of correct responses (D'Souza et al., 2004) and impairs performance in a dose- and delay-dependent manner (Lane et al., 2005) in healthy subjects performing delayed match to sample tasks. In addition, healthy subjects perform more poorly with increasing working memory load in N-back tasks during acute cannabis intoxication (Ilan et al., 2004).

In addition to these cognitive deficits, acute cannabis intoxication has also been shown to produce temporary drug-induced 'cannabis psychosis' in some cannabis users without a history of schizophrenia (Arseneault et al., 2004). These psychoses appear following large doses of cannabis and often resemble schizophrenia-like symptoms including hallucinations, altered judgment, depersonalization, and paranoid psychosis (Kupfer et al., 1973; Chopra and Smith, 1974; Leweke et al., 2004).

1.3.2   Cannabis use is a risk factor for schizophrenia

Convergent findings demonstrate a significant association between cannabis use and an increased risk of schizophrenia. For example, cannabis use by those afflicted with schizophrenia is associated with a poorer outcome, increased severity of symptoms, especially cognitive impairments, and more frequent hospitalization, suggesting that these individuals have increased sensitivity to the effects of cannabis (Negrete et al., 1986; Grech et al., 2005; Pencer et al., 2005; D'Souza et al., 2005). Furthermore, epidemiological studies have consistently reported dose-response relationships between prior cannabis use and the later development of the illness (reviewed in Henquet et al., 2005b; Fergusson et al., 2006). In a follow-up study of Swedish conscripts, individuals with the greatest self-reported history of cannabis use by age 18 had a 6-fold increased risk of developing schizophrenia diagnosed 15 years later, even after controlling for a number of other risk factors for schizophrenia (Andreasson et al., 1987). Studies in several other cohorts have demonstrated similar relationships between the degree of cannabis use and the predicted risk of developing schizophrenia (van Os et al., 2002; Zammit et al., 2002). Importantly, several studies have demonstrated that the association between reported cannabis

use and schizophrenia cannot be explained by reverse causality (van Os et al., 2002; Arseneault et al., 2002; Stefanis et al., 2004). For example, in a Dutch cohort, all individuals who had ever reported any prodromal psychotic symptoms were excluded and an association between cannabis use and schizophrenia in the psychosis-free group at follow-up was still evident (van Os et al., 2002). This temporal effect between the use of cannabis and the subsequent development of psychosis discounts the argument that the illness causes cannabis use as an attempt at self-medicating in order to cope with their distress (Henquet et al., 2005b).

Together, the above findings converge on the idea that cannabis use confers an increased risk of later schizophrenia. Indeed, a recent meta-analysis of prospective studies found that cannabis exposure nearly doubles the risk (pooled ODDS ratio of 2.1) of later developing the illness (Henquet et al., 2005a), a risk that matches that of the most promising reported susceptibility genes, and a risk factor of particular importance given the prevalence of cannabis use.

1.3.3   Risk of schizophrenia is increased with cannabis use during adolescence

Studies also indicate that the early use of cannabis during adolescence is particularly associated with the later development of schizophrenia. For example, even after taking into account pre-existing symptoms and other confounding factors, young individuals who met diagnostic criteria for cannabis dependence disorder at age 18 had a 3.7 fold increased risk of psychosis, whereas the increase in risk of psychosis was only 2.3 fold in those who did not develop dependence until age 21 (Fergusson et al., 2003). Similarly, the initiation of cannabis use by age 15 was associated with a greater likelihood of developing schizophreniform disorder at age 26 than was cannabis use at age 18 (Arseneault et al., 2002). Finally, in individuals who develop schizophrenia, cannabis use during adolescence is associated with an earlier onset of first psychotic episode than in those who are not exposed to cannabis during this period (Veen et al., 2004; Arendt et al., 2005; Barnes et al., 2006).

Together, these findings converge on the idea that cannabis use represents an environmental risk factor for schizophrenia because 1) the association between cannabis use and schizophrenia is consistent across studies (replicated effect); 2) the association cannot be explained by other confounding factors (specificity of effect); 3) the degree of cannabis exposure

is positively correlated with the risk of schizophrenia (dose-response effect); 4) the exposure to cannabis precedes the development of schizophrenia (temporal effect); and 5) cannabis use during early adolescence is associated with greater risk (developmental effect) (reviewed in Henquet et al., 2005b). However, it is important to note that although some subjects with schizophrenia have been exposed to cannabis, not all individuals who are exposed to the drug develop the illness. Although this suggests that cannabis exposure is neither a necessary nor a sufficient cause of schizophrenia, the reviewed evidence strongly implicates that exposure to cannabis is an environmental risk factor for schizophrenia (Henquet et al., 2005b).

1.4   THE CANNABINOID 1 (CB1) RECEPTOR: A POTENTIAL PATHOPYSIOLOGICAL ENTITY IN SCHIZOPHRENIA

1.4.1   The endocannabinoid system

An endogenous system of cannabinoid receptors and ligands with cannabis-mimicking activity has recently been discovered in the mammalian brain (reviewed in Freund et al., 2003; Piomelli, 2003). The search for the molecular constituents of this system was fueled in the late 1980's following the demonstration of selective and specific binding of a radiolabelled synthetic derivative of Δ^9-THC in brain tissue, indicating the presence of a central brain cannabinoid receptor (Devane et al., 1988). To date, two cannabinoid receptors, CB1 (Matsuda et al., 1990) and CB2 (Munro et al., 1993), have been identified and cloned. Both cannabinoid receptors are seven-transmembrane-domain receptors coupled to G-protein second messenger systems (Freund et al., 2003). Whereas the CB2 receptor is mainly expressed in the immune system, the CB1 receptor is the principal cannabinoid receptor expressed in the brain and mediates the psychoactive and behavioral effects of cannabis (Freund et al., 2003). The two chief and best studied endocannabinoids, anandamide (Devane et al., 1992) and 2-arachidonoyl-glycerol (2-AG) (Mechoulam et al., 1995), are lipid-based compounds that are synthesized within the plasma membrane of neurons in an activity dependent manner and are released extracellularly through passive diffusion and/or facilitated transport (Freund et al., 2003).

1.4.2 Anatomical distribution of CB1 receptors

The CB1 receptor is one of the most abundant G-protein-coupled receptors expressed in the mammalian brain (Herkenham et al., 1990). In particular, high levels of the CB1 receptor are expressed in neocortical association areas such as the prefrontal cortex and the cingulate cortex (Herkenham et al., 1991; Matsuda et al., 1993; Glass et al., 1997), which are known to mediate executive functions. Other regions involved in cognitive functioning, such as the hippocampus, basal ganglia, and cerebellum, also express high levels of the CB1 receptor (Herkenham et al., 1991; Matsuda et al., 1993; Glass et al., 1997). Therefore, CB1 receptors in these regions may mediate certain deficits in cognitive functions observed following cannabinoid administration in humans and animals (Winsauer et al., 1999; Schneider and Koch, 2003; D'Souza et al., 2004).

In rodents, the CB1 receptor is predominantly expressed by GABA interneurons in the neocortex, hippocampus, and basal nuclei of the amygdala. Indeed, *in situ* hybridization experiments in the mouse neocortex and hippocampus have demonstrated that 100% of neurons that express high levels of CB1 mRNA also express mRNA for the 65-kDa isoform of glutamic acid decarboxylase 65 (GAD_{65}), a synthesizing enzyme of GABA (Marsicano and Lutz, 1999). Furthermore, dual-label *in situ* hybridization and dual-label electron microscopy experiments in the rodent neocortex, hippocampus, and amygdala revealed that the CB1 receptor is preferentially expressed by, and predominantly localized in, the terminals of the subtype of GABA basket interneurons that contain the neuropeptide cholecystokinin (CCK). In contrast, CB1 is not found in GABA neurons containing the calcium-binding protein parvalbumin (PV) (Katona et al., 1999; Marsicano and Lutz, 1999; Hajos et al., 2000a; Katona et al., 2001; Bodor et al., 2005). A number of physiological studies suggest that the CB1 receptor is also contained in excitatory pyramidal neurons (Auclair et al., 2000; Hajos et al., 2001) and recent immunocytochemical studies have confirmed this localization (Kawamura et al., 2006; Katona et al., 2006).

1.4.3 CB1 receptor signaling: Modulation of GABA neurotransmission and role in cortical circuitry

Consistent with the cellular localization of the CB1 receptor, electrophysiological studies have demonstrated that CB1 agonists affect GABA neurotransmission. For instance, in *in vitro* slices of rodent neocortex, hippocampus, and amygdala, CB1 agonists inhibit the release of GABA from neurons and reduce the amplitude of inhibitory postsynaptic currents (Katona et al., 1999; Hajos et al., 2000b; Katona et al., 2001; Trettel et al., 2004; Bodor et al., 2005). Furthermore, systemic administration of CB1 agonists decreases GABA levels in the rat neocortex *in vivo* as measured by microdialysis (Pistis et al., 2002). The CB1 receptor is a $G_{i/o}$-coupled receptor (reviewed in Freund et al., 2003) and in culture has been shown to inhibit N- and P/Q-type voltage-dependent Ca^{2+} channels, and activate inwardly rectifying K^+ channels (Mackie et al., 1995; Twitchell et al., 1997; Guo and Ikeda, 2004). These data suggests that CB1 receptor activation prevents vesicle fusion by blocking the depolarization of, and Ca^{2+} influx into, terminals. Under physiological conditions, CB1 receptor-mediated inhibition of GABA release results from a direct interaction of $G_{i/o}$-protein β-γ subunits with Ca^{2+} channels rather than through negative coupling to adenylyl cyclase or activation of inwardly rectifying K^+ channels (Wilson and Nicoll, 2002) **(Fig. 2)**. Importantly, CB1 receptor-mediated inhibition of GABA release in hippocampal slices primarily involves N-type Ca^{2+} channels, which are expressed by CCK-containing neurons, and not P/Q-type Ca^{2+} channels, which are expressed in PV-containing neurons (Wilson et al., 2001).

In the rodent hippocampus and neocortex, endocannabinoids and CB1 receptors mediate a phenomenon known as depolarization-induced suppression of inhibition (DSI) (Pitler and Alger, 1992; Trettel et al., 2004; Bodor et al., 2005) **(Fig. 2)**. In this phenomenon, pyramidal cell depolarization produces elevated intracellular Ca^{2+} levels, which initiates the synthesis and retrograde release of endocannabinoids (Freund et al., 2003). The released endocannabinoids bind to presynaptic CB1 receptors located on CCK terminals resulting in the reduction of perisomatic inhibitory input to that same pyramidal neuron (Wilson and Nicoll, 2002) **(Fig. 2)**. Thus, DSI in the neocortex is a mechanism by which pyramidal neurons can self-regulate their perisomatic inhibitory input.

This suggests a mechanism by which inhibition from CB1/CCK-containing neurons may serve to spatially and temporally shape and fine tune the firing of DLPFC pyramidal cells necessary for working memory function (Sawaguchi et al., 1988; Sawaguchi et al., 1989; Rao et al., 2000; Constantinidis et al., 2002). In the rodent neocortex, CB1/CCK-containing neurons are chemically and electrically coupled (Galarreta et al., 2004) and in the hippocampus entrain oscillatory patterns of rhythmic activity (Klausberger et al., 2005; Robbe et al., 2006). Interestingly, in the rodent hippocampus the administration of CB1 agonists reduce the power of gamma oscillations presumably by interrupting the temporal coordination of CB1/CCK-containing neurons that leads to a disruption of the organization of cell assemblies (Hajos et al., 2000b; Klausberger et al., 2005; Robbe et al., 2006). Based on these data, CB1 receptor-mediated disruption of gamma oscillations may be an underlying mechanism of impaired working memory performance in both humans and animals following chronic or acute cannabis use (Winsauer et al., 1999; Schneider and Koch, 2003; D'Souza et al., 2004).
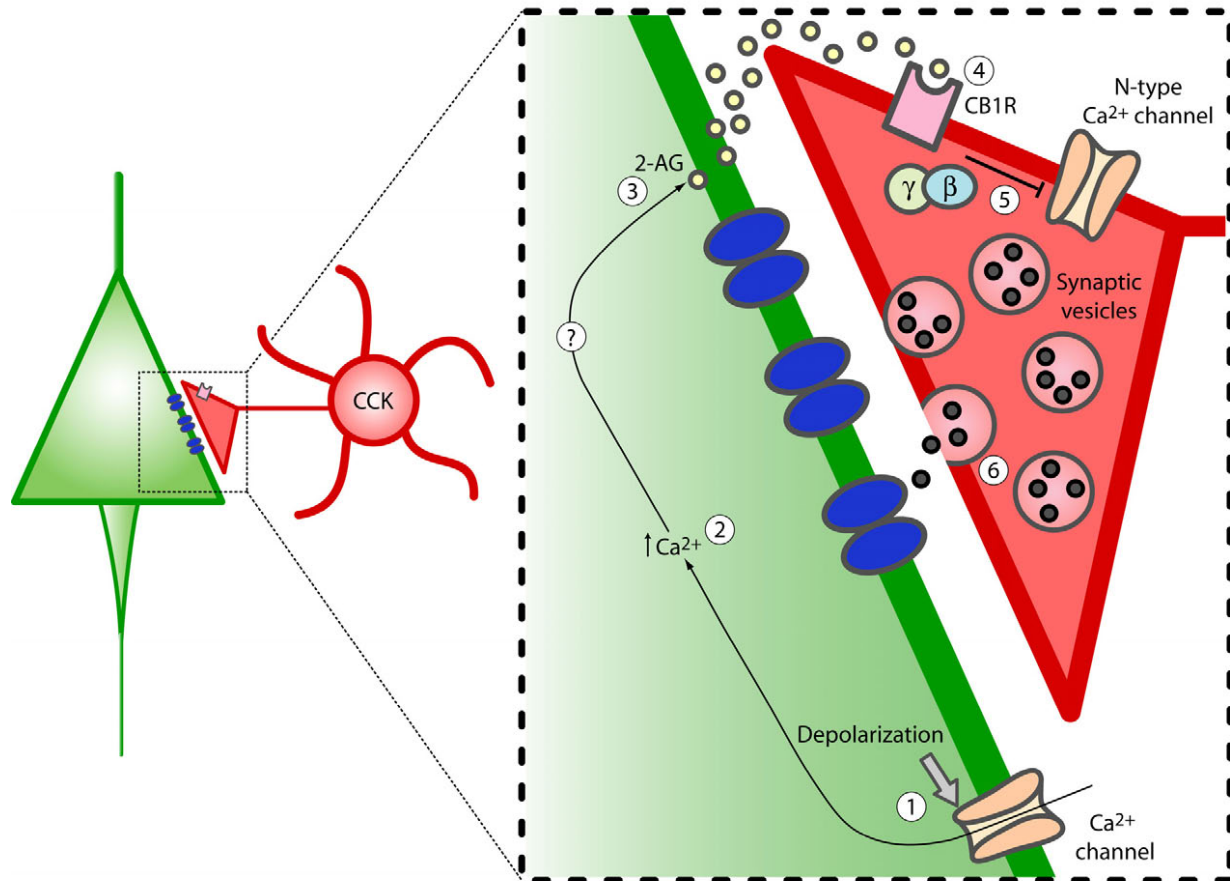
Figure 2. CB1 receptor- and endocannabinoid-mediated depolarization-induced suppression of inhibition (DSI). In the rodent neocortex, pyramidal neuron depolarization through Ca2+ channels (1) produces an increase in intracellular calcium concentration (2). Intracellular calcium triggers the synthesis and retrograde release of endocannabinoids (3), which activate CB1 receptors on presynaptic terminals of CCK-containing neurons (4). Binding of endocannabinoids to CB1 receptors activate G-protein β-γ subunits that inhibit N-type Ca2+ channels (5) and inhibit GABA release (6).

1.4.4 Evidence for CB1 as a potential neuropathological entity

To summarize, in humans, 1) chronic cannabis users and acute cannabis intoxication in normal individuals produce impairments in working memory performance, a core feature of schizophrenia and 2) cannabis exposure represents a significant environmental risk factor for schizophrenia, especially when exposure occurs during adolescence. In rodents, the CB1 receptor 1) is highly expressed in the prefrontal cortex, 2) is preferentially contained in a specific subpopulation of GABA basket interneurons that express CCK and that furnish perisomatic input to pyramidal neurons, 3) inhibits the release of GABA and reduces inhibitory postsynaptic currents upon activation, and 4) mediates network activity patterns that are necessary for working memory function. Consequently, alterations in the expression of the CB1 receptor might represent a neuropathological entity in the DLPFC of subjects with schizophrenia.

1.5   GOALS AND RELEVANCE OF THIS DISSERTATION

Despite the evidence implicating cannabis use as an environmental risk factor of schizophrenia and data from the rodent indicating that the CB1 receptor participates in circuitry that subserves working memory function, little is known about the anatomical distribution and localization of the CB1 receptor in the primate cortex or whether the expression of the CB1 receptor is altered in the DLPFC of individuals with schizophrenia. The research in this dissertation is aimed at elucidating these issues. The experimental results illuminate important functional roles of CB1 receptors in primate DLPFC circuitry and identify novel drug targets for the treatment of cognitive deficits in schizophrenia. In brief, the results of the experimental chapters are outlined:

1.5.1 Immunocytochemical distribution of the cannabinoid CB1 receptor in the primate neocortex: A regional and laminar analysis

In this study, we set out to characterize the anatomical distribution of the CB1 receptor in the brains of macaque monkeys and humans, focusing on the neocortex. The results demonstrate that in both monkeys and humans, CB1 receptors are preferentially contained in axons and that the DLPFC contains the highest density of CB1-containing axons in the neocortex. In addition, in the monkey neocortex, CB1 receptors are primarily contained in cells and axon terminals that have the morphologic features characteristic of GABA neurons.

1.5.2 Synaptic targets of cannabinoid CB1 receptor- and cholecystokinin-containing axon terminals in macaque monkey prefrontal cortex

The goal of this chapter was to determine the relationship between, and synaptic targets of, CB1 and CCK axon terminals in the monkey DLPFC. We found that, in the monkey DLPFC, a majority of CB1- and CCK-IR axons and axon terminals, particularly those in layer 4, are overlapping and arise from a common population of intrinsic interneurons. However, axons and terminals that colocalize CB1- and CCK-IR represent a subset of both CB1 and CCK neurons. The findings suggest that several classes of CB1- and/or CCK-containing neurons are present in monkey DLPFC and may play distinct functional roles, including perisomatic inhibition that is important for working memory function.

1.5.3 Reduced CB1 receptor mRNA and protein expression in schizophrenia: Implications for cognitive deficits

This series of experiments explored the potential role of the CB1 receptor in DLPFC dysfunction in schizophrenia by examining the expression of CB1 receptor mRNA and protein in the DLPFC of subjects with schizophrenia. We also examined the relationship between changes in CB1 mRNA expression and markers of GABA neurotransmission in schizophrenia. We found that 1) the levels of CB1 receptor mRNA and protein are significantly reduced in the DLPFC of subjects

with schizophrenia; 2) these reductions cannot be explained by potential confounding factors, suggesting that a reduction in CB1 receptors is intrinsic to the disease process of schizophrenia; and 3) the observed changes in CB1 receptor mRNA expression correlated with expression changes in GAD_{67} and CCK mRNA in the same subjects with schizophrenia.

2.0 IMMUNOCYTOCHEMICAL DISTRIBUTION OF THE CANNABINOID CB1 RECEPTOR IN THE PRIMATE NEOCORTEX: A REGIONAL AND LAMINAR ANALYSIS

2.1 ABSTRACT

Delta-9-tetrahydrocannabinol (Δ^9-THC) has profound effects on higher cognitive functions, and exposure to Δ^9-THC has been associated with the appearance or exacerbation of the clinical features of schizophrenia. These actions appear to be mediated via the CB1 receptor, the principle cannabinoid receptor expressed in the brain. However, the distribution of the CB1 receptor in neocortical regions of the primate brain that mediate cognitive functions is not known. We therefore investigated the immunocytochemical localization of the CB1 receptor in the brains of macaque monkeys and humans using antibodies that specifically recognize the N- or C-terminus of the CB1 receptor. In monkeys, intense CB1 immunoreactivity was observed primarily in axons and boutons. Across neocortical regions of the monkey brain, CB1-immunoreactive (IR) axons exhibited considerable heterogeneity in density and laminar distribution. Neocortical association regions, such as the prefrontal and cingulate cortices, demonstrated a higher density, and exhibited a unique laminar pattern of CB1-IR axons, compared to primary sensory and motor cortices. Similar regional and laminar distributions of CB1-IR axons were also present in the human neocortex. CB1-IR axons had more prominent varicosities in human tissue, but this difference appeared to represent a postmortem effect as similar morphological features increased in unperfused monkey tissue as a function of postmortem interval. In electron microscopy studies of perfused monkey prefrontal cortex, CB1 immunoreactivity was predominantly found in axon terminals that exclusively formed symmetric synapses. The high density, distinctive laminar distribution, and localization to inhibitory terminals of CB1 receptors in primate higher order association regions suggests that the CB1

receptor may play a critical role in the circuitry that subserves cognitive functions such as those that are disturbed in schizophrenia.

2.2 INTRODUCTION

Marijuana, a preparation of the hemp plant *Cannabis sativa*, is one of the oldest known recreational drugs and today, it is one of the most widely abused illicit drugs (Watson et al., 2000). Delta-9-tetrahydrocannabinol (Δ^9-THC), the chief psychoactive cannabinoid in cannabis, has profound effects on mood and a number of cognitive functions (reviewed in Childers and Breivogel, 1998; Ameri, 1999). In addition, cannabis use has been associated with both an increased risk of, and greater symptom severity in, psychiatric disorders such as schizophrenia (reviewed in Smit et al., 2004; Ujike and Morita, 2004). Thus, understanding the molecular mechanisms by which cannabinoids elicit their effects is of substantial interest and clinical importance.

The demonstration of selective and specific binding of a radiolabelled synthetic derivative of Δ^9-THC to brain tissue revealed the presence of a central brain cannabinoid receptor (designated CB1) (Devane et al., 1988). This finding led to the cloning of the brain CB1 receptor (Matsuda et al., 1990) and the identification of a peripheral CB_2 receptor (Munro et al., 1993), both of which are G protein-coupled receptors. The discovery of the endogenous cannabinoids anandamide (Devane et al., 1992) and 2-arachidonoyl-glycerol (2-AG) (Mechoulam et al., 1995), and the development of selective synthetic ligands that bind to the two receptor types (Rinaldi-Carmona et al., 1994; Rinaldi-Carmona et al., 1998), soon followed.

Most of the physiological and behavioral effects of cannabinoids appear to be mediated by the CB1 receptor (Zimmer et al., 1999), which is highly expressed and widely distributed in the brain (Herkenham et al., 1991; Matsuda et al., 1993; Glass et al., 1997). In particular, high levels of the CB1 receptor are expressed in neocortical association areas such as the prefrontal cortex and the cingulate cortex (Herkenham et al., 1991; Matsuda et al., 1993; Glass et al., 1997), which are known to mediate executive functions. Other regions involved in cognitive functioning, such as the hippocampus, basal ganglia, and cerebellum, also express high levels of the CB1 receptor (Herkenham et al., 1991; Matsuda et al., 1993; Glass et al., 1997). Therefore,

CB1 receptors in these regions may mediate certain deficits in cognitive functions observed following cannabinoid administration in humans and animals (Winsauer et al., 1999; Schneider and Koch, 2003; D'Souza et al., 2004).

In rodents, the CB1 receptor is almost exclusively expressed by GABA interneurons in the neocortex, hippocampus, and basal nuclei of the amygdala. Indeed, *in situ* hybridization experiments in the mouse neocortex and hippocampus have demonstrated that 100% of neurons that express high levels of CB1 mRNA also express mRNA for the 65-kDa isoform of glutamic acid decarboxylase 65 (GAD_{65}), a synthesizing enzyme of GABA (Marsicano and Lutz, 1999). Furthermore, dual-label *in situ* hybridization and dual-label electron microscopy experiments in the rodent neocortex, hippocampus, and amygdala revealed that the CB1 receptor is preferentially expressed by, and predominantly localized in, the terminals of the subtype of GABA basket interneurons that contain the neuropeptide cholecystokinin (CCK). In contrast, CB1 is not found in GABA neurons containing the calcium-binding protein parvalbumin (PV) (Katona et al., 1999; Marsicano and Lutz, 1999; Hajos et al., 2000b; Katona et al., 2001; Bodor et al., 2005). Consistent with this anatomical localization of the CB1 receptor, electrophysiological studies have demonstrated that CB1 agonists affect GABA neurotransmission. For instance, in *in vitro* slices of rodent neocortex, hippocampus, and amygdala, CB1 agonists inhibit the release of GABA from neurons and reduce the amplitude of inhibitory postsynaptic currents (Katona et al., 1999; Hajos et al., 2000b; Katona et al., 2001; Trettel et al., 2004; Bodor et al., 2005). Furthermore, systemic administration of CB1 agonists decreases GABA levels in the rat neocortex *in vivo* as measured by microdialysis (Pistis et al., 2002).

Together, these observations suggest that the endogenous cannabinoid system plays an integral role in modulating GABA synaptic neurotransmission. However, understanding the involvement of CB1 receptor-mediated signaling in cognitive functions, and in the impairment of these abilities in schizophrenia, requires knowledge of the anatomical localization of this receptor in the primate neocortex, especially in areas such as the prefrontal cortex where GABA neurotransmission is critical for cognitive functions (Sawaguchi et al., 1988; Rao et al., 2000). However, in the two studies that previously investigated the immunocytochemical distribution of the CB1 receptor in the monkey neocortex, the antibody that was used produced a pattern of labeling not entirely consistent with electrophysiological and pharmacological affects of CB1

24

agonists or the anatomical localization of the CB1 receptor in rodents (Ong and Mackie, 1999; Lu et al., 1999). Furthermore, although the immunocytochemical localization of CB1 in CCK interneurons in the human hippocampus (Katona et al., 2000) and the autoradiographic distribution of CB1 receptor binding sites across certain human neocortical regions (Glass et al., 1997; (Biegon and Kerman, 2001) appear to be conserved from the rodent (Herkenham et al., 1991; Katona et al., 1999), the immunocytochemical distribution of the CB1 receptor in the human brain has not been examined outside of the hippocampus. Consequently, we used immunocytochemical techniques and antibodies that specifically recognize the N- or C-terminus of the CB1 receptor to examine the regional and laminar distribution of the CB1 receptor in the neocortex of macaque monkeys and humans. In addition, we used immunoelectron microscopy in order to determine the cellular localization and cell types that express the CB1 receptor in the monkey dorsolateral prefrontal cortex.

2.3   MATERIALS AND METHODS

2.3.1   Light microscopy

2.3.1.1 Perfused monkey specimens

Eight adult male long-tailed macaque monkeys (*Macaca fascicularis*) were utilized for light microscopy. Housing and experimental procedures were conducted in accordance with USDA and NIH guidelines and with approval of the University of Pittsburgh's Institutional Animal Care and Use Committee. Monkeys were deeply anesthetized with ketamine hydrochloride (25 mg/kg) and sodium pentobarbital (30 mg/kg), intubated, mechanically ventilated with 28% O_2/air, and perfused transcardially with ice-cold 1% paraformaldehyde in 0.1 M phosphate buffer (pH 7.4) followed by 4% paraformaldehyde in phosphate buffer, as previously described (Oeth and Lewis, 1993). Brains were immediately removed, blocked into 5-6 mm-thick coronal or sagittal blocks, and postfixed for 6 hours in phosphate buffered 4% paraformaldehyde at 4°C. Tissue blocks were subsequently immersed in cold sucrose solutions of increasing concentrations (12%, 16%, and 18%) and then stored at -30°C in a cryoprotectant solution containing glycerin and ethylene

glycol in dilute phosphate buffer. We have previously shown that this storage procedure does not affect immunoreactivity for a number of antigens (see Cruz et al., 2003). Tissue blocks from either the left or the right hemisphere were sectioned coronally or sagittally at 40 µm on a cryostat and every 10th section was stained for Nissl substance with thionin.

2.3.1.2 Human autopsy subjects

Brain specimens from six (four male and two female) human subjects (20-38 years of age; postmortem interval [PMI] 4.5-8.5 hours) were obtained from autopsies conducted at the Allegheny County Coroner's Office, Pittsburgh, PA, following informed consent for brain donation from the next-of-kin. None of the subjects had a history of psychiatric or neurologic disorders as determined by information obtained from clinical records and a structured interview conducted with a surviving relative. Neuropathological examinations revealed no abnormalities in any subject. All procedures were performed with the approval of the University of Pittsburgh's Institutional Review Board for Biomedical Research.

Following retrieval of brain specimens, the left hemisphere was cut into 1.0 cm coronal blocks, and immersed in phosphate buffered 4% paraformaldehyde for 48 hours at 4°C. Tissue blocks were subsequently immersed in graded sucrose solutions and stored as described above. Tissue blocks containing the superior frontal gyrus (dorsolateral prefrontal cortex) or the calcarine sulcus (primary visual cortex) were sectioned coronally as described above.

2.3.1.3 Unperfused monkey specimens

One adult male long-tailed macaque monkey (Macaca fascicularis) was used to investigate the effect of PMI on CB1 immunoreactivity. The monkey was deeply anesthetized as described above and the brain was immediately removed, cut into 3-5 mm-blocks, and immersed in ice-cold 0.01 M phosphate buffered saline (PBS; pH 7.4). Following PMIs of 2, 12, 24, or 48 hours, adjacent tissue blocks were transferred to cold phosphate buffered 4% paraformaldehyde for 48 hours. Tissue blocks were then immersed in sucrose solutions and stored as described above. Blocks containing the dorsolateral prefrontal cortex for each PMI were sectioned on a cryostat as described above.

2.3.1.4 Immunocytochemistry

For perfused monkeys, free-floating tissue sections were thoroughly washed in 0.01 M PBS and then treated for 30 minutes with a blocking solution containing 0.3% Triton X-100 and 4.5% normal donkey (NDS) and normal human sera (NHuS) at room temperature in PBS. Tissue sections were subsequently incubated for 48 hours at 4°C in PBS containing 0.3% Triton X-100, 3% NDS and NHuS, 0.05% bovine serum albumin (BSA), and an affinity-purified polyclonal rabbit anti-CB1 antibody raised against either the N-terminus of the human CB1 receptor (residues 1-99; Sigma, St. Louis, MO; diluted 1:1000), the entire C-terminus of the rat CB1 receptor (anti-CB1-CT) (residues 401-473; diluted 1:5000), or the last 15 amino acid residues of the rat CB1 receptor (anti-CB1-L15) (diluted 1:5000). Both of the C-terminus antibodies were kindly provided by Dr. Ken Mackie (Indiana University, Bloomington, IN). Sections were then incubated for 1 hour in a biotinylated goat anti-rabbit IgG secondary antibody made in donkey (diluted 1:200; Jackson ImmunoResearch, West Grove, PA) followed by processing with the avidin-biotin peroxidase method (Hsu et al., 1981) using the Vectastain Avidin-Biotin Elite Kit (Vector Laboratories, Burlingame, CA). The immunoperoxidase reaction was visualized using 3,3'-diaminobenzidine (DAB; Sigma, St. Louis, MO), and sections were then mounted on gel-coated slides, and air-dried. The DAB reaction product was stabilized by serial immersions in osmium tetroxide (0.005%) and thiocarbohydrazide (0.5%) as previously described (Lewis et al., 1986).

Human and unperfused monkey tissue sections were processed with the anti-CB1-L15 in the same manner except that they were initially pretreated with 1% hydrogen peroxide for 15 minutes to remove endogenous peroxidase activity.

2.3.1.5 Analysis of neocortical laminar patterns

The laminar patterns of CB1 immunoreactivity observed across different neocortical regions were assessed using a Microcomputer Imaging Device (MCID) system (Imaging Research Inc, London, Ontario, Canada). Slide-mounted sections containing selected neocortical regions were trans-illuminated on a light box and images were captured by a video camera under precisely controlled conditions and digitized. Within each cytoarchitectonic region, a rectangle ~1 mm wide extending from pial surface to white matter was drawn and the optical density within each rectangle was measured. Optical density values were divided into 100 bins using Matlab

software (The MathWorks, Natick, Massachusetts) and normalized within each cytoarchitectonic region by dividing the value of each bin by the value of the maximum bin. Laminar boundaries were determined by calculating the percent depth of each layer in adjacent Nissl stained sections using the Neurolucida program (MicroBrightfield, Inc., Colchester, VT). Values from layer 1 were not reported due to edge effects that produced high optical density values even though layer 1 did not contain CB1-IR axons in most regions. Optical density values for each selected region were obtained from a single traverse from one animal each. A systematic analysis across multiple animals was not performed due to a lack of available tissue containing each region studied from every animal. However, the overall density and laminar patterns were confirmed in at least two animals for each region qualitatively.

2.3.2 Electron microscopy

2.3.2.1 Animals and tissue preparation

For electron microscopy studies, two additional adult male long-tailed macaque monkeys (*Macaca fascicularis*) were deeply anesthetized as described above and transcardially perfused with room temperature 1% paraformaldehyde and 0.05% glutaraldehyde in 0.1 M phosphate buffer followed by 4% paraformaldehyde and 0.2% glutaraldehyde in the same buffer as previously reported (Melchitzky et al., 2005). Brains were immediately removed, blocked coronally into 5 mm-thick blocks, and postfixed for 2 hours in phosphate buffered 4% paraformaldehyde at 4°C. Tissue blocks were subsequently washed in 0.1 M phosphate buffer and blocks containing prefrontal cortex area 46 were sectioned coronally at 50 µm on a vibrating microtome.

2.3.2.2 Immunocytochemistry

Free floating tissue sections were initially treated with 1% sodium borohydride in 0.1 M phosphate buffer for 30 minutes followed by several washes in 0.1 M phosphate buffer to improve antigenicity and reduce nonspecific immunoreactivity (Sesack et al., 1998). Sections were incubated for 30 min in a blocking solution containing 0.2% BSA, 0.04% Triton-X 100, 3% NDS, and 3% NHuS in 0.01 M PBS (pH 7.4) to further reduce nonspecific labeling. Sections were subsequently incubated overnight in blocking solution containing the anti-CB1-CT primary

antibody (diluted 1:5,000). On the following day, sections were rinsed in PBS and incubated for 1 hour in blocking solution containing a biotinylated anti-rabbit IgG secondary antibody made in donkey (diluted 1:200; Jackson ImmunoResearch, West Grove, PA). Following rinses in PBS, sections were processed with the avidin-biotin peroxidase method and visualized with DAB as described above. Tissue sections were then post-fixed in 2% osmium tetroxide for 1 hour in phosphate buffer, dehydrated in ascending alcohol solutions and embedded in Epon 812 (EM bed 812; Electron Microscopy Sciences, Fort Washington, PA) as previously described (Sesack et al., 1995b).

2.3.2.3 Sampling regions and procedures

For each animal, trapezoid blocks were cut from layer 4 of area 46 **(Fig. 3A)** and sectioned on a Reichert ultramicrotome (Nussloch, Germany) at 80 nm. Two to four ultrathin sections were serially collected on 200-mesh copper grids and counterstained with uranyl acetate and lead citrate. For each trapezoid block two to three grids, separated by at least ten grids, were examined. Grids were examined on an FEI Morgagni transmission microscope (Hillsboro, OR) and micrographs containing CB1 labeled structures were captured as digital images using an AMT XP-60 digital camera (Danvers, MA) and stored for later analysis.

2.3.2.4 Identification of neuronal and synaptic elements

Neuronal elements encountered in electron micrographs were identified according to previous descriptions (Peters et al., 1991). Briefly, perikarya were identified by the presence of a nucleus. Dendritic shafts were identified by the presence of synaptic inputs, mitochondria, microtubules, and neurofilaments, whereas dendritic spines were characterized by the absence of both organelles and microtubules. Asymmetric synapses (Gray's Type I) were identified by the widening and parallel spacing of apposed plasmalemmal surfaces, the presence of a prominent postsynaptic density, and round small synaptic vesicles. Symmetric synapses (Gray's type II) were identified by the presence of intercleft filaments, a thin postsynaptic density, and pleomorphic small synaptic vesicles.

29

2.3.3 Antibody specificity

The specificity of the antibodies raised against the entire C-terminus of the rat CB1 receptor has been verified by several lines of evidence. First, when tested in tissue from CB1 knockout mice, no immunolabeling was observed (Hajos et al., 2000b; Katona et al., 2001). Second, Western blotting of rat brain homogenates produced bands at the predicted molecular weights based on the amino acid sequence of the CB1 receptor. Third, the CB1 antibody labeled ATt20 cells transfected with the CB1 receptor, but did not label untransfected cells (Hajos et al., 2000b; Katona et al., 2001). In addition, we preadsorbed the anti-CB1-CT and anti-CB1-L15 antibodies with 1 µg/ml of their respective cognate peptides. We also preadsorbed the anti-CB1-L15 antibody with the anti-CB1-CT fusion peptide and visa versa (see results).

2.3.4 Nomenclature

Neocortical regions were identified on adjacent Nissl-stained sections based on previously published cytoarchitectonic and connectional analyses in the macaque monkey and the atlas of Paxinos et al. (2000) (for regional abbreviations see **Table 1**). Frontal lobe cytoarchitectonic delineations used the criteria and terminology of Barbas and Pandya (1989) and Carmichael and Price (1994). Regions of the cingulate cortex were identified following the divisions of Vogt et al. (1987) and Morecraft et al. (2004). In the temporal lobe, the terminology of Amaral et al. (1987) was used for the subregions of the entorhinal cortex, and regions of the superior temporal sulcus (TE and TEO) were defined according to Seltzer and Pandya (1989). The auditory regions in the superior temporal gyrus were identified according to the cytoarchitectonic criteria of Galaburda and Pandya (1983), using the updated parcellation and nomenclature of Hackett et al. (1998). In this nomenclature, AI and R compose the core auditory cortex, association belt regions are designated RM, AL, and ML, and parabelt regions are designated RP and CP. Divisions of the insular cortex were classified according to Mesulam and Mufson (1982). In the parietal post central gyrus, primary somatosensory areas 3, 1, and 2 were identified based on the studies of Burton et al. (1995) and Cipolloni and Pandya (1999). Regions of the posterior parietal cortex were defined in accordance with Cavada and Goldman-Rakic (1989) in which area 5 corresponds to area PE and areas 7m, 7a, and 7b correspond to areas PGm, PG, and PF of

Pandya and Seltzer (1982), respectively. Regions of the intraparietal sulcus were designated as physiologically-defined areas MIP, VIP, and LIP (reviewed in Colby and Goldberg, 1999), but are architectonically analogous to area PEa and POa of Pandya and Seltzer (1982) and area 7ip of Cavada and Goldman-Rakic (1989). Visual regions of the parieto-occipital cortex (MT, MST, FST) were defined based on the studies of Boussaoud et al. (1990) and Lewis and Van Essen (2000). The laminar boundaries of area 17 were delineated based on the divisions of Fitzpatrick et al. (1985). The nuclear divisions of the amygdala were defined according to Amaral and Bassett (1989) and Pitkanen and Amaral (1998). Regions of the hippocampal formation and layers of the dentate gyrus and CA regions followed the terminology of Alonso and Amaral (1995) and Jongen-Relo et al. (1999). Cerebellar lobules and folia were defined according to the atlas of Madigan, Jr. and Carpenter (1971). Finally, laminar boundaries in human neocortical regions were identified using published cytoarchitectonic criteria (Braak, 1976; Rajkowska and Goldman-Rakic, 1995) **(Table 1)**.

Table 1. Abbreviations

ABmc	accessory basal nucleus, magnocellular division	**FST**	fundus of the superior temporal area	**PLdg**	polymorphic layer of the dentate gyrus
ABpc	accessory basal nucleus, parvicellular division	**G**	granular layer of the cerebellum	**PN**	paralaminar nucleus
AI	auditory area I (core primary auditory)	**GL**	granule cell layer of the dentate gyrus	**PrS**	presubiculum
AL	anterior lateral auditory belt	**GPe**	globus pallidus, external	**ps**	principal sulcus
amt	anterior middle temporal sulcus	**GPi**	globus pallidus, internal	**Pu**	putamen
as	arcuate sulcus	**Id**	insula, dysgranular	**R**	rostral auditory area (core primary auditory)
Bi	basal nucleus, intermediate division	**Ig**	insula, granular	**rf**	rhinal fissure
Bmc	basal nucleus, magnocellular division	**ips**	intraparietal sulcus	**RM**	rostromedial auditory belt
Bpc	basal nucleus, parvicellular division	**lf**	lateral fissure	**RP**	rostral auditory parabelt
CA1, CA3	fields of the hippocampus	**LIP**	lateral intraparietal cortex	**S**	subiculum
CC	corpus collosum	**Ldi**	lateral nucleus, dorsal intermediate division	**SII**	second somatosensory cortex
Cd	caudate nucleus	**Lv**	lateral nucleus, ventral division	**SL**	stratum lucidum
Ce	central amygdaloid nucleus	**Lvi**	lateral nucleus, ventral intermediate division	**SLM**	stratum lacunosum-moleculare
Cgs	cingulate sulcus	**M**	molecular layer of the cerebellum	**SP**	stratum pyramidale
Cl	claustrum	**Me**	medial amygdaloid nucleus	**SR**	stratum radiatum
COp	posterior cortical nucleus	**MIP**	medial intraparietal cortex	**sts**	superior temporal sulcus
CP	caudal auditory parabelt	**MLdg**	molecular layer of the dentate gyrus	**TE**	inferotemporal cortex
cs	central sulcus	**ML**	middle lateral auditory belt	**TEO**	temporal area TE, occipital part
DG	dentate gyrus	**OML**	outer molecular layer	**Th**	thalamus
E$_C$	entorhinal cortex, caudal field	**PaS**	parasubiculum	**TPO**	temporal parietooccipital associated area in sts
E$_I$	entorhinal cortex, intermediate field	**PCL**	pyramidal cell layer	**VIP**	ventral intraparietal cortex

2.3.5 Photography

Brightfield photomicrographs were obtained with a Zeiss Axiocam camera. Digital electron micrographs and brightfield photomontages were assembled and the brightness and contrast were adjusted in Adobe Photoshop.

2.4 RESULTS

2.4.1 Specificity of the CB1 antibodies

The specificity of the C-terminus CB1 antibodies was tested by omission of the primary antibodies and by preadsorption of the anti-CB1-CT and anti-CB1-L15 antibodies with their respective fusion proteins. All specific immunoreactivity was eliminated in monkey tissue under these conditions. When the anti-CB1-L15 antibody was preadsorbed with the anti-CB1-CT fusion peptide, all specific immunoreactivity was eliminated. However, when the anti-CB1-CT antibody was preadsorbed with the anti-CB1-L15 fusion peptide, some specific labeling of axons remained, indicating that the overlapping but shorter anti-CB1-L15 fusion peptide contained some, but not all, epitopes recognized by the anti-CB1-CT antibody. Furthermore, although raised against different amino acid sequences of the CB1 receptor, all three antibodies produced identical patterns of immunoreactivity in the neocortex **(Fig. 3)**. Specifically, each of the CB1 antibodies labeled numerous thin, highly varicose axons with a distinctive laminar pattern of distribution **(Fig. 3A-C)**. In addition, dense perisomatic arrays of labeled processes around unlabeled cell bodies **(Fig. 3D-F)** and a small number of intensely-immunoreactive cell bodies restricted to neocortical layers 2 and superficial 3 were observed with all three antibodies **(Fig. 3A-C)**. Consistent with other reports (Hajos et al., 2000b; Katona et al., 2001), the C-terminus antibodies **(Fig. 3A, B, D, E)** produced more intense immunoreactivity with a better signal-to-noise ratio than the N-terminus antibody **(Fig. 3C, F)**. We therefore used the C-terminus antibodies in our analyses.
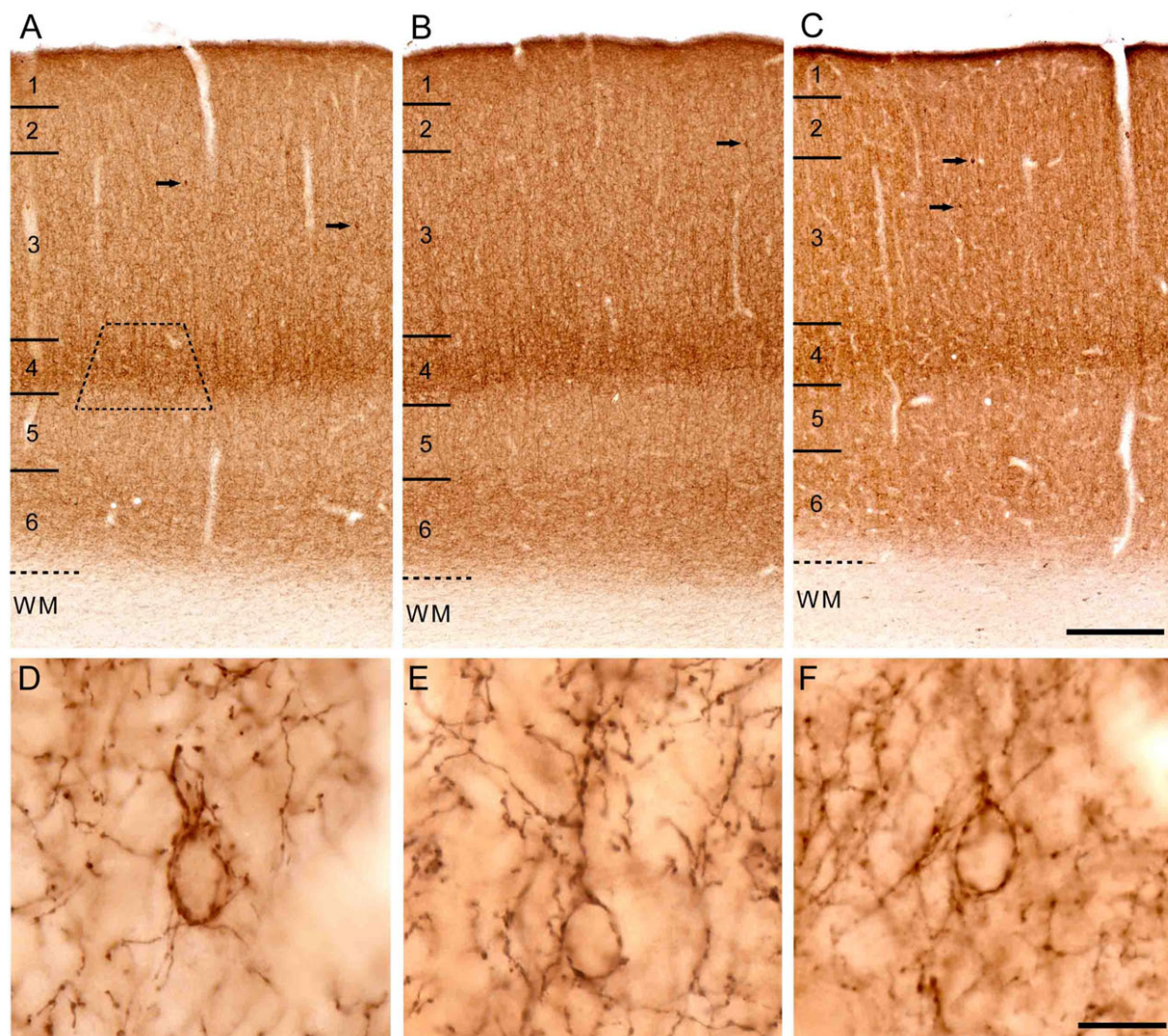
Figure 3. Brightfield photomicrographs of CB1 immunoreactivity in area 46 of the monkey prefrontal cortex produced by the anti-CB1-CT (A, D), anti-CB1-L15 (B, E), and the N-terminus antibodies (C, F). All 3 antibodies labeled numerous fibers that were thin and rich in varicosities and produced similar laminar patterns of immunoreactivity. Some labeled axons formed dense ''baskets'' surrounding unlabeled cell bodies **(D–F)**. In addition, intensely labeled CB1-IR neurons were present in layers 2 and superficial 3 (arrows). In panels **A–C** numbers and hash marks to the left indicate the relative positions of the cortical layers, and the dashed lines denote the layer 6-white matter (WM) border. The trapezoid in panel **A** shows the approximate laminar location of blocks examined for electron microscopy. Scale bars = 300 μm in **C** (applies to **A, B, C**) and 10 μm in **F** (applies to **D, E, F**).

2.4.2 Distribution of CB1 immunoreactivity in monkey neocortex

2.4.2.1 Regional densities

The overall distribution of CB1-IR axons varied substantially across different neocortical regions in each of the animals examined **(Table 2)**. Specifically, the highest densities of CB1-IR axons in the neocortex were present in higher order association regions, such as the prefrontal cortex, whereas the primary visual cortex had the lowest density of CB1-IR axons. Within the frontal lobe, dorsolateral prefrontal area 46, followed by dorsal area 9 and rostral area 10, contained the highest densities of CB1-IR axons. From these areas the density of CB1-IR axons progressively declined both caudally (across areas 8, 6, and 4) and ventrally (across areas 11 and 13) **(Fig. 4)**. Primary motor cortex (area 4) contained the lowest overall density of CB1-IR axons in the frontal lobe **(Table 2; Fig. 4)**. Regions of the cingulate cortex also expressed a high density of CB1-IR axons **(Table 2; Fig. 5)**. For instance, the densities CB1-IR axons in areas 24b-d, 23b-d, and 31 were similar to that observed in prefrontal areas 9 and 10. However, areas 24a, 23a, 29, and 30 exhibited a lower density of CB1 immunoreactivity **(Table 2; Fig. 5)**.

Table 2. Relative intensity of CB1 immunoreactivity in selected regions of macaque monkey brain

Region	Relative Density	Region	Relative Density
Frontal cortex		**Parietal cortex (cont.)**	
Area 46	8 (Fig. 4)	Area LIP	5
Area 10	7	Area VIP	5
Area 9	7	Areas 3, 1, 2	4
Area 32	7	Area MT	5
Area 8	6	Area MST	5
Area 6	5	Area FST	5
Area 4	4 (Fig. 4)	Area SII	5
Area 11	7	**Occipital cortex**	
Area 13	6	Area 18	3
Area 14	6	Area 17	2 (Fig. 7B)
Cingulate cortex		**Amygdala**	
Area 24b-d	7	Bmc	8
Area 23b-d	7	Bi	8
Area 31	7	ABmc	8
Area 24a	5	Lvi	8
Area 23a	5	ABpc	7
Area 29	5	Bpc	7
Area 30	5	COp	7
Temporal cortex		Ldi	7
Area 36	7	Lv	7
Area TE	6	PN	7
Area TEO	5	Ce	0
EI	7	Me	0
EC	7	**Hippocampus**	
CP	7	Dentate gyrus	8
RM	7	CA fields	8
RP	7	Subiculum	7
AL	6	**Basal Ganglia**	
ML	6	Globus pallidus	10 (Fig. 5)
AI	5	SNr	10
R	5	Caudate	1
Area Idg	6 (Fig. 5)	Putamen	1
Area Ig	5	**Claustrum**	6
Parietal cortex		**Thalamus**	0 (Fig. 5)
Area 7	7	**Cerebellum**	
Area 5	7	Molecular layer	9
Area MIP	5	Granular layer	4

Note: Relative density values represent qualitative assessments of the intensity of CB1 immunoreactivity on a scale of 0-10 with 0 representing the absence of detectable CB1 immunoreactivity and 10 representing the highest intensity of CB1 immunoreactivity. Examples of points along this scale are provided as follows: 0 (**Fig. 5**), 2 (**Fig. 7B**); 4 (**Fig. 4**); 6 (**Fig. 5**); 8 (**Fig. 4**), 10 (**Fig. 5**).

cs

4

as

6

9

8

ps

46

10

11

Cd

Cd

13

Th

Pu

GP

37
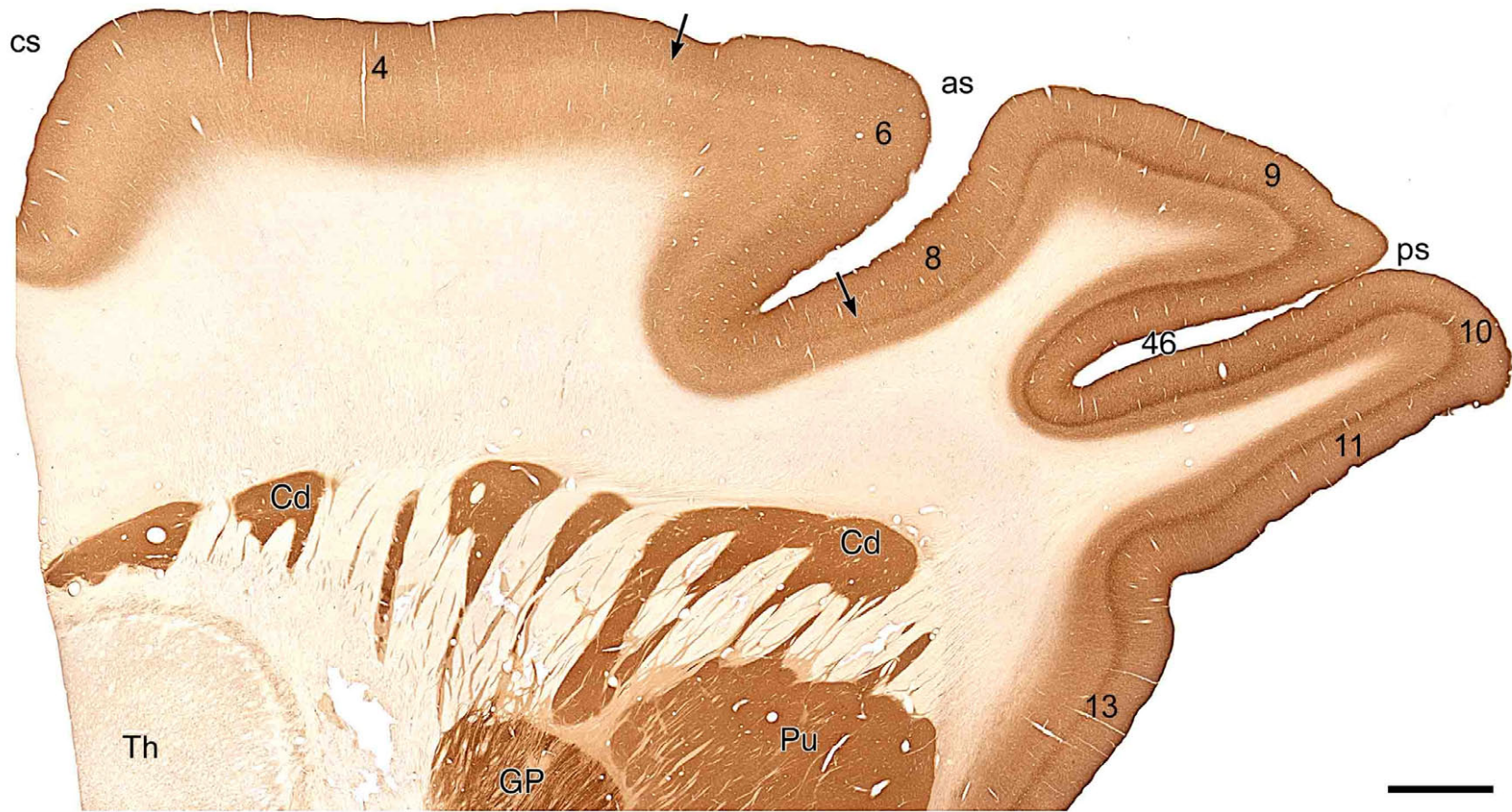
Figure 4. Brightfield photomicrograph of a parasagittal section through macaque monkey frontal lobe processed for CB1 immunoreactivity. CB1-IR axon density was greatest in prefrontal regions such as the dorsolateral prefrontal cortex (area 46) within the principal sulcus (ps). The overall density of CB1-IR axons decreased and the laminar patterns changed (arrows) from rostral prefrontal areas to motor areas (areas 4 and 6) caudal to the arcuate sulcus (as). On the orbital surface, labeled axon density also decreased from dorsal (area 10) to ventral (area 13) regions. Scale bar = 2 mm.

In the medial temporal cortex, all fields of the entorhinal cortex (E_I and E_C illustrated) and adjacent area 36 exhibited a high density of CB1-IR axons **(Table 2; Figs. 5 and 10A)**. Visual area TEO in the inferior temporal cortex contained an intermediate density of CB1-IR axons, whereas rostral region TE **(Fig. 5)** contained a moderate to high CB1-IR axon density. In the superior temporal gyrus, auditory association areas contained a high CB1-IR axon density, with parabelt regions RP and CP exhibiting slightly higher CB1-IR axon densities than the adjacent belt regions AL and ML **(Table 2; Figs. 5 and 9A)**. Primary auditory regions R and AI exhibited only an intermediate density of CB1-IR axons **(Table 2; Figs. 5 and 9A)**. The dysgranular region of the insula (Idg) contained a lower density of CB1-IR axons than the prefrontal cortex and labeled axon density was further reduced in the granular region of the insula (Ig) **(Table 2; Fig. 5)**.

In the post central gyrus of the parietal cortex, primary somatosensory areas 3, 1, and 2 had a relatively low density of CB1-IR axons, similar to that observed in primary motor area 4 **(Table 2; Fig. 5)**. Area SII on the dorsal bank of the lateral fissure showed a slightly higher density of CB1-IR axons. Areas 7 and 5 of the posterior parietal cortex contained a high density of CB1-IR axons similar to that observed in the prefrontal cortex, whereas areas MIP, VIP, and LIP in the intraparietal sulcus exhibited only an intermediate expression of CB1-IR axons **(Table 2)**.

The lowest overall density of CB1-IR axons in the neocortex was present in the primary visual cortex (area 17), with area 18 demonstrating a slightly higher density of CB1-IR axons **(Table 2)**. Higher order visual areas MT, MST, and FST demonstrated intermediate densities of CB1-IR axons **(Table 2)**.

cs

4

1

2

ips

cgs

3

2

23c

23a

CC

Cd

Ig

SII

If

A

Th

Pu

AL

GPi

Idg

RP

B

R

GPe

RM

Cl

TPO

Ce

sts

Me

C

COp

ABmc

Bmc

Ldi

ABpc

Bi

Lvi

Bpc

Lv

PN

E_l

TE

rf

36

40
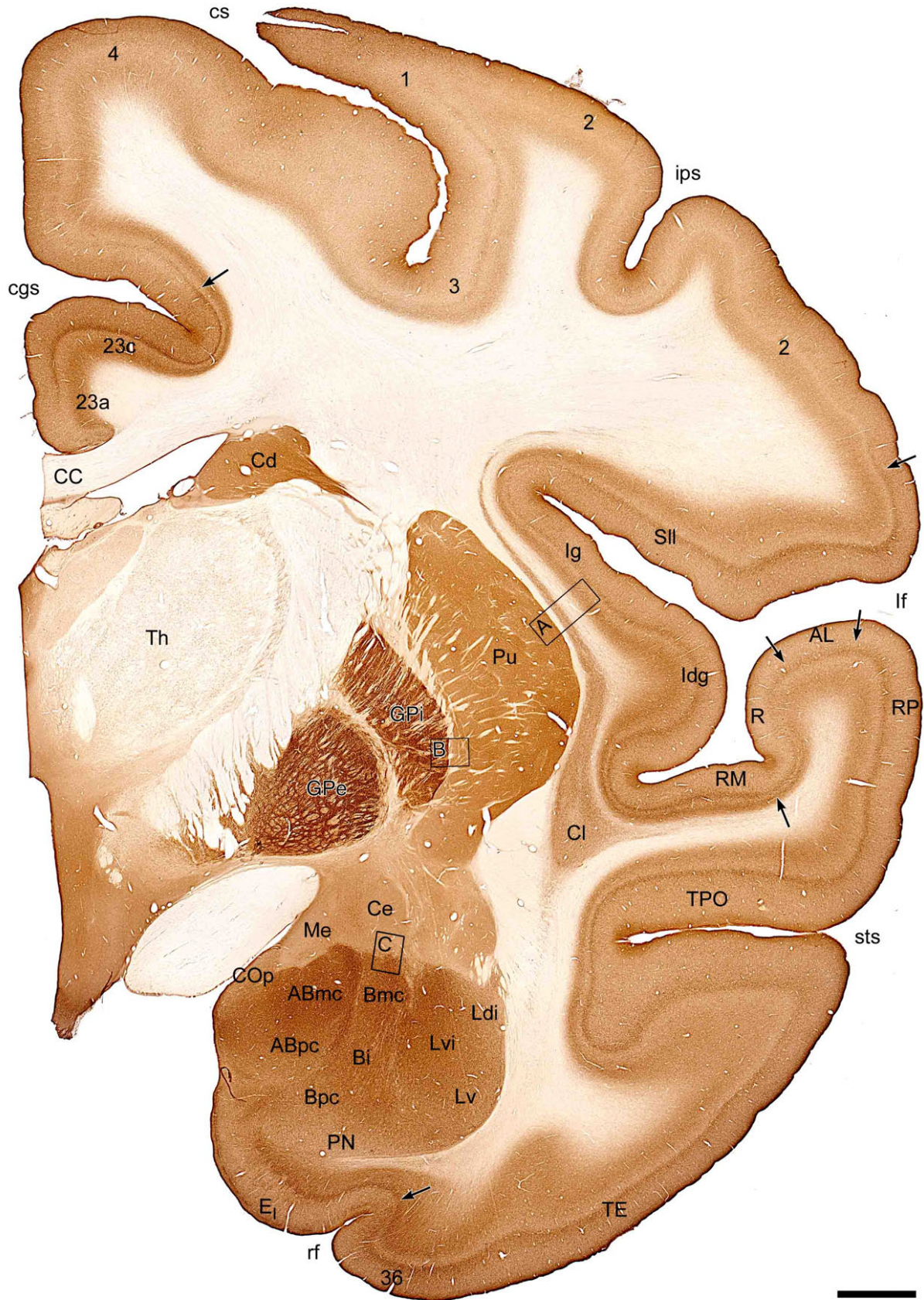
Figure 5. Photomicrograph of a coronal section through macaque monkey brain illustrating the distribution of CB1-IR axons. Association areas such as the cingulate cortex (area 23), insula (Ig, Idg), auditory association cortex (RP), and the entorhinal cortex (E$_I$) had an overall higher density of CB1-IR axons than primary somatosensory areas (areas 3, 1, 2) and primary motor cortex (area 4). Also note the distinct differences in the laminar distribution of labeled processes at the boundaries of some cytoarchitectonic regions (arrows). In subcortical structures, the intensity of CB1 immunoreactivity was high in the claustrum (Cl), the basal and lateral nuclei of the amygdala, and both segments of the globus pallidus (GP); intermediate to low in the caudate (Cd) and putamen (Pu) and the central and medial nuclei of the amygdala; and not detectable in the thalamus (Th). Boxes indicate regions shown at higher magnification in **Figure 11**. Scale bar = 2 mm.

2.4.2.2 Laminar patterns

      The laminar distribution of CB1-IR axons also varied substantially across different neocortical regions in each of the animals examined. Most association areas, such as the prefrontal cortex **(Figs. 3 and 4)**, parietal area 7m **(Fig. 6A)**, and cingulate areas 23b-d, 24b-d, and 31 **(Fig. 5)**, had a similar laminar distribution of CB1-IR axons. For example, in prefrontal area 46 **(Fig. 3)**, the density of CB1-IR axons was lowest in layer 1 and progressively increased from superficial to deep across layers 2 and 3. Layer 4 contained a very dense band of immunoreactive axons and varicosities and layer 6 contained a band of lower density. The low level of immunoreactivity in layer 5 sharply demarcated the borders with layers 4 and 6. The presence of distinct radial fibers also distinguished layers 3 and 5. The somewhat lower overall density of CB1-IR axons in some other association regions was due to a lower density of positive axons in layer 4. For instance, areas 24a **(Fig. 6B)** and 23a **(Fig. 5)** of the cingulate cortex showed a fairly homogenous distribution of CB1 positive axons across layers 2-6.

      In contrast, in the E_I and E_C subdivisions of the entorhinal cortex **(Fig. 6C)**, layers 2 and 5 contained the highest density of CB1-IR axons and varicosities, and the density was lower in layers 3 and 6. The lower density of radially-oriented CB1-IR axons in layer 3 in E_C and layers 3 and 4 in E_I highlighted distinct borders with layers 2 and 5. Layer 2 of E_I contained patches of high and low densities of CB1-IR axons that correspond to the islands of multipolar cells separated by cell-sparse zones that are characteristic of this region **(Fig. 5)**. Layer 1 of the entorhinal cortex contained diffuse horizontally oriented CB1-IR axons unlike other neocortical association regions **(Fig. 6)**.
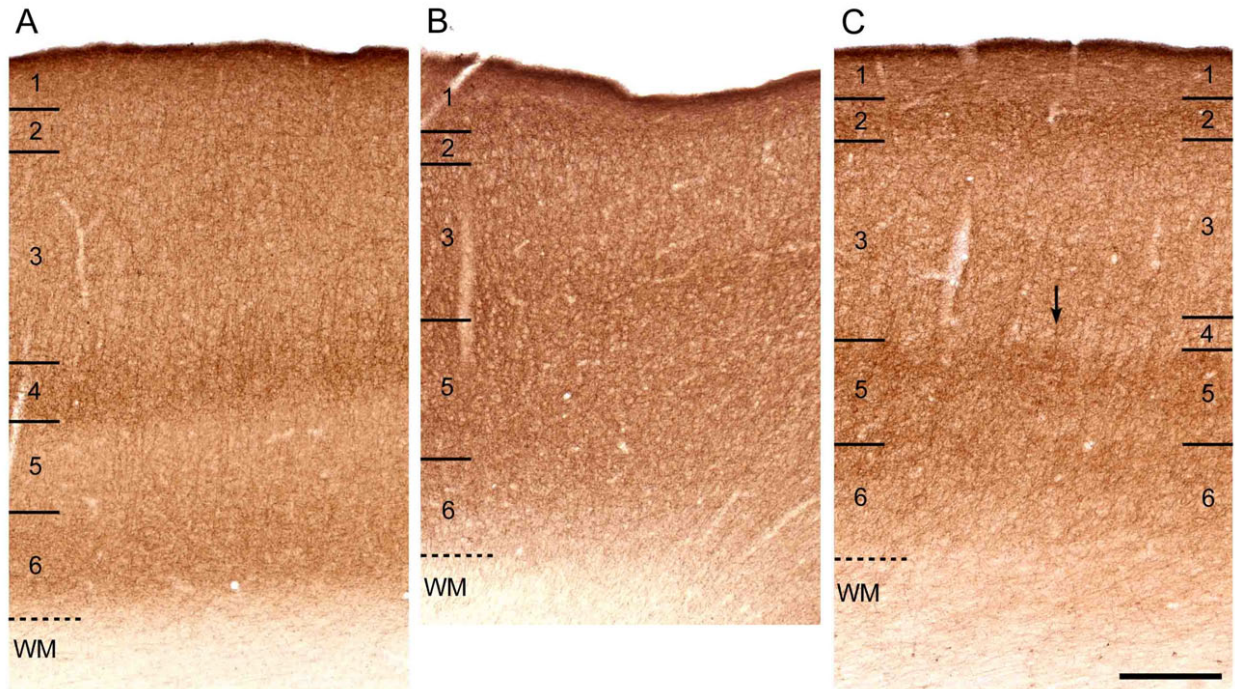
Figure 6. Brightfield photomicrographs demonstrating regional differences in the laminar distribution of CB1-IR axons across association cortices of monkey brain. **(A)** In the medial posterior parietal cortex (area 7m), the overall density and laminar distribution of CB1-IR axons were similar to those present in prefrontal area 46 **(Fig. 3)**. **(B)** In contrast, area 24a of the cingulate cortex showed a more homogenous laminar distribution of CB1-positive axons. **(C)** In a sagittal section of the entorhinal cortex, the transition from the caudal entorhinal cortex (E_C) to the intermediate entorhinal cortex (area E_I) is marked by a decreased density of CB1-IR axons in the lamina dessicans, a cell-sparse layer 4 present in E_I (arrow). Throughout the entorhinal cortex, layers 2 and 5 demonstrated the highest density of CB1-IR axons and varicosities, and layers 3 and 6 exhibited a lower density of CB1-IR axons. Numbers and hash marks in each panel indicate the relative positions of the cortical layers, and the dashed lines denote the layer 6-white matter (WM) border. Scale bar = 300 μm in **C** (applies to **A, B, C**).
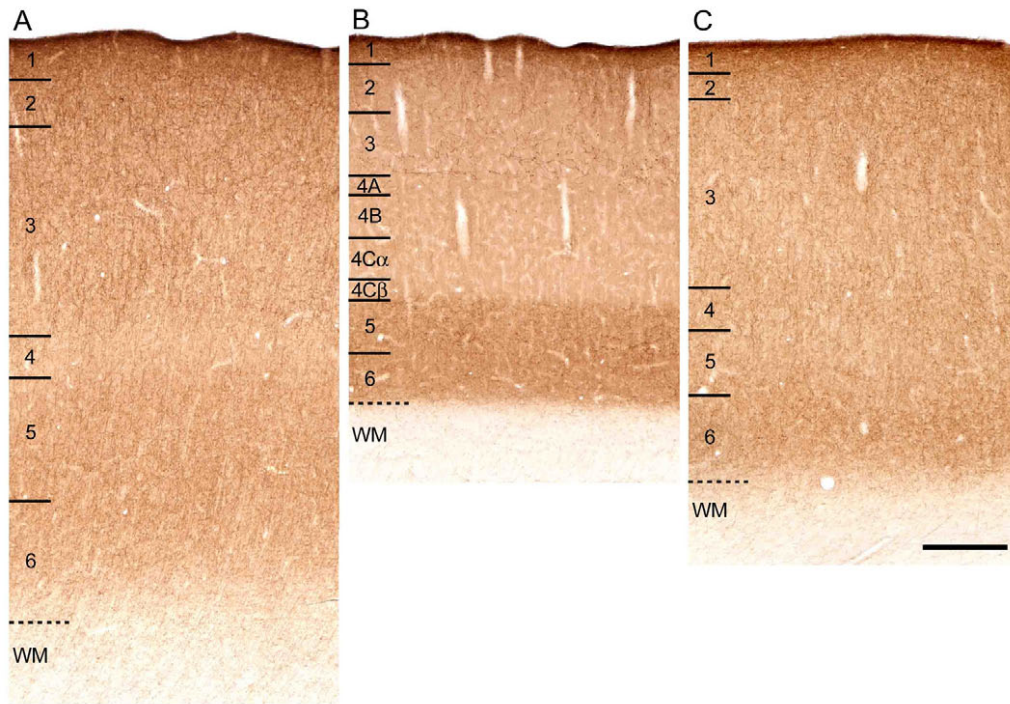
Figure 7. Brightfield photomicrographs demonstrating differences in density and laminar distribution patterns of CB1-IR axons across sensory regions. All sensory regions showed an overall lower density of CB1-IR axons than association regions. **(A)** Primary somatosensory cortex (area 2) contained a relatively low density of CB1-IR axons. The density of CB1- IR axons was similar across layers 2–3 and 5–6, and there was a paucity of labeling in layer 4. **(B)** Primary visual cortex (area 17) showed the overall lowest density of CB1-IR axons in the cortex. The laminar pattern of CB1-IR axons in area 17 was unique in that layers 5–6 contained the highest density of labeled axons and layer 4 contained no labeled axons. **(C)** Higher-order visual areas, such as area FST, contained an overall CB1-IR axon density that was lower than other association regions, and the laminar distribution of CB1-IR axons was homogeneous across layers. Numbers and hash marks to the left of each panel indicate the relative positions of the cortical layers, and the dashed lines denote the layer 6-white matter (WM) border. Scale bar = 300 μm in **C** (applies to **A, B, C**).

The laminar pattern of CB1-IR axons was quite different in primary motor **(Fig. 4)** and somatosensory cortices **(Fig. 7A)**, where the density of CB1-IR axons was greatest in layers 2-3 and 5-6 and lowest in layer 4. The primary visual cortex was unique in that the highest density of CB1-IR axons was observed in layers 5-6, layers 1-3 exhibited diffuse horizontally oriented axons, and layer 4 demonstrated a complete absence of CB1-IR axons **(Fig. 7B)**. The laminar distribution of CB1-IR axons in higher order visual areas such as area FST was homogeneous across layers **(Fig. 7C)**.

These qualitative regional differences in laminar distribution of CB1 immunoreactive axons were confirmed by optical density measures **(Fig. 8)**. For example, optical density across layers in area 46 **(Fig. 8A)**, area 24a **(Fig. 8B)**, area 2 **(Fig. 8C)**, and area 17 **(Fig. 8D)** precisely matched the laminar distribution of CB1-IR axons observed in these areas qualitatively.

The differences in density and laminar distribution of CB1-IR axons were so striking that many boundaries between cytoarchitectonic regions were clearly delineated by CB1 immunoreactivity **(Fig. 9)**. For instance, the boundary between primary auditory cortex AI and the adjacent auditory association belt cortex area ML in the superior temporal gyrus was clearly distinguished by the appearance of a dense band of CB1 immunoreactive axons in layer 4 of ML **(Fig. 9A)**. In the posterior parietal cortex, the border between area 5 and MIP could be delineated by the disappearance of a dense band of CB1-IR axons in layer 4 of MIP **(Fig. 9B)**. In the visual cortex, the area 17/18 border was clearly identified by an increase in axon density in layers 2-4 of area 18 (data not shown).
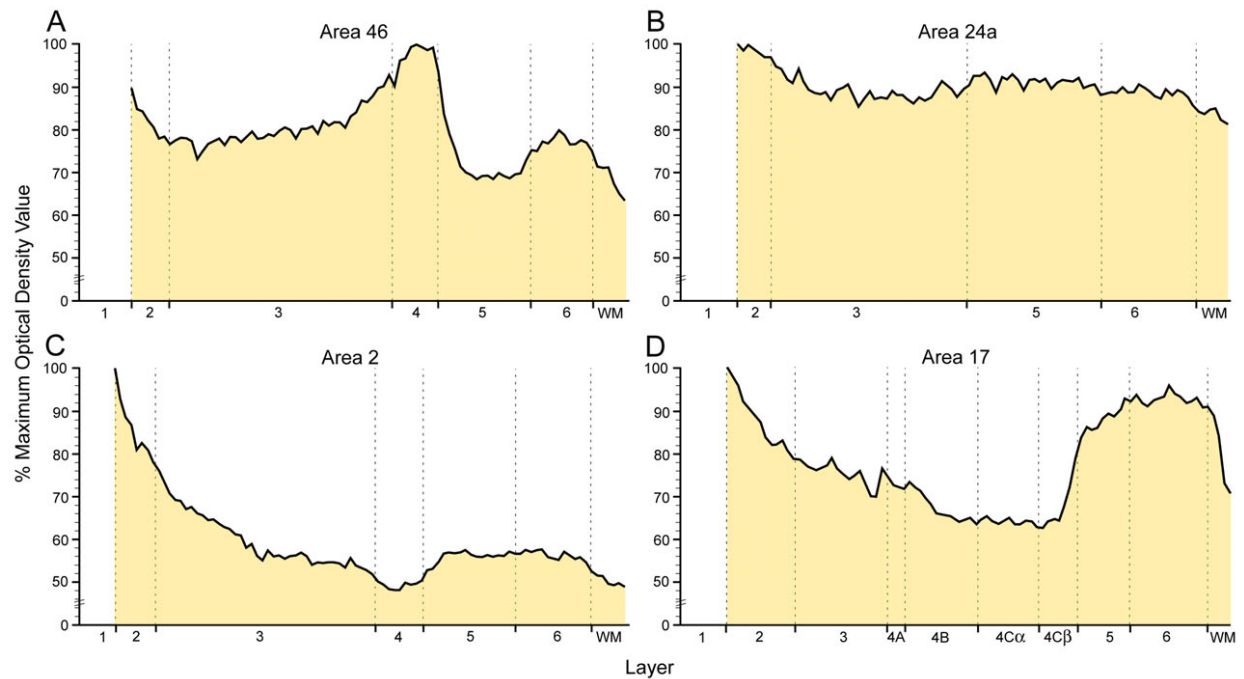
Figure 8. Plots of CB1 optical density as a function of cortical layer in 4 regions of the macaque monkey neocortex. Optical density values in A-D were obtained from the identical cortical traverses shown in **Figure 3B** (area 46), **Figure 6B** (area 24a), and **Figure 7A** (area 2) and **B** (area 17). For each area optical density measures were divided into 100 bins, and within each region optical density measures were normalized by dividing the value of each bin by the value of the maximum bin. Note the marked regional differences in laminar distribution patterns.
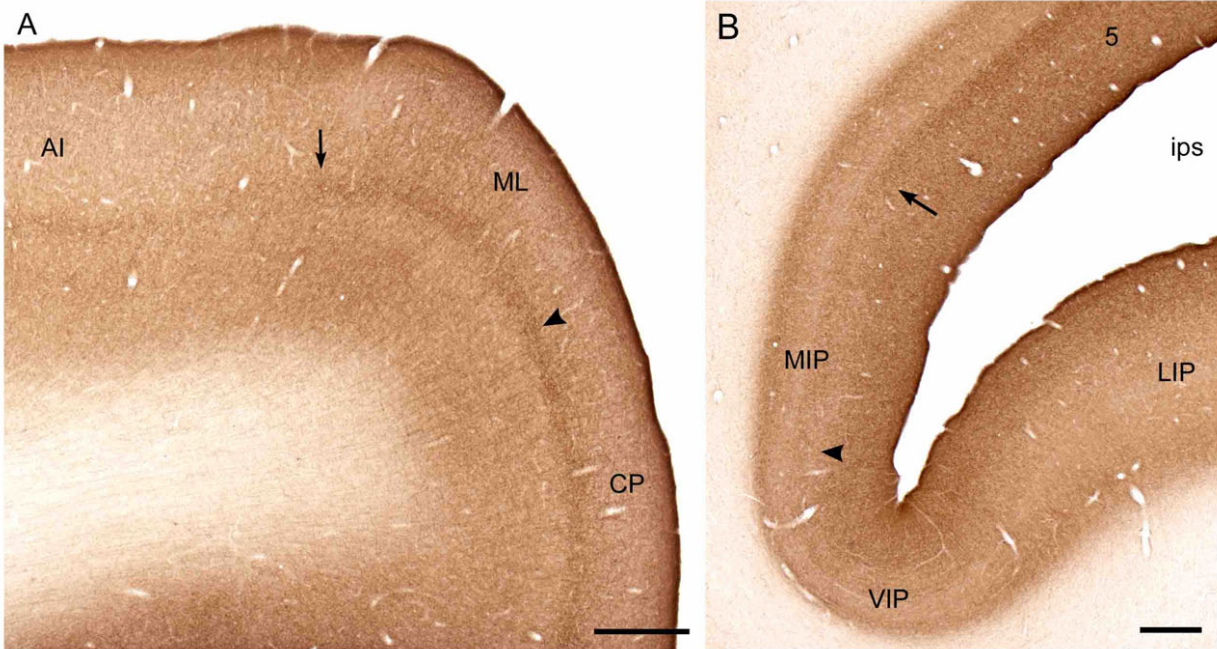
Figure 9. Brightfield photomicrographs illustrating shifts in CB1-IR axon density and laminar distribution at cytoarchitectonic boundaries. (A) CB1-IR axon density was greater in association auditory cortex (ML and CP) compared with primary auditory cortex (AI). Note the appearance of a dense band of CB1-IR axons in layer 4 at the border of AI–ML (arrow) that becomes even more distinct at the border of ML–CP (arrowhead). **(B)** In posterior parietal cortex, the boundary between area 5 and MIP was marked by a decrease in overall CB1-IR axon density and disappearance of a dense layer 4 band of CB1-IR axons (arrow). The transition between areas MIP and VIP was also marked by a slight decrease in overall CB1-IR axon density (arrowhead). Scale bars = 500 μm.

2.4.3 Other brain regions

In order to place the relative density of CB1-labeled structures in the neocortex in a broader context, we also evaluated a sampling of other telencephalic regions.

2.4.3.1 Hippocampal formation

The hippocampus contained overall a high density of CB1-IR axons that was similar to the density of labeled axons observed in the prefrontal cortex **(Table 2)**. A dense meshwork of immunolabeled beaded axons was present throughout all regions of the hippocampal formation **(Table 2; Fig. 10)**. In the CA1-CA3 fields, the pyramidal cell layer (PCL) demonstrated a high density of CB1-IR axons that surrounded unlabeled pyramidal cells **(Fig. 10A, B)**. The stratum lacunosum-moleculare (SLM) also exhibited a high density of CB1-IR axons **(Table 2; Fig. 10A, B)**, whereas the stratum oriens (SO) and stratum radiatum (SR) in CA1-CA3 of the hippocampus showed a slightly lower density of CB1-IR axons **(Table 2; Fig. 10A, B)**. The stratum lucidum (SL) of the CA3 region demonstrated the lowest density of CB1-IR axons **(Table 2; Fig. 10A, B)**. CB1-IR axons appeared to radiate through the SL in parallel with pyramidal cell dendrites, whereas in the SO, SR, and SLM regions, CB1-IR axons appeared to travel perpendicular to dendrites originating from pyramidal cells in the PCL **(Fig. 10B)**. The subicular regions demonstrated a high density of CB1-IR axons, although the density was somewhat lower than that present in the CA regions **(Fig. 10A)**.

The dentate gyrus (DG) was distinguished by an extremely low density of CB1 labeling in the granule cell layer (GL), which appeared as a prominent immunonegative strip at low magnification **(Fig. 10A)**. Similar to the PCL in the CA regions, granule cells were always immunonegative for CB1; however, in contrast to the PCL, CB1-IR axons appeared to radiate through the GL without surrounding unlabeled granule cells except at the border of the infragranular plexus **(Fig. 10C)**. The outer molecular layer (OML) contained a very high density of CB1-IR axons, whereas the molecular layer (MLdg) contained a slightly lower density of CB1-IR axons **(Fig. 10A, C)**. The polymorphic layer (PLdg) had a somewhat lower density of CB1-IR axons compared to MLdg **(Fig. 10C)**.
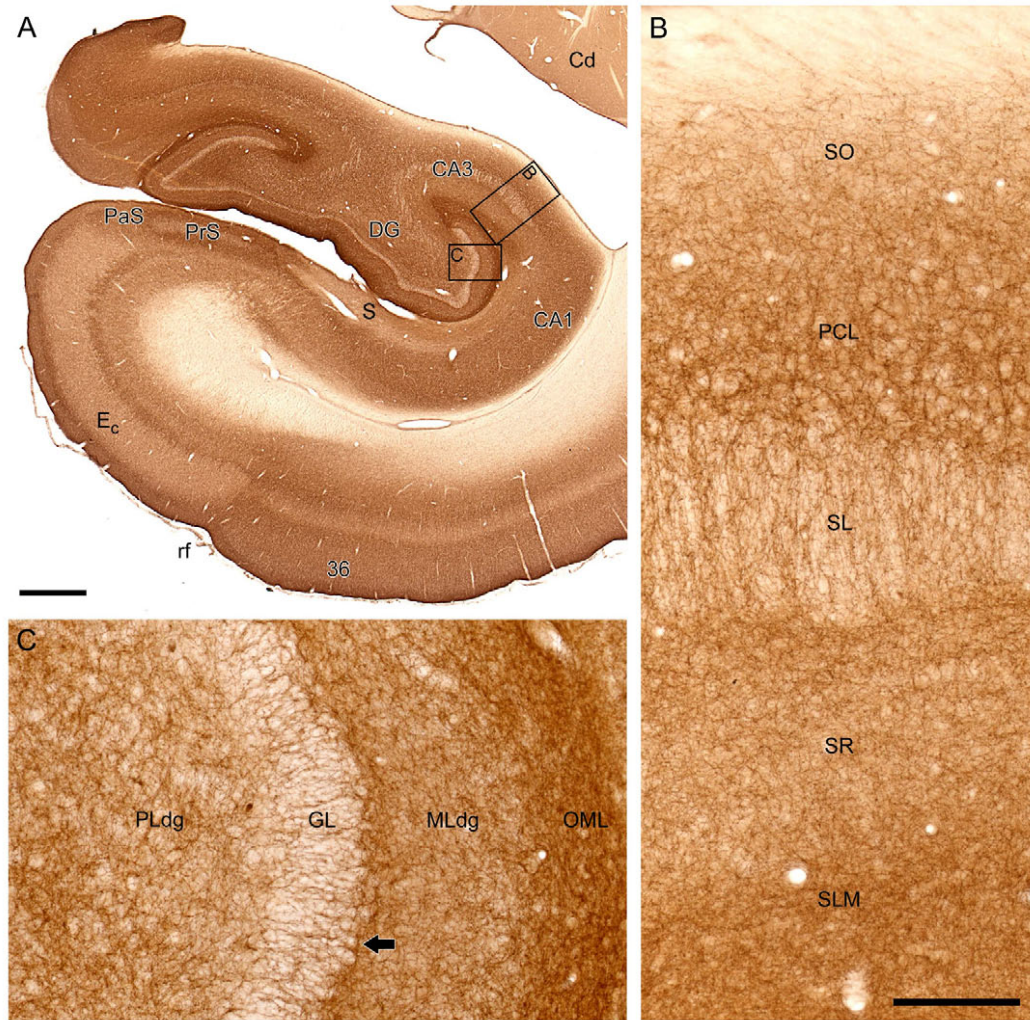
Figure 10. (A) Brightfield photomicrograph of a coronal section through macaque medial temporal lobe illustrating the distribution of CB1-IR axons in the hippocampal formation and adjacent entorhinal cortex (E$_C$). A dense meshwork of CB1-IR beaded axons was observed throughout the entire hippocampal formation. Note the distinct laminar pattern of CB1-IR axons in the E$_C$ compared with area 36. **(B)** In the CA regions of the hippocampus, the highest density of CB1-IR axons was located in the pyramidal cell layer (PCL) and stratum lacunosum-moleculare (SLM) and the lowest density of CB1-IR axons was located in the stratum oriens (SO) stratum lucidum (SL). **(C)** In the dentate gyrus, the highest density of CB1-IR axons was observed in the outer molecular layer (OML) and infragranular plexus (arrow). The granule cell layer (GL) contained the lowest density of CB1-IR axons, and granule neurons were always CB1 immunonegative. Scale bar = 1 mm in **A**; 150 μm in **B** (applies to **B, C**).

2.4.3.2 Amygdala

The pattern of CB1 immunolabeling clearly followed the boundaries of several nuclei in the monkey amygdala **(Figs. 5 and 11C)**. The most intense CB1 immunoreactivity was observed in the cortical-like basolateral complex **(Table 2; Figs. 5 and 11C)**, where a dense meshwork of varicose axons surrounded CB1-immunonegative cell bodies **(Fig. 11C)**. In the basolateral complex, the density of CB1-IR axons was greatest in the Bmc, Bi, ABmc and Lvi nuclei **(Fig. 5)**, whereas the more ventral and lateral ABpc, Bpc, Ldi, and Lv nuclei contained slightly fewer CB1-IR axons. The overall density of CB1-IR axons in the basolateral nuclei was similar to that observed in the prefrontal cortex **(Table 2)**. In the striatal-like central (Ce) and medial (Me) nuclei of the monkey amygdala, no CB1-IR axons were evident **(Table 2; Figs. 5 and 11C)**. In these nuclei, light labeling above that in the white matter was observed; however, this immunoreactivity was morphologically indistinct.

2.4.3.3 Basal ganglia, cerebellum, thalamus, and claustrum

As summarized in **Table 2**, CB1 immunoreactivity was present throughout the basal ganglia, but each nucleus exhibited a pattern of immunoreactivity that differed from other components of the basal ganglia and from regions of the neocortex. The caudate nucleus (Cd) and putamen (Pu) contained sparsely-distributed, thin, varicose, labeled processes, as well as a diffuse immunoreactivity that was morphologically indistinct **(Table 2; Figs. 5 and 11A, B)**. The globus pallidus (GP), which exhibited the most intense CB1 immunoreactivity of the brain regions examined **(Table 2; Figs. 5 and 11B)**, contained a very dense meshwork of thin, smooth, CB1-IR processes that encircled large unstained fascicles, cell bodies, and wooly fibers **(Fig. 11B)**. The substantia nigra pars reticulata (SNr) demonstrated CB1 immunoreactivity identical to that observed in the GP (data not shown). The thalamus (Th) appeared to be completely devoid of CB1-IR axons **(Fig. 5)**. The claustrum (Cl) exhibited a high density of CB1-IR highly varicose, axonal processes **(Table 2)**, similar to those present in the adjacent insular cortex **(Fig. 11A)**. As in the neocortex, axons in the Cl were found to surround immunonegative cell bodies.

In the cerebellum, most lobules contained a high intensity of CB1 immunoreactivity with a distinctive laminar pattern **(Fig. 12)**. The intensity of CB1 immunoreactivity was greatest in the molecular layer and lowest in the granular layer **(Table 2; Fig. 12)**. Intense CB1

immunoreactivity coated the basilar portion of Purkinje cell bodies in a triangular cap-like fashion reminiscent of the pinceau synapses furnished by basket interneurons **(Fig. 12B)**. However, Purkinje cell bodies and dendrites were always CB1 immunonegative **(Fig. 12B)**. Although this pattern of CB1 immunoreactivity was present in most lobules, lobule X was notable for containing a very low level of CB1 immunoreactivity in the molecular layer **(Fig. 13)**.
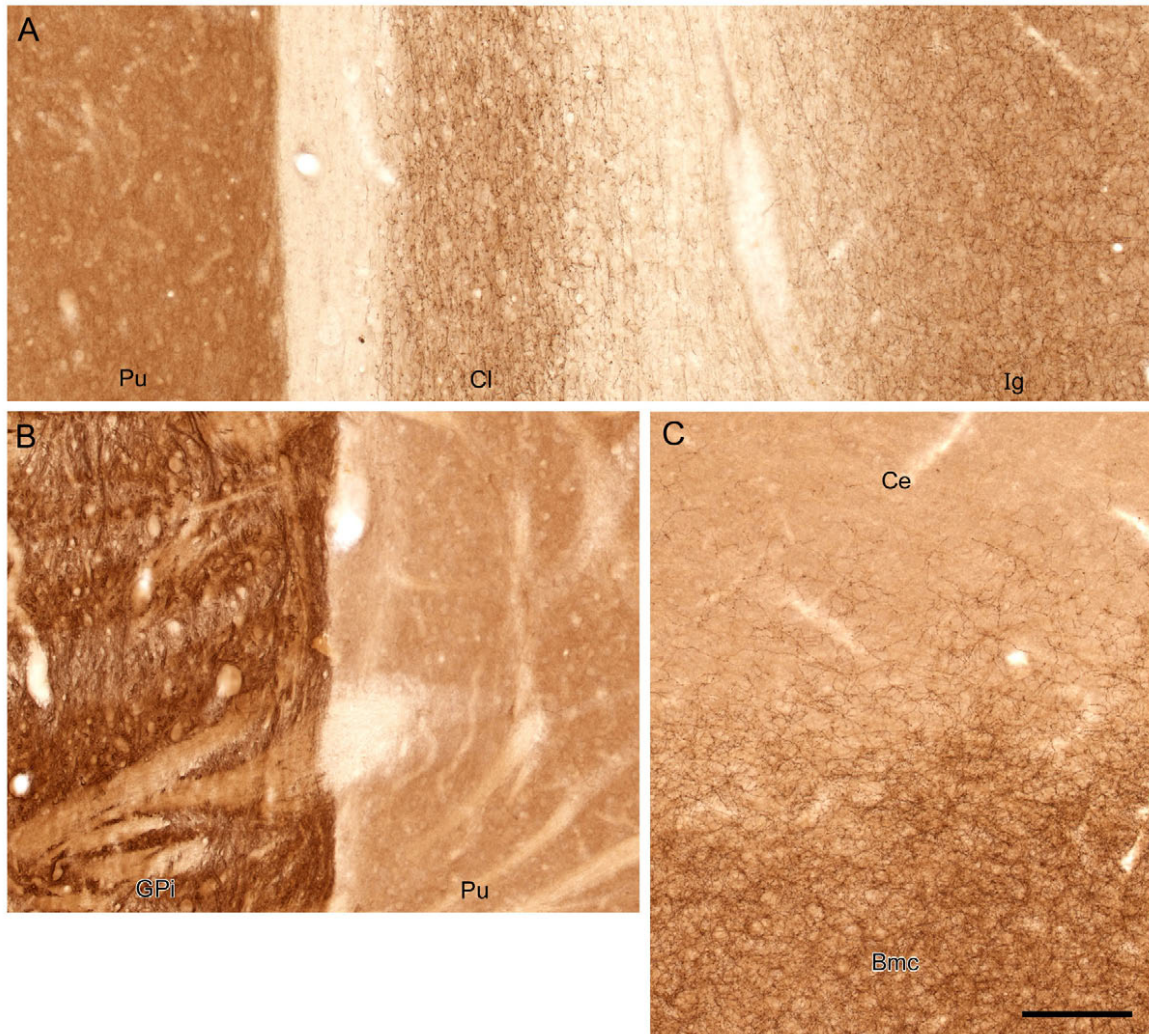
Figure 11. Higher magnification photomicrographs of boxed regions in Figure 5 illustrating different patterns of CB1 immunoreactivity in subcortical structures. (A, B) Immunoreactivity in the putamen (Pu) was enhanced pericellularly with some evidence of sparsely distributed, thin, varicose processes, but most immunoreactivity was morphologically indistinct. Immunoreactivity in the claustrum (Cl) was localized to axon processes and boutons, similar to that found in the adjacent granular insular cortex (Ig). **(B)** The globus pallidus (GP) contained a very dense meshwork of thin smooth CB1-IR processes that appeared to encircle unstained compartments such as cell bodies and wooly fibers. **(C)** The basal and lateral nuclei of the amygdala (Bmc illustrated) contained a very dense plexus of thin varicose axons that surrounded unlabeled cell bodies. In contrast, the central nucleus (Ce) of the amygdala contained few CB1-IR axons. Scale bar = 150 μm in **B** (applies to **A, B, C**)

52
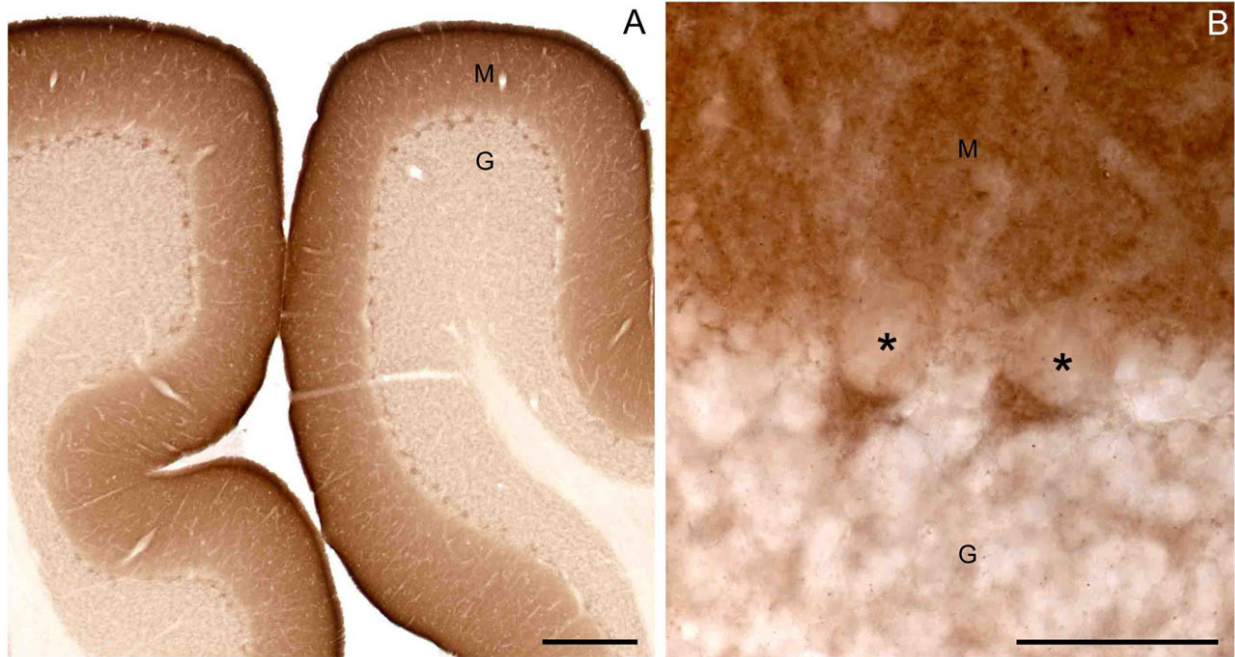
Figure 12. CB1 immunoreactivity in the monkey cerebellar cortex. (A) Low-power brightfield photomicrograph demonstrating intense CB1 immunoreactivity in the molecular layer (M) and lower CB1 immunoreactivity in the granular layer (G) of the cerebellum. **(B)** High-power brightfield photomicrograph illustrating CB1 immunoreactivity in the molecular, Purkinje, and granule cell layers of the cerebellum. The somata and dendrites of Purkinje cells were always CB1 immunonegative (asterisks). Note the dense triangular, pinceau synapse-like immunolabeling surrounding the basal portion of Purkinje cells. Scale bars = 300 μm in **A**; 50 μm in **B**.
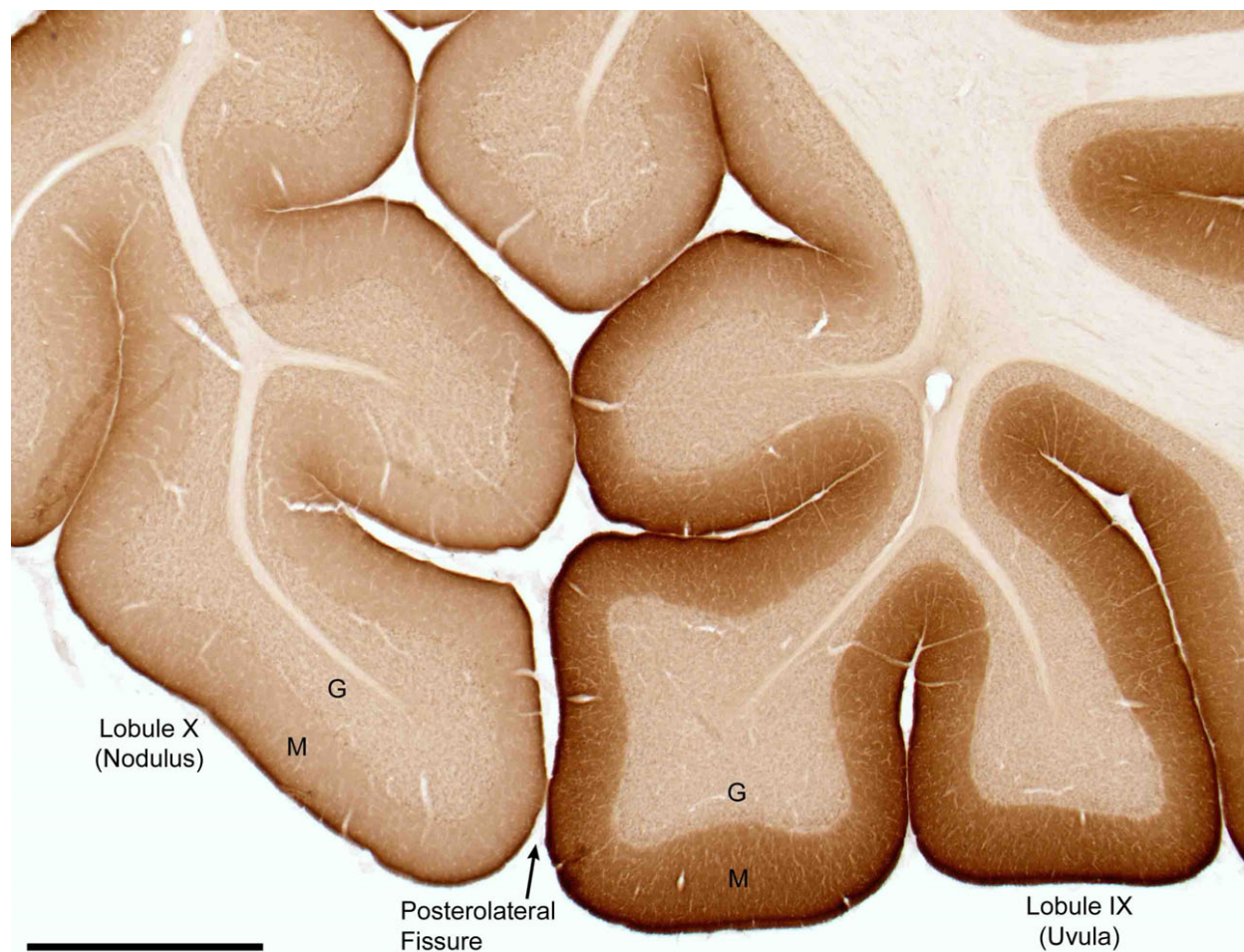
Figure 13. Low-power brightfield photomicrograph illustrating CB1 immunoreactivity in the nodulus (lobule X) and uvula (lobule IX) of the cerebellum. The intensity of CB1 immunoreactivity was very low in the molecular layer (M) of lobule X and increased caudally in lobule IX. Lobular differences in the granular layer (G) were much less marked. Scale bar = 1 mm.

2.4.4 Comparison to human neocortex

The distribution of CB1-IR axons in the human prefrontal and primary visual cortices was very similar to that observed in homologous regions of the monkey neocortex with a few exceptions. As in the monkey, human prefrontal area 46 exhibited a much higher density of CB1-IR axons than primary visual cortex area 17 **(Fig. 14)**. In the human prefrontal cortex **(Fig. 14A)**, layer 5 contained the lowest density of CB1-IR axons, layers 2-3 contained a moderate density of CB1-IR axons, and layer 4 contained the highest density of CB1-IR axons, similar to that observed in the monkey. However, in contrast to the monkey, the density of CB1-IR in layer 6 did not appear to be greater than in layer 5. In human area 17 **(Fig. 14B)**, the laminar distribution of CB1-IR axons was identical to the monkey. However, layers 1-3 contained a greater density of CB1-IR axons and layer 4 appeared to contain slightly more CB1-IR radial axons, whereas layers 5-6 exhibited a lower density of CB1-IR axons than in the monkey **(Fig. 14B)**. Finally, the morphology of CB1-IR axons in the human neocortex differed slightly from that observed in the monkey. In the human neocortex **(Fig. 15C)**, the intervaricose segments of CB1-IR axons were less distinct and boutons appeared to be larger and swollen compared to those in the perfused monkey neocortex **(Fig. 15A)**. These morphological differences appeared to reflect a postmortem effect. In unperfused monkey tissue with different postmortem delays before fixation, the intervaricose segments of CB1-IR axons became less distinct and boutons became more swollen with longer delays **(Fig. 15B)**.
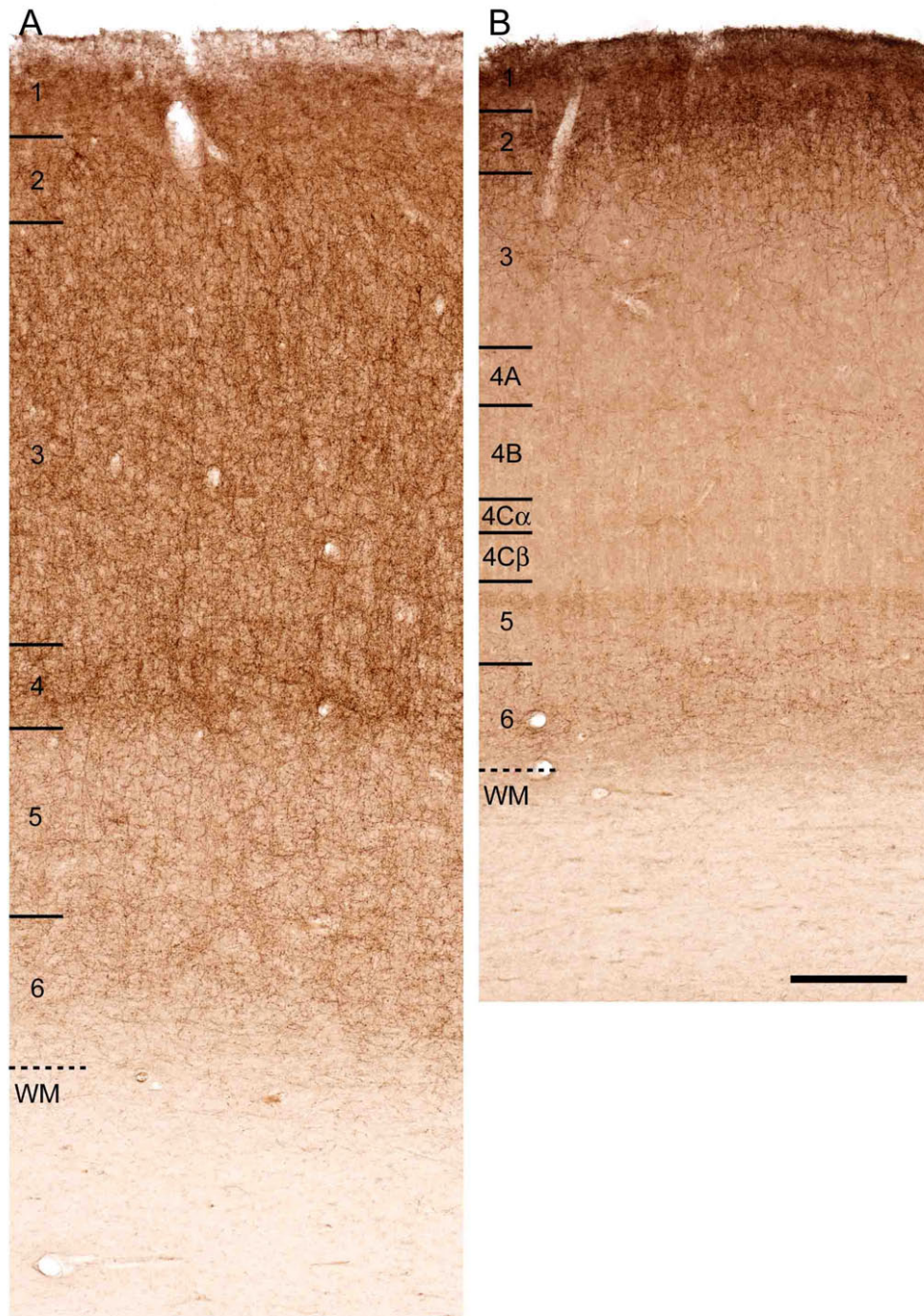
Figure 14. Brightfield photomicrographs demonstrating CB1 immunoreactivity in human prefrontal cortex area 46 (A) and primary visual cortex area 17 (B). The differences in relative density and laminar distribution between these regions were quite similar to those between the homologous areas in monkeys. Scale bar = 300 μm in **B** (applies to **A, B**).
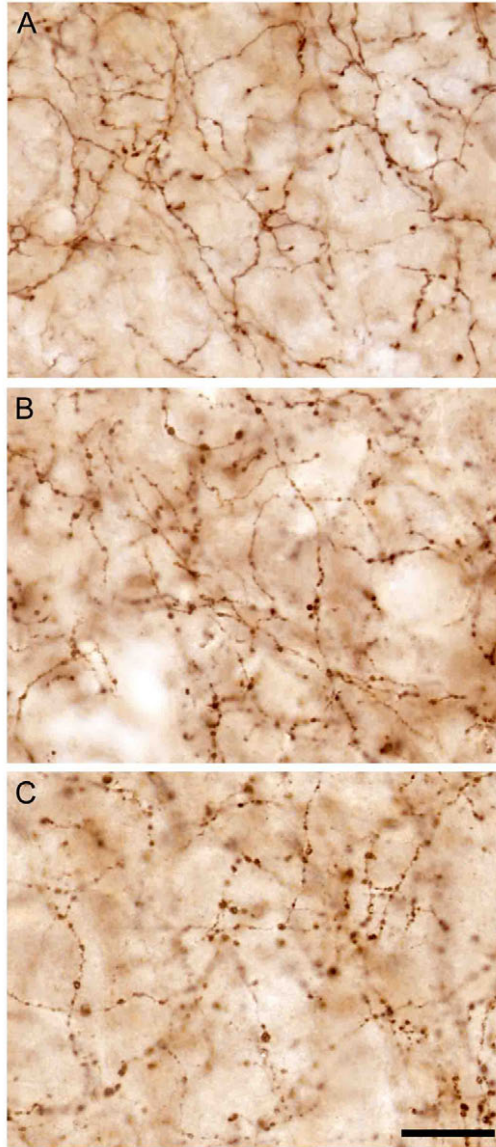
Figure 15. High-power, brightfield photomicrographs of CB1-IR axons in layer 5 of monkey (A, B) and human (C) prefrontal cortex area 46 demonstrating the effect of PMI on axon morphology. (A) In a perfused monkey with no PMI, CB1-IR boutons are relatively small, and the axons have distinct intervaricose axon segments. **(B)** In a nonperfused monkey after a 24-h PMI, boutons appear larger and intervaricose axon segments less well defined. **(C)** In a 33-year-old male human subject with a PMI of 8 h, boutons appear enlarged and intervaricose axon segments are less distinct, similar to observations in the 24-h PMI monkey. Scale bar = 20 µm in **C** (applies to **A, B, C**).

2.4.5 Electron microscopy

Electron microscopy studies were performed in layer 4 of monkey area 46 in order to assess the cellular distribution of the CB1 receptor **(Fig. 3A)**. CB1 immunoreactivity was found in axon terminals forming symmetric synapses (Gray's type II) **(Fig. 16A)**. Asymmetric synapses (Gray's type I), dendrites, and dendritic spines did not appear to be immunoreactive for the CB1 receptor **(Fig. 16A)**. When CB1 immunoreactivity was observed in cell bodies, they had the characteristic features of GABA neurons such as invaginated nuclei. The immunoperoxidase reaction product in cell somas was associated with the Golgi apparatus and endoplasmic reticulum, but was not found near the plasma membrane **(Fig. 16B)**.
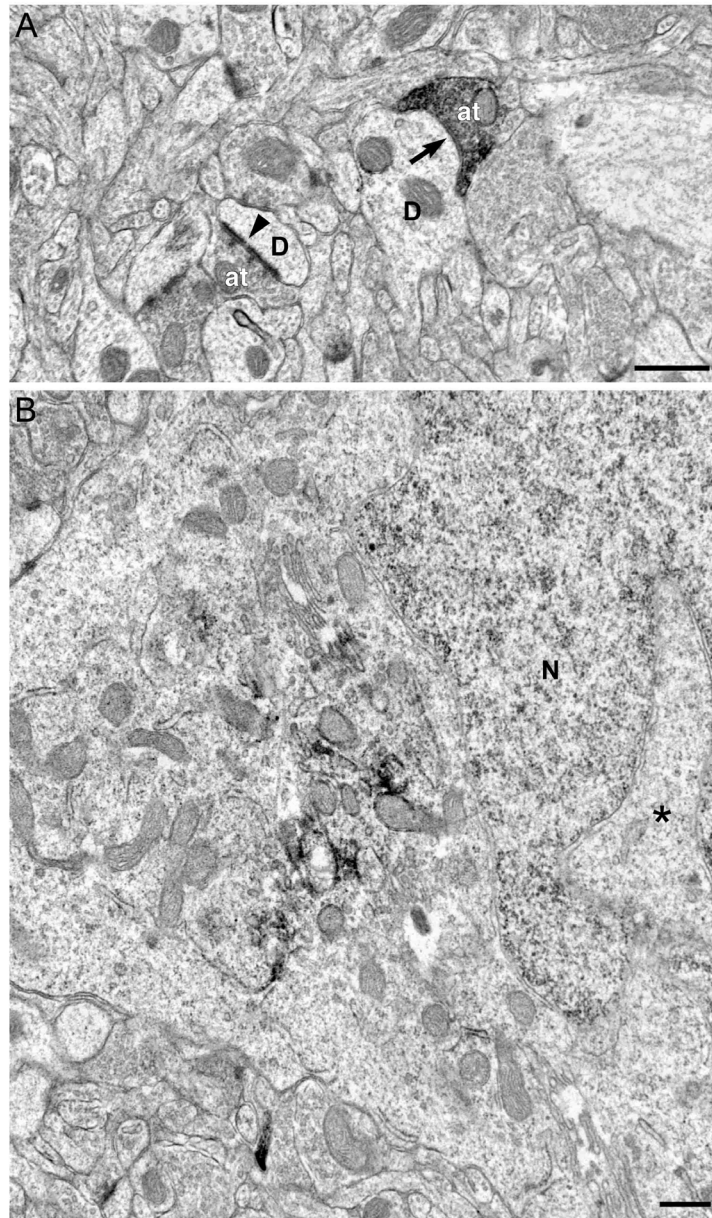
Figure 16. Electron micrographs demonstrating CB1 immunoperoxidase labeling in area 46 of monkey prefrontal cortex. (A) CB1 immunoreactivity in an axon terminal (at) forming a symmetric synapse (arrow) onto an unlabeled dendrite (D). Terminals forming asymmetric synapses (arrowhead) were always CB1 immunonegative. **(B)** Low-power electron micrograph demonstrating CB1 labeling in the cell body of a putative GABA interneuron as evidenced by an invaginated (asterisk) nucleus (N). Reaction product was associated with the Golgi apparatus and rough endoplasmic reticulum but not found near the plasma membrane. Scale bars = 500 nm.

2.5   DISCUSSION

The results of this study demonstrate that 1) the distribution of CB1-IR axons is heterogeneous across neocortical regions of the macaque monkey with regions associated with higher cognitive functions, such as the prefrontal cortex, containing higher densities of CB1-IR axons than primary motor and sensory cortices; 2) different neocortical regions exhibit distinctive laminar distributions of CB1-IR axons, which precisely mark the cytoarchitectonic boundaries between many regions; 3) the density and distribution of CB1-IR axons also differ substantially across other regions of the primate brain; 4) the regional and laminar distributions of CB1-IR axons in the human neocortex are quite similar to those in monkey, although the morphology of labeled axons is altered by postmortem delay and; 5) in the monkey neocortex CB1 immunoreactivity is primarily contained in cells and axon terminals that have the morphologic features characteristic of GABA neurons.

2.5.1   Methodological considerations

Several lines of evidence indicate that the antibodies used in this study are selective for the central CB1 receptor. First, three antibodies raised against different portions of the CB1 receptor produced identical patterns of immunoreactivity. Second, preadsorption with the cognate peptides eliminated specific immunoreactivity. Third, previous studies confirmed the specificity of the anti-CB1-CT antibody by demonstrating the elimination of immunoreactivity in CB1 knock-out mice, the identification of bands of appropriate molecular weight in Western blot analysis, and the labeling of cultured cells transfected with the CB1 receptor (Hajos et al., 2000b; Katona et al., 2001).

Previous studies employing immunocytochemistry in both rat (Tsou et al., 1998) and monkey (Ong and Mackie, 1999; Lu et al., 1999) using antibodies raised against the first 77 N-terminus amino acids of the CB1 receptor reported a significantly lower density and less distinct laminar pattern of axon labeling, and a much greater density of labeled cells including

interneurons and pyramidal neurons. These differences in patterns of immunoreactivity could reflect the phosphorylation state of the C-terminus of the CB1 receptor, which mediates CB1 receptor internalization (Hsieh et al., 1999). As suggested by Egertová and Elphick (2000), the last 13 amino acids of the CB1 receptor contain six sites that, when phosphorylated, may render the CB1 receptor nonimmunoreactive to antibodies directed against the C-terminus. Therefore, internalized receptors in cell bodies may not be recognized by C-terminus antibodies. However, we observed immunoreactivity within cell bodies, including labeling associated with cytoplasmic organelles, as has been reported in rodents using the same C-terminus antibodies (Hajos et al., 2000b; Katona et al., 2001; Bodor et al., 2005). Furthermore, in the present study we observed identical patterns of immunoreactivity with both C-terminus and N-terminus antibodies. Together, these data indicate that the C-terminus antibodies used in this study recognize CB1 receptors whether they are inserted in the plasma membrane or internalized.

Some studies suggest that CB1 receptors might be present presynaptically in pyramidal cell axon terminals where they could affect glutamate release. For instance, low levels of CB1 mRNA have been observed in pyramidal neurons (Marsicano and Lutz, 1999) and the application of CB1 agonists has been reported to reduce the amplitude of excitatory postsynaptic currents (Auclair et al., 2000; Hajos et al., 2001). These findings could reflect alternative splicing of the N-terminus CB1 receptor to form a variant of the CB1 receptor ($CB1_A$) (Shire et al., 1995; Egertová and Elphick, 2000). In the proposed $CB1_A$ splice variant, the first 61 amino acids of the CB1 receptor are replaced by 28 amino acids that are unrelated to the full CB1 receptor. It could be argued that it is the $CB1_A$ splice variant that is expressed by pyramidal neurons; however, the C-terminus antibodies used in this study would recognize both isoforms of the CB1 receptor, yet only inhibitory neurons, axons, and terminals were found to contain CB1 immunoreactivity. Alternatively, a yet unidentified cannabinoid receptor (or receptors) might be present in glutamatergic neurons (Begg et al., 2005). This hypothesis is supported by findings that the ability of WIN 55,212-2 (a CB1 receptor agonist) to block inhibitory postsynaptic currents is abolished in CB1 knock-out mice, whereas its ability to prevent excitatory postsynaptic currents persists (Hajos et al., 2001). In addition, WIN 55,212-2 binds to tissue of CB1 knock-out mice, but with lower affinity than in wild type mice (Breivogel et al., 2001).

2.5.2   Regional and laminar distributions of CB1-containing axons

CB1-IR axons were present throughout the monkey and human neocortex, but showed marked regional variations in overall densities and laminar distributions. For example, the overall density of CB1-IR axons was much higher in association areas, such as the prefrontal cortex, than in primary sensory and primary motor regions. The distribution of CB1 immunoreactivity across monkey neocortical regions was broadly similar to that observed in the rat with several C-terminus antibodies (Egertová and Elphick, 2000; Hajos et al., 2000b; Katona et al., 2001; Bodor et al., 2005) and to the distribution of CB1 receptor binding sites (Herkenham et al., 1991). However, some species differences in the laminar distribution of CB1-IR axons are worth noting. For instance, Egertová and Elphick (2000) reported that CB1-IR axons were most densely - localized in layers 2-3 and 6, and least dense in layer 4, of the rat frontal and cingulate cortices, whereas in the monkey layer 4 contained the highest density of CB1-IR axons in these regions. Furthermore, the dense band of CB1-IR axons in layer 5A, bordered by sparse axon labeling in layers 4 and 5B, in the rat somatosensory cortex (Bodor et al., 2005) differs from the relatively similar density of axons across layers 2-3 and 5-6 and sparse axonal labeling in layer 4 in the monkey primary somatosensory cortex. In contrast to the differences observed in the laminar distribution of CB-IR axons in the monkey and rat, the laminar distribution of CB1-IR axons across homologous regions of the monkey and human is nearly identical. Furthermore, the laminar distribution of CB1 receptor binding sites in the human revealed by autoradiography (Glass et al., 1997) is quite similar to that of CB1-IR axons observed here.

The various laminar distributions of CB1-IR axons across the monkey neocortex raise the question of whether some CB1-IR axons could arise from extrinsic sources. Although the band of CB1-IR axons in layer 4 of some regions suggests a thalamic source for these axons, the absence of labeling in terminals forming asymmetric synapses (this study; Katona et al., 1999; Hajos et al., 2000b; Katona et al., 2001; Bodor et al., 2005) and the complete absence of CB1 immunoreactivity in the thalamus excludes this source. In contrast, the presence of CB1 immunoreactivity in cell bodies and terminals with the morphological features of GABA neurons suggests that the most likely source of neocortical CB1-IR axons is intrinsic inhibitory local circuit interneurons. This idea is supported by a recent study demonstrating that the axons of intracellularly-labeled CB1-IR cells in layers 2-3 of the mouse neocortex arborized extensively

within layers 2-3, but also projected into layers 4-6 (Galarreta et al., 2004). Furthermore, recent evidence suggests that neocortical neurons containing CB1 receptors belong to the subpopulation of large basket GABA neurons that contain the neuropeptide CCK (Bodor et al., 2005). Indeed, experiments in the rodent neocortex revealed that nearly all neurons expressing high levels of CB1 mRNA also express CCK mRNA (Marsicano and Lutz, 1999) and that inhibitory terminals containing CB1 immunoreactivity also contain CCK immunoreactivity (Bodor et al., 2005). Furthermore, both the laminar pattern of CB1-IR neurons and axons and the perisomatic arrays formed by CB1-IR processes observed in this study directly match the findings of CCK-IR structures in monkey neocortex (Oeth and Lewis, 1990; Oeth and Lewis, 1993).

2.5.3   Functional implications

In the rodent, activation of CB1 receptors inhibits the release of GABA from presynaptic terminals and reduces $GABA_A$ receptor-mediated inhibitory postsynaptic currents in pyramidal neurons in the neocortex (Trettel et al., 2004; Galarreta et al., 2004; Bodor et al., 2005). Furthermore, the binding of endocannabinoids to CB1 receptors *in vitro* mediates depolarization suppression of inhibition (DSI) in the rodent neocortex (Trettel et al., 2004; Bodor et al., 2005). In this phenomenon, repetitive firing of pyramidal neurons produces elevated intracellular calcium levels, which initiates the synthesis and retrograde release of endocannabinoids. The released endocannabinoids bind to presynaptic CB1 receptors located on CCK terminals resulting in the reduction of proximal inhibitory input to that same pyramidal neuron (reviewed in Wilson and Nicoll, 2002). Thus, DSI in the neocortex is a mechanism by which pyramidal neurons can self-regulate their perisomatic inhibitory input.

These data suggest that CB1 receptors play an important role in regulating network activity patterns by controlling proximal inhibitory input to pyramidal neurons during prolonged firing. Synchronous rhythmic activity appears to arise from the coordinated firing of electrically-coupled interneurons belonging to the same population which then entrain the spike timing of large cell ensembles (reviewed in Connors and Long, 2004). Although fast-spiking, parvalbumin-containing neurons are the major cell type necessary for rhythmically entraining pyramidal cells to fire in the gamma range, CB1/CCK basket neurons may be necessary for fine tuning network oscillations (Freund, 2003). Indeed, in the rat hippocampus CB1 agonists

significantly reduce the amplitude of gamma band oscillations suggesting that the activation of CB1 receptors disinhibit pyramidal cells and prevent them from firing in synch (Hajos et al., 2000b).

These functional data in rodents, in concert with the high density of CB1-IR axons in the prefrontal cortex of monkeys and humans observed in this study, suggest that the endocannabinoid system may modulate cognitive functions, such as working memory. Indeed, in the human prefrontal cortex gamma band power increases directly and in proportion to working memory load (Howard et al., 2003), and the systemic administration of cannabinoids disrupts the ability to perform working memory tasks in both humans and animals (Winsauer et al., 1999; Schneider and Koch, 2003; D'Souza et al., 2004). This disruption in cognitive abilities following cannabis use might be due, at least in part, to decreased GABA transmission in the prefrontal cortex (Pistis et al., 2002), which is critical for performance of working memory tasks (Sawaguchi et al., 1988; Rao et al., 2000). Interestingly, the working memory deficits commonly observed in individuals with schizophrenia (Weinberger et al., 1986; Callicott et al., 2003) are associated with both reduced gamma band power and deficient perisomatic input to pyramidal neurons from parvalbumin-containing GABA neurons (Lewis et al., 2005). Thus, activation of CB1 receptors through the use of exogenous cannabinoids could result in an additional deficit in perisomatic GABA input to pyramidal neurons in individuals with schizophrenia by inhibiting GABA release from CCK basket interneurons. Future studies investigating the physiological role of CB1 receptors in the monkey prefrontal cortex, and of the integrity of the CB1 in the prefrontal cortex of individuals with schizophrenia, may provide critical insight into the role of exogenous cannabinoids and CB1 receptors in the cognitive deficits associated with schizophrenia.

3.0   SYNAPTIC TARTGETS OF CB1- AND CHOLECYSTOKININ-CONTAINING AXON TERMINALS IN MACAQUE MONKEY PREFRONTAL CORTEX

3.1   ABSTRACT

Exposure to cannabis impairs certain cognitive functions reliant on the circuitry of the dorsolateral prefrontal cortex (DLPFC), including working memory, and is a risk factor for the development of schizophrenia. The actions of cannabis are mediated via the brain cannabinoid 1 (CB1) receptor, which in rodents is heavily localized to the axon terminals of the subpopulation of GABA basket neurons that contain cholecystokinin (CCK). However, neither the relationship of the CB1 receptor to CCK-containing interneurons, nor the postsynaptic targets of CB1 and CCK axon terminals, have been examined in primate DLPFC, a region that contains high levels of both CB1- and CCK-immunoreactive (IR) axons. Therefore, we compared the synaptic type and postsynaptic targets of CB1- and CCK-IR axon terminals in macaque monkey DLPFC. At the light microscopic level, CB1- and CCK-IR axons exhibited a similar laminar distribution, with the greatest density present in layer 4. Dual-label experiments showed that CB1 and CCK immunoreactivities were extensively, but not completely, colocalized. At the electron microscopic level, all synapses formed by CB1-IR axon terminals were symmetric, whereas CCK-labeled axon terminals formed both symmetric (88%) and asymmetric (12%) synapses. The primary postsynaptic target of both CB1- and CCK-IR axon terminals forming symmetric synapses was dendritic shafts (81-88%). The synaptic targets of CB1- and CCK-IR axon terminals were similar in layer 4, but differed in layers 2-superficial 3, where 11% of CCK-IR terminals, but no CB1-IR terminals formed synaptic contacts with cell bodies. Thus, in the monkey DLPFC, CB1 and CCK are colocalized in a subset of GABA neurons that principally target dendrites. These findings provide an anatomical substrate for the impaired function of the DLPFC associated with cannabis use.

3.2   INTRODUCTION

In both humans and animals, exposure to marijuana and other forms of cannabis produces impairments in complex cognitive functions including those subserved by the dorsolateral prefrontal cortex (DLPFC), such as working memory (Winsauer et al., 1999; Schneider and Koch, 2003; D'Souza et al., 2004). In addition, cannabis use during adolescence increases the risk of developing schizophrenia (Henquet et al., 2005a; Fergusson et al., 2006), a disorder characterized by both dysfunction of the DLPFC and working memory impairments (Lewis et al., 2005). The effects of cannabis are mediated by the cannabinoid CB1 receptor, the principal cannabinoid receptor in the brain (Freund et al., 2003), which in the primate neocortex is most heavily expressed in the DLPFC (Eggan and Lewis, 2007).

In primates, working memory function depends critically on the synaptic connectivity and patterns of activity within the DLPFC (reviewed in Goldman-Rakic, 1995; Fuster, 2001). In particular, networks of interconnected GABA interneurons are essential for the synchronization of large cell ensembles of neurons (Connors and Long, 2004) and the pacing of oscillatory patterns required for working memory (Howard et al., 2003). Consistent with these findings, working memory performance in monkeys is disrupted by $GABA_A$ receptor antagonists injected into the DLPFC (Sawaguchi et al., 1988; Rao et al., 2000).

In the rodent neocortex, the CB1 receptor is heavily expressed by, and localized in the terminals of, the subtype of GABA basket interneurons that contain the neuropeptide cholecystokinin (CCK), but is not present in GABA basket neurons that contain the calcium binding protein parvalbumin (PV) (Marsicano and Lutz, 1999; Bodor et al., 2005). In line with this anatomical localization, activation of CB1 receptors by either exogenous or endogenous cannabinoids inhibits the release of GABA from CCK terminals and strongly suppresses $GABA_A$ receptor-mediated inhibitory postsynaptic currents in pyramidal neurons (Trettel et al., 2004; Galarreta et al., 2004; Bodor et al., 2005). Furthermore, CB1/CCK-containing neurons are electrically coupled in the neocortex (Galarreta et al., 2004) and in the hippocampus entrain oscillatory patterns of activity which are disrupted following administration of CB1 agonists (Klausberger et al., 2005; Robbe et al., 2006).

In concert, these data suggest that CB1 receptors may play an important role in regulating network activity in the primate DLPFC by controlling proximal inhibitory input to pyramidal

neurons; consequently, CB1 receptor alterations in the DLPFC in schizophrenia might contribute to the working memory impairments in the illness. However, the relationship between, and synaptic targets of, CB1 and CCK axon terminals has not been examined in the primate DLPFC. Consequently, in this study we used immunocytochemistry and light and electron microscopy to 1) determine whether CB1 and CCK are co-localized in cell bodies and axon terminals, 2) identify the type(s) of synapses formed by, and the synaptic targets of, CB1- and CCK-immunoreactive (IR) axon terminals, and 3) determine whether these targets differ as a function of cortical layer in monkey DLPFC area 46.

3.3   MATERIALS AND METHODS

3.3.1   Light Microscopy

3.3.1.1 Animals and Tissue Preparation

For light microscopy studies, four adult, male long-tailed macaque monkeys (*Macaca fascicularis*) were utilized. Monkeys were deeply anesthetized with 25 mg/kg ketamine hydrochloride and 30 mg/kg sodium pentobarbital and then perfused transcardially with ice-cold 1% paraformaldehyde in 0.1 M phosphate buffer (PB; pH 7.4) followed by 4% paraformaldehyde in PB, as previously described (Oeth and Lewis, 1993). Brains were immediately removed and coronal blocks (5-6 mm-thick) were postfixed in phosphate-buffered 4% paraformaldehyde at 4°C for 6 hours. Tissue blocks were subsequently cryoprotected and then stored at -30°C as previously described (Oeth and Lewis, 1993). We have previously shown that immunoreactivity for a number of antigens are unaffected by this storage procedure (Cruz et al., 2003). Coronal blocks containing DLPFC area 46 from either the left or the right hemisphere were sectioned at 40 µm on a cryostat and every 10th section was stained for Nissl substance with thionin.

Housing and experimental procedures were conducted in accordance with guidelines set by the United States Department of Agriculture and the National Institutes of Health *Guide for the Care and Use of Laboratory Animals* and with approval of the University of Pittsburgh's

Institutional Animal Care and Use Committee. All efforts were made to minimize the number of animals used and their suffering.

3.3.1.2 Immunocytochemistry and dual label immunofluorescence

For standard single-label immunocytochemistry, free-floating coronal tissue sections were washed several times in 0.01 M phosphate-buffered saline (PBS; pH 7.4) and then incubated in blocking solution containing 3% Triton X-100, and 4.5% normal donkey sera (NDS) and normal human sera (NHuS; Jackson ImmunoResearch, West Grove, PA) in PBS for 30 min to reduce background. Tissue sections were then incubated in a PBS solution containing 0.3% Triton-X, 3% NDS and NHuS, 0.05% bovine serum albumin (BSA; Jackson), and either an affinity-purified polyclonal rabbit anti-CB1 antibody raised against the last 15 amino acid residues of the rat CB1 receptor (diluted 1:5000), an affinity-purified polyclonal guinea pig anti-CB1 antibody raised against the entire C-terminus of the rat CB1 receptor (diluted 1:4000; both CB1 antibodies were generously provided by Dr. Ken Mackie, Indiana University, Bloomington, IN), or a monoclonal mouse anti-CCK antibody raised against gastrin (diluted 1:4000; antibody #9303 provided by the CURE Digestive Diseases Research Center, Antibody/RIA Core, Los Angeles, CA, NIH Grant DK41301). Sections were subsequently washed in PBS and incubated in either a biotinylated donkey anti-rabbit or anti-mouse IgG secondary antibody (diluted 1:200; Jackson) solution containing 0.3% Triton-X and 3% NDS and NHuS in PBS for 1 hour. Sections were washed in PBS and then processed with the avidin-biotin-peroxidase method (Hsu et al., 1981) using the Vectastain Avidin-Biotin Elite Kit (Vector Laboratories, Burlingame, CA) and the immunoperoxidase reaction was visualized using 3,3'-diaminobenzidine (DAB; 0.005%; Sigma, St. Louis, MO). Sections were subsequently mounted on gel-coated slides, air dried, and immersed serially in osmium tetroxide (0.005%) and thiocarbohydrazide (0.5%) to stabilize the DAB reaction product (Lewis et al., 1986). All incubations and washes were performed on a shaker at room temperature (RT) except for the primary antibody incubation.

For dual-label immunofluorescence experiments, free floating coronal tissue sections were washed in PBS and then pretreated in a blocking solution containing 0.3% Triton X-100, 5% normal goat serum (NGS) and NHuS, 1% BSA, 0.1% glycine, and 0.1% lysine in PBS (used in all antibody solutions) at RT for 3 hours to reduce background. Sections were then incubated at 4°C for 48 hours in the same blocking solution containing the guinea pig anti-CB1 antibody

(diluted 1:3000) and either the monoclonal mouse anti-CCK antibody (diluted 1:2000) or a monoclonal mouse IgG1 antibody against PV (diluted 1:8000; Swant, Bellinzona, Switzerland). Sections were then washed in PBS and incubated for 24 hours in blocking solution containing an anti-guinea pig Alexa 633 secondary antibody to visualize the CB1 antibody and an anti-mouse Alexa 488 secondary antibody (both raised in goat; diluted 1:500; Invitrogen, Carlsbad, California) to visualize the CCK and PV antibodies. Sections were subsequently washed in PBS, mounted on gel-coated slides, and coverslipped with Vectashield (Vector).

Fluorescent images were collected on an Olympus BX51 microscope fitted with an Olympus DSU spinning disk confocal (Olympus America Inc., Melville, NY), a Hamamatsu C4742-98 CCD camera (Hamamatsu Corporation, Bridgewater, NJ), and a Ludl motorized XYZ stage (LEP Ltd., Hawthorne, NY). Data was captured using a 60X 1.4 NA plan apochromat objective or a 40X 1.3 plan fluorite objective and was deconvolved using Intelligent Imaging Innovations' constrained iterative algorithm in Slidebook 4.2 (Denver, CO). Images are projected images of 20-30 sequential confocal slices taken 0.22-0.5 µm apart.

3.3.2   Electron Microscopy

3.3.2.1 Animals and Tissue Preparation

For electron microscopy studies, three additional adult male long-tailed macaque monkeys (*M. fascicularis*) were perfused as described above except that the perfusate was room temperature 1% paraformaldehyde and 0.05% glutaraldehyde in 0.1 M PB followed by 4% paraformaldehyde and 0.2% glutaraldehyde in 0.1 M PB as previously reported (Melchitzky et al., 2005; Eggan and Lewis, 2007). Brains were immediately removed and coronal blocks (5-mm-thick) were immersed in phosphate buffered 4% paraformaldehyde at 4°C for 2 hours. Coronal tissue blocks containing DLPFC area 46 were washed several times in 0.1 M PB and sectioned at 50 µm on a vibrating microtome.

3.3.2.2 Immunocytochemistry

To improve antigenicity and reduce nonspecific immunoreactivity, free-floating tissue sections containing DLPFC area 46 were initially treated with 1% sodium borohydride in 0.1 M PB for 30 min, washed extensively in 0.1 M PB, and then incubated in a blocking solution containing

0.2% BSA, 0.04% Triton X-100, 3% NDS, and 3% NHuS in 0.01 M PBS for 30 min as previously described (Sesack et al., 1998; Eggan and Lewis, 2007). Sections from each animal were subsequently incubated overnight in blocking solution containing either the rabbit anti-CB1 (diluted 1:5000) or the monoclonal mouse anti-CCK antibody (diluted 1:2000 or 1:1500). On the following day, sections were rinsed in PBS and incubated for 1 h in blocking solution containing either a biotinylated anti-rabbit or anti-mouse IgG secondary antibody made in donkey (diluted 1:200; Jackson). Following rinses in PBS, sections were processed with the avidin-biotin-peroxidase method and visualized with DAB as described earlier, postfixed in 2% osmium tetroxide for 1 h and embedded in Epon 812 (EM bed 812; Electron Microscopy Sciences, Fort Washington, PA) as previously described (Sesack et al., 1995b; Melchitzky et al., 2005).

3.3.2.3 Sampling Regions and Procedures

For each animal and each primary antibody condition, separate trapezoid blocks from two tissue sections were cut from layers 2-superficial 3 (2-3s) and layer 4 in DLPFC area 46 **(Fig. 17A)**. Trapezoid blocks were sectioned on a Reichert ultramicrotome (Nussloch, Germany) at 80 nm and two to four ultrathin sections were serially collected on 200- or 400-mesh copper grids and counterstained with uranyl acetate and lead citrate. For each trapezoid block 1-2 grids, separated by at least 10 grids, were examined on a FEI Morgagni transmission microscope (Hillsboro, OR). One section per grid was arbitrarily chosen as the starting point for analysis and within each selected section all CB1- or CCK-labeled structures were captured and stored for later analysis. All labeled axon terminals were identified, photographed at X22,000, and classified according to their synaptic specialization and appositional or postsynaptic target.

3.3.2.4 Identification of Neuronal and Synaptic Elements

Neuronal elements encountered in electron micrographs were identified according to previous descriptions (Peters et al., 1991). Axon terminals were identified by the presence of small vesicles and often contained mitochondria. Axon terminals forming asymmetric synapses (Gray's type I) were distinguished by the widening and parallel spacing of apposed plasmalemmal surfaces and small round synaptic vesicles. In addition, asymmetric synapses were identified by the presence of a prominent postsynaptic density. In contrast, axon terminals forming symmetric synapses (Gray's type II) were identified by the presence of intercleft

70

filaments, pleomorphic small synaptic vesicles, and a thin postsynaptic density. The presence of a nucleus identified somata. Dendritic shafts were identified by the presence of postsynaptic specializations, mitochondria, microtubules, and neurofilaments. Dendritic spines were characterized by the absence of both organelles and microtubules.

3.3.3 Antibody Specificity

The specificity of the rabbit anti-CB1 antibody has been previously demonstrated by several lines of evidence including preadsorption experiments, Western blot analysis, and testing in tissue from CB1 knockout mice (see Eggan and Lewis, 2007). The specificity of the guinea pig anti-CB1 antibody has also been determined by testing in tissue from CB1 knockout mice (Ken Mackie, personal communication). The mouse monoclonal anti-CCK antibody was raised against gastrin, but recognizes CCK due to a homologous terminal pentapeptide shared by gastrin and CCK. Gastrin is not present in the neocortex (Rehfeld, 1978; Geola et al., 1981); thus, only CCK was detected in this study. The specificity of the anti-CCK antibody has been demonstrated by its high affinity for the CCK peptide (ID50 = 30-70 pM; Kovacs et al., 1989), by preadsorption experiments in monkey tissue (Oeth and Lewis, 1990), and by experiments in which an excess of antigen added to the incubation serum produced no labeling (Hefft and Jonas, 2005). The specificity of the PV antibody has been previously demonstrated (Celio et al., 1988) and has been used in multiple studies (Melchitzky et al., 1999; DeFelipe et al., 1999; Cruz et al., 2003).

3.3.4 Statistical Analyses

Individual 2x3 or 2x2 χ^2 analyses were performed to compare laminar differences in the relative proportions of postsynaptic targets of CB1- or CCK-IR axon terminals forming symmetric synapses or appositions. Individual 2x3 or 2x2 χ^2 analyses were also performed to compare the differences in the relative proportions of postsynaptic targets of CB1- and CCK-IR postsynaptic targets within layers.

3.3.5   Photography

The brightfield photomicrographs presented were obtained with a Zeiss Axiocam camera. Digital electron micrographs images were captured using an AMT XP-60 digital camera (Danvers, MA). Brightfield photomontages and digital electron micrographs were assembled, and the brightness and contrast were adjusted in Adobe Photoshop. Immunofluorescent images were obtained and assembled as described earlier.

3.4   RESULTS

3.4.1   General observations

CB1 immunoreactivity was localized to a small number of somata of non-pyramidal neurons that were most frequently present in layers 2-3s. A small number of CB1- immunoreactive (IR) non-pyramidal neurons were observed in layers deep 3 and 6. CB1-IR neurons had either a vertically oriented oval cell body or a large multipolar somal morphology **(Fig. 17D)**. CB1 immunoreactivity produced a distinctive laminar pattern of intensely labeled numerous axons that were thin and rich in varicosities. Layer 1 contained few CB1-IR axons, the density of CB1-IR axons increased across layers 2-3, layer 4 contained the highest density of CB1-IR axons and varicosities, and layer 6 contained a moderate density of CB1-IR axons. Layer 5 contained the lowest density of CB1-IR axons, which distinctly marked the borders with layers 4 and 6. Layers deep 3 and 5 were unique in that they contained distinct bundles or fascicles of radial immunoreactive axons **(Fig 17A)**. From layers deep 3 to 4 these fascicles were associated with putative pyramidal neuron apical dendrites then diverged and formed dense "baskets" around unlabeled cell bodies **(Fig. 17C)**. These perisomatic arrays of CB1-IR axons were also found surrounding unlabeled putative non-pyramidal cell bodies, based on their small size and round shape, and around CB1-IR neurons **(Fig. 17D)**.

The mouse anti-CCK antibody labeled non-pyramidal cell bodies, dendrites, and thin, highly varicose axons **(Fig. 17B, E, F)** as described previously (Oeth and Lewis, 1990; Oeth and

Lewis, 1993). The density of CCK-IR neurons was highest in layers 2-3s; however, scattered CCK-labeled neurons were observed across all cortical layers **(Fig. 17B)**. Consistent with previous reports (Oeth and Lewis, 1990; Oeth and Lewis, 1993; Kawaguchi and Kubota, 1997), many CCK-IR neurons were vertically-oriented, oval, large, and multipolar **(Fig. 17B, F)**. The laminar distribution of CCK-IR axons and varicosities exhibited a distinct laminar pattern very similar to that of CB1-IR axons and varicosities. The density of CCK-IR axons and varicosities was lowest in layer 1. In contrast, layers 2-3s contained a moderate density of CCK-IR axons and varicosities and layers 4 and 6 contained dense bands CCK-IR axons and varicosities. Layers 3 and 5 contained low densities of CCK-IR axons and varicosities and contained distinct radially traversing axons similar to that described for CB1-IR axons; however, these axons were less prominent and did not form fascicles **(Fig. 17B)**. Unlike CB1-IR axons, the intervaricose segments of CCK-IR axons were less distinct and CCK immunoreactivity was predominantly contained in axon varicosities **(Fig. 17E)**. However, similar to CB1-IR axons, CCK-IR axons were found to form perisomatic arrays around putative pyramidal **(Fig. 17E)** and non-pyramidal cell bodies.
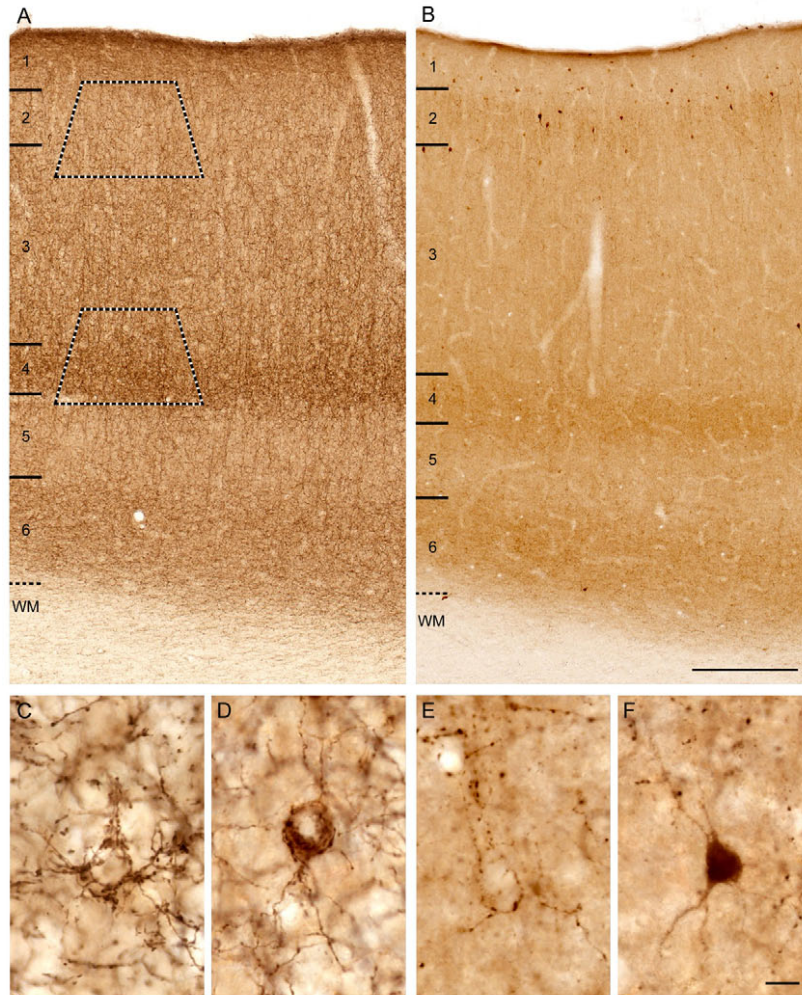
Figure 17. Brightfield photomicrographs of immunoreactivity produced by the guinea pig anti-CB1-CT and mouse anti-CCK antibodies in area 46 of monkey DLPFC. Both CB1 (**A, C, D**) and CCK (**B, E, F**) antibodies labeled numerous fibers that were thin and rich in varicosities distributed with similar laminar patterns (**A, B**). Both CB1- and CCK-labeled neurons were most frequently present in layers 2 and superficial 3 (**A, B**). CB1- and CCK-IR neurons were often large and multipolar in shape (**D, F**). Some CB1- and CCK-labeled axons formed "baskets" surrounding unlabeled cell bodies (**C, E**). In panels **A** and **B** numbers and hash marks to the left indicate the relative positions of the cortical layers, and the dashed lines denote the layer 6-white matter (WM) border. The trapezoids in panel **A** show the approximate laminar location of blocks examined for electron microscopy. Scale bars = 300 µm in **B** (applies to **A, B**) and 10 µm in **F** (applies to **D, E, F**).

3.4.2 Analysis of dual-labeled tissue

CB1 and CCK immunoreactivities were colocalized in many profiles in DLPFC area 46 **(Fig. 18)**. In layers 2-3s, most CB1-IR neurons were also CCK-IR **(Fig. 18A-C)**, but some CCK-IR neurons were CB1 immunonegative. In addition, there was a high degree of colocalization of CB1 and CCK immunoreactivity in axon varicosities **(Fig. 18A-C)**. CB1/CCK-IR axons frequently formed perisomatic baskets around unlabeled putative pyramidal and small, round putative non-pyramidal cell bodies that had the morphologic shape and appearance of pyramidal or nonpyramidal neurons (data not shown). Perisomatic appositions were also found surrounding CB1/CCK dual-labeled neurons **(Fig. 18)**.

In contrast, no colocalization was found for CB1 and PV immunoreactivity **(Fig. 19)**. All CB1-IR cells were PV immunonegative and all PV-IR cells were CB1 immunonegative **(Fig 19)**. Furthermore, axons and varicosities were always single-labeled for either CB1 or PV, even at the border of layers 3 and 4 where the density of both CB1- and PV-IR axons is highest in monkey area 46 **(Fig 19A-C)**. However, CB1- and PV-IR single-labeled axons formed baskets around the same unlabeled cell bodies.
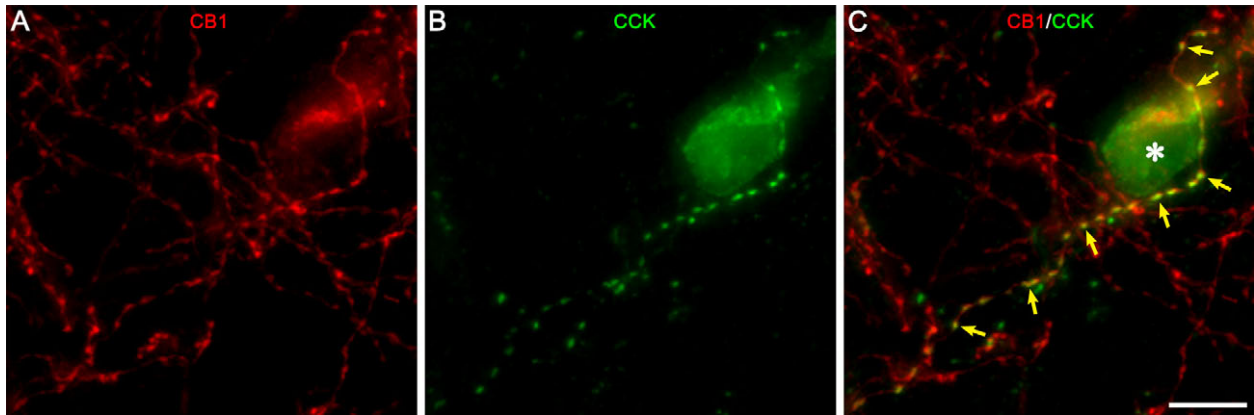
Figure 18. Fluorescent photomicrographs of CB1 and CCK immunoreactivity in area 46 of monkey DLPFC. (A) CB1-IR neuron and axons labeled with Alexa 633 (red). **(B)** CCK-IR neuron and axons labeled with Alexa 488 (green). **(C)** Overlay of panels **A** and **B** showing the colocalization (yellow) of CB1 and CCK in the same cell (asterisk) and in a subpopulation of axons and boutons (arrows). Note single-labeled axons and boutons for each protein are also present. Scale bar = 10 µm in **C** (applies to **A, B, C**).
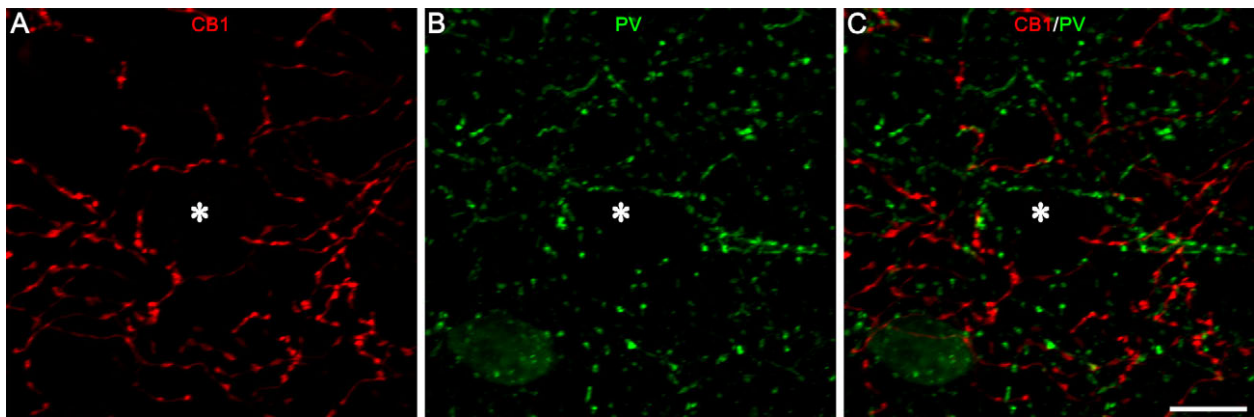
Figure 19. Fluorescent photomicrographs of CB1 and PV immunoreactivity in area 46 of monkey DLPFC. (A) CB1-IR neuron and axons labeled with Alexa 633 (red). **(B)** PV-IR neuron and axons labeled with Alexa 488 (green). **(C)** Overlay of panels **A** and **B** showing an absence of colocalization of CB1 and CCK immunoreactivity. Asterisk denotes an unlabeled pyramidal cell body receiving single-labeled CB1- and PV-IR perisomatic appositions. Scale bar = 10 µm in **C** (applies to **A, B, C**).

3.4.3 Synapses formed by and postsynaptic targets of CB1- or CCK-IR axon terminals

Of 111 CB1-IR axon terminals with an identifiable synaptic specialization, 100% formed classic symmetric synapses onto small and large unlabeled dendritic shafts (**Fig. 20A, D**), dendritic spines **(Fig. 20C)**, or somata. Some dendritic shafts that were contacted by CB1-IR axon terminals exhibited morphologic characteristics of interneuron dendrites, such as a varicose shape and a high density of synapses (McGuire et al., 1991; Smiley and Goldman-Rakic, 1993; Sesack et al., 1995a); however, most contacted dendritic shafts were cut in cross-section, precluding the identification of the origin of the neuron type (pyramidal versus nonpyramidal). In addition, a small number of CB1-IR axon terminals were found forming symmetric synapses onto CB1-IR dendrites **(Fig 20B)**. Occasionally, CB1-IR axons were observed forming basket-like appositions around unlabeled cell bodies **(Fig. 20E)**.

Of 95 CCK-IR axon terminals with identifiable synaptic specializations, 88% (n = 84) formed symmetric synapses onto large and small unlabeled dendritic shafts **(Fig. 21A, B)**, dendritic spines **(Fig. 21C)**, or somata **(Fig. 21D)**. Some dendritic shafts contacted by CCK-IR axon terminals were varicose in shape and received other synaptic inputs **(Fig. 21A)**. The remaining 12% (n = 11) of CCK-IR axon terminals formed classic asymmetric synapses primarily onto spines **(Fig. 22B)** and to a lesser extent onto unlabeled dendritic shafts **(Fig. 22A)**.
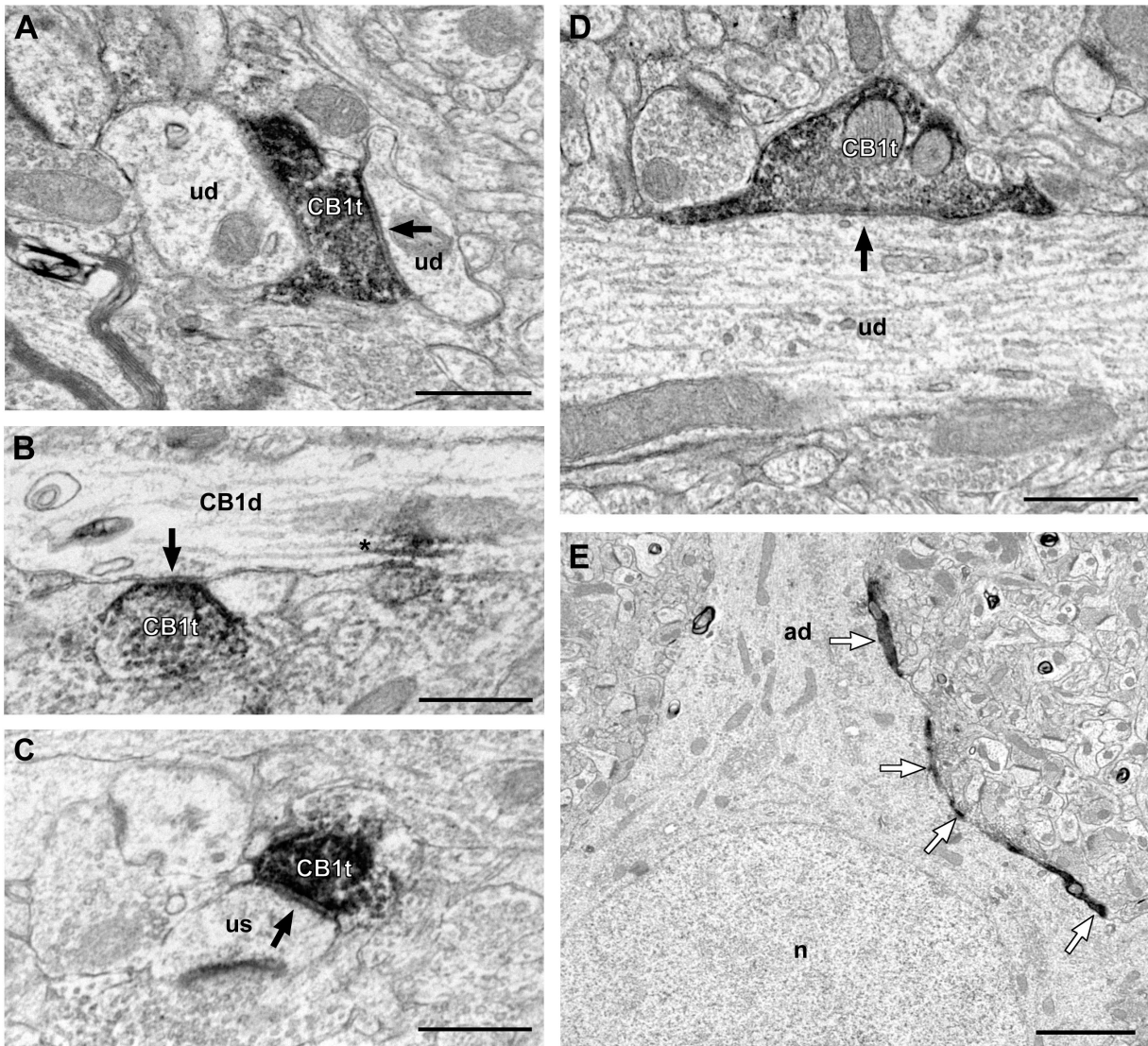
Figure 20. Electron micrographs of CB1-IR axon terminals forming symmetric synapses in area 46 of monkey DLPFC. (A, D) CB1-IR axon terminals (CB1t) form symmetric synapses (arrows) onto small and large unlabeled dendritic shafts (ud). **(B)** CB1-IR axon terminal (CB1t) forms a symmetric synapse (arrow) onto a CB1-labeled dendritic shaft (CBd). Reaction product in dendrites (asterisk) was associated with microtubules. **(C)** A CB1t forms a symmetric synapse onto an unlabeled dendritic spine (us). **(E)** Low power electron micrograph demonstrating a CB1-IR axon forming "basket-like" appositions (white arrows) around an unlabeled cell body (ad = apical dendrite, n = nucleus). Scale bars = 500 nm in **A-D** and 2 µm in **E**.

78

Table 3. Synaptic and appositional targets of CB1-IR axon terminals in layer 2-superficial 3 and layer 4 of monkey DLPFC area 46

	Layers 2-superficial 3	Layer 4	Statistical Results
Number (%) of axon terminals forming symmetric synapses onto:			
Dendritic shafts	49 (88%)	48 (87%)	$\chi^2 = 2.34$
Somata	0 (0%)	2 (4%)	p = 0.311
Dendritic spines	7 (12%)	5 (9%)	
Number (%) of axon terminals apposed to:			
Dendritic shafts	199 (90%)	100 (85%)	$\chi^2 = 7.53$
Somata	7 (3%)	12 (10%)	p = 0.023
Dendritic spines	16 (7%)	6 (5%)	

Table 4. Synaptic and appositional targets of CCK-IR axon terminals in layer 2-superficial 3 and layer 4 of monkey DLPFC area 46

	Layers 2-superficial 3	Layer 4	Statistical Results
Number (%) of axon terminals forming symmetric synapses onto:			
Dendritic shafts	21 (81%)	48 (83%)	$\chi^2 = 2.54$
Somata	3 (11%)	2 (3%)	p = 0.280
Dendritic spines	2 (8%)	8 (14%)	
Number (%) of axon terminals apposed to:			
Dendritic shafts	58 (85%)	97 (83%)	$\chi^2 = 0.245$
Somata	4 (6%)	9 (8%)	p = 0.885
Dendritic spines	6 (9%)	11 (9%)	

Table 5. Comparison of the synaptic targets of CB1- and CCK-IR axon terminals in layers 2-superficial 3 and layer 4 of monkey DLPFC area 46

	Dendritic Shafts	Somata	Dendritic Spines	Statistical Results
Layers 2-superficial 3				
Number (%) of CB1-IR axon terminals	49 (88%)	0 (0%)	7 (12%)	$\chi^2 = 6.93$ p = 0.031
Number (%) of CCK-IR axon terminals	21 (81%)	3 (11%)	2 (8%)	
Layer 4				
Number (%) CB1-IR axon terminals	48 (87%)	2 (4%)	5 (9%)	$\chi^2 = 0.56$ p = 0.755
Number (%) CCK-IR axon terminals	48 (83%)	2 (3%)	8 (14%)	

3.4.4   Laminar analysis of CB1- or CCK-IR axon terminal postsynaptic targets

No significant laminar differences were present in the postsynaptic targets of CB1-IR terminals that had an identifiable synaptic specialization **(Table 3; Fig. 23A)**. In both layers 2-3s and layer 4, the majority of symmetric synapses were onto dendritic shafts (88% and 87%, respectively). In addition, the smaller proportions of symmetric synapses onto dendritic spines and somata were similar in both layers **(Table 3; Fig. 23A)**. Consistent with these observations, most CB1-IR axon terminals without identifiable synapses were in apposition to dendritic shafts in both layer 2-3s (90%) and layer 4 (85%). However, the proportion of appositions to somata in layer 4 (10%) was greater than in layers 2-3s (3%). This difference was confirmed by χ^2 analysis, which revealed a significant difference in the postsynaptic targets of CB1-IR axon terminal appositions by layer ($\chi^2 = 7.53$, $P = 0.023$, $df = 2$; **Table 3**).

CCK-IR terminals showed no significant differences in postsynaptic targets by layer **(Table 4; Fig. 23B)**. The major postsynaptic target of CCK-IR axon terminals forming symmetric synapses was dendritic shafts in both layers 2-3s (81%) and layer 4 (83%). Likewise, CCK-IR axon terminal appositions were also predominantly with dendritic shafts in both layers **(Table 4)**.

The postsynaptic targets of CB1- and CCK-IR symmetric synapses revealed no significant difference in layer 4 **(Table 5)**. In contrast, the postsynaptic targets of CB1- and CCK-IR symmetric synapses in layers 2-3s were significantly different ($\chi^2 = 6.93$, $P = 0.031$, $df = 2$; **Table 5**). 2x2 χ^2 analyses revealed that this difference was due to a larger proportion of CCK-IR symmetric synapses targeting somata (11%) than CB1-IR symmetric synapses (0%).
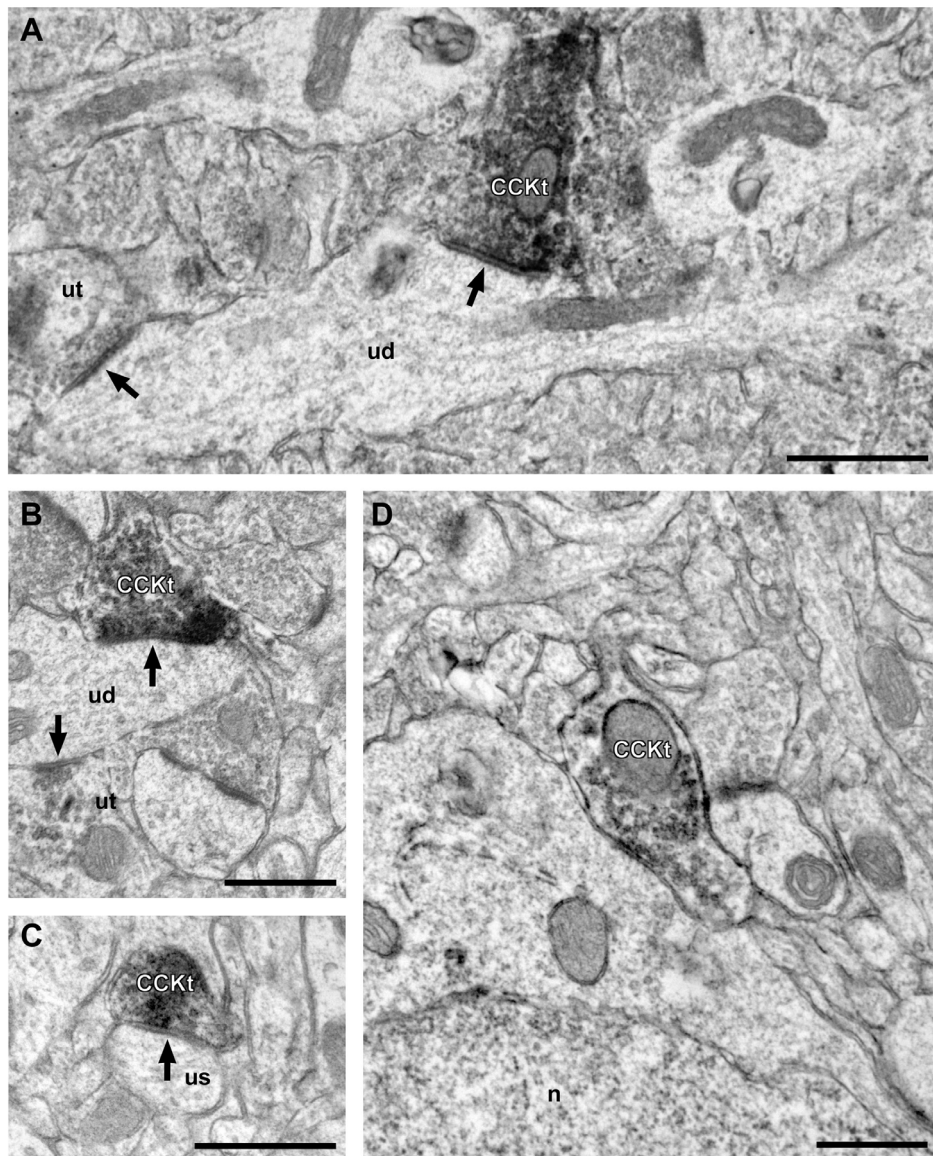
Figure 21. Electron micrographs of CCK-IR axon terminals forming symmetric synapses in area 46 of monkey DLPFC. (A, B) A CCK-IR axon terminal (CCKt) forms a symmetric synapse (arrow) onto an unlabeled dendritic shaft (ud). Note that the dendritic shaft in **(A)** is varicose in shape and receives a synaptic input from another, unlabeled axon terminal (ut; arrow), which are morphologic characteristics of GABA neuron dendrites. **(C)** A CCKt forms a symmetric synapse onto a dendritic unlabeled spine (us). **(D)** A CCKt forms a symmetric synapse (arrow) onto an unlabeled soma (n = nucleus). Scale bars = 500 nm in all panels.
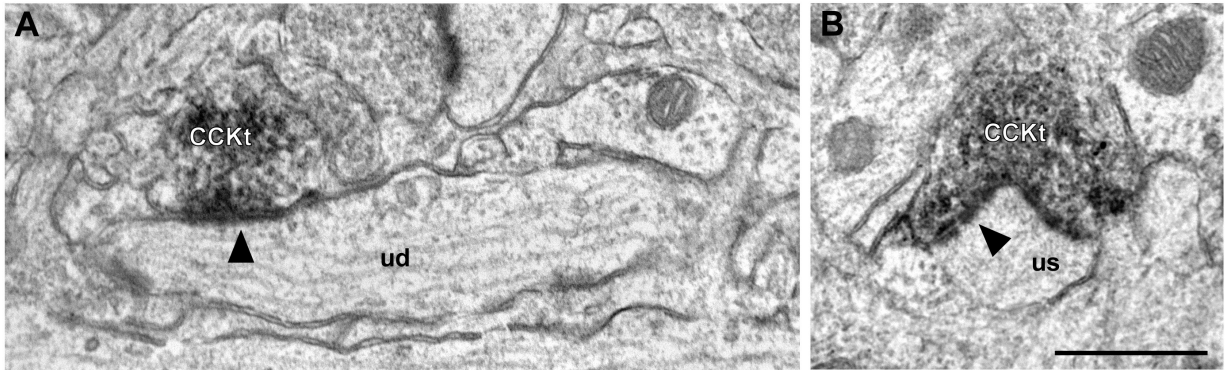
Figure 22. Electron micrographs of CCK-IR axon terminals forming asymmetric synapses in area 46 of monkey DLPFC. (A) A CCK-IR axon terminal (CCKt) forms an asymmetric synapse (arrowhead) onto an unlabeled dendritic shaft (ud). **(B)** A CCKt forms an asymmetric synapse (arrowhead) onto an unlabeled dendritic spine (us). Scale bar = 500 nm in **B** (applies to **A, B**).
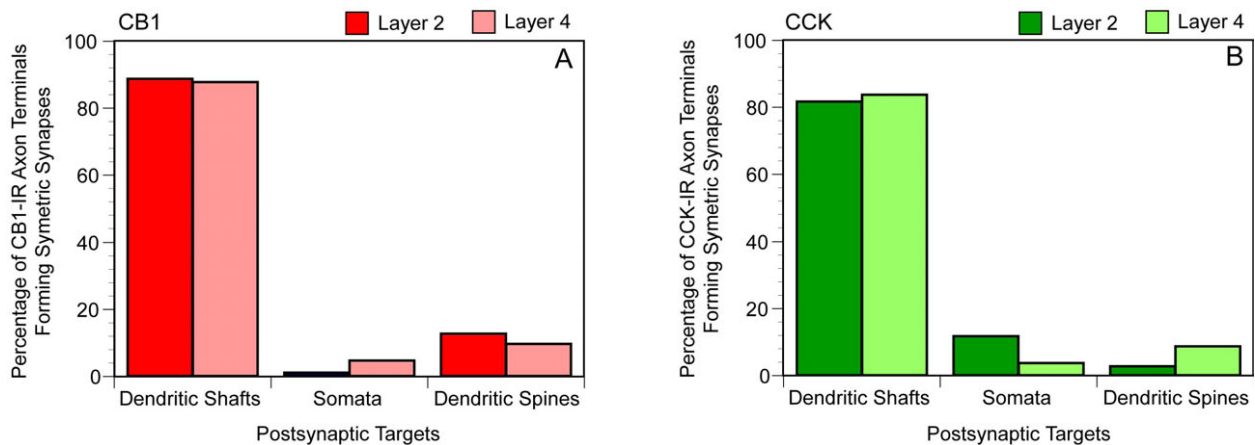
Figure 23. Synaptic targets of CB1- or CCK-IR axon terminals in area 46 of monkey DLPFC. Percentages of CB1- **(A)** or CCK-IR **(B)** axon terminals that form symmetric synapses onto unlabeled dendritic shafts, somata or dendritic spines in layers 2-3s or layer 4.

3.5   DISCUSSION

The results of this study demonstrate that in the macaque monkey DLPFC 1) the laminar distributions of CB1- and CCK-IR neurons and axons are very similar; 2) CB1 and CCK immunoreactivities are colocalized in neurons, axons, and axon terminals although structures single-labeled for each protein are also present; 3) CB1-IR axon terminals exclusively form symmetric synapses, whereas CCK-IR axon terminals form both symmetric and asymmetric synapses; 4) the majority of both CB1- and CCK-IR axon terminals forming symmetric synapses contact dendritic shafts; and 5) the synaptic targets of CB1- and CCK-IR axon terminals are similar in layer 4 but different in layers 2-3s, where CCK-IR terminals are more likely to contact cell bodies and less likely to contact spines than are CB1-IR terminals.

3.5.1   Sources of CB1- and CCK-IR axon terminals

The source of the axons containing both CB1 and CCK is most likely intrinsic inhibitory interneurons. This idea is supported by the presence of CB1 and CCK immunoreactivities in somata and terminals with the morphological features of GABA neurons and the observed colocalization of CB1 and CCK in neurons in layers 2-3s. In addition, the monkey and human DLPFC contain high densities of CB1 and CCK mRNA-expressing neurons, especially in layers 2-superficial 3 (Hashimoto et al., 2007; Eggan et al., 2007). Furthermore, in the rodent neocortex all neurons expressing high levels of CB1 also express the mRNA for glutamic acid decarboxylase-65 (GAD_{65}), a synthesizing enzyme of GABA (Marsicano and Lutz, 1999). In the monkey DLPFC, layers 2-3s contain the highest density of CB1- and CCK-IR neurons and a moderate density of axons and terminals, whereas layer 4 contains a high density of CB1 and CCK-IR axons and terminals but few immunoreactive neurons (this study). This disproportionate distribution of immunoreactive neurons and axons is explained by previous studies in the monkey DLPFC demonstrating that the axons of CCK-containing neurons in layers 2-3s project radially into, and collateralize within, layer 4 (Oeth and Lewis, 1990; Lund and Lewis, 1993;

Oeth and Lewis, 1993). Furthermore, in the mouse neocortex intracellularly filled CB1/CCK-containing neurons in superficial layers project to and arborize within layer 4 (Galarreta et al., 2004). Thus, the presence of interneurons in layer 2-3s that express both CB1 and CCK could account for the high degree of colocalization and the similar postsynaptic targets of CB1- and CCK-IR axon terminals observed in layer 4.

In the rodent neocortex, two distinct populations of CCK-containing cells have been identified: Small bipolar CCK-IR neurons frequently contain calretinin (CR), whereas the less common, large, multipolar CCK-IR neurons lack this calcium binding protein (Kubota and Kawaguchi, 1997; Kawaguchi and Kondo, 2002). In addition, CB1-IR neurons in the rat cortex are either large and contain CCK or small and contain the calcium binding protein calbindin (Bodor et al., 2005). Based upon these findings, the CCK-positive, CB1-negative axons and terminals observed in the monkey DLPFC in this study likely arise from CR-containing GABA neurons, whereas the CCK-negative, CB1-positive axons and terminals likely arise from calbindin-containing GABA neurons. These different sources of CB1 and CCK-IR axons may account for the different synaptic targets of CB1- and CCK-IR axons in layers 2-3s.

However, the single-labeled CCK and CB1-containing axons and terminals could also arise from extrinsic sources. For instance, anterograde tract-tracing studies have shown that GABA-containing neurons in the rodent ventral mesencephalon innervate layers 5-6 of the prefrontal cortex (Carr and Sesack, 2000), and retrograde tract-tracing studies in the monkey demonstrated that CCK neurons in the ventral mesencephalon project to the DLPFC (Oeth and Lewis, 1992). However, the termination pattern of these axons in layers 5-6 does not explain the difference in postsynaptic targets of CCK and CB1 terminals in layers 2-3s. Recently, CB1 immunoreactivity was demonstrated in norepinephrine-containing axons in the rodent cortex (Oropeza et al., 2007) suggesting that CB1-IR axons in layers 2-3s could arise from the locus coeruleus. Although this source cannot be excluded, in the monkey DLPFC dopamine-β-hydroxylase-containing terminals form both symmetric and asymmetric synapses (Aoki et al., 1998), whereas CB1 terminals were only found to form symmetric synapses. Furthermore, the distribution of dopamine-β-hydroxylase-containing axons in the primate DLPFC does not match the laminar pattern observed for CB1-containing axons (Lewis and Morrison, 1989; Gaspar et al., 1989).

The CCK-IR terminals forming asymmetric synapses could arise from several sources. For instance, CCK-IR asymmetric synapses could arise from intrinsic nonpyramidal neurons that do not utilize GABA. Indeed, about 5-10% of CCK-IR neurons in the monkey cortex do not exhibit immunoreactivity for GAD, a synthesizing enzyme of GABA (Hendry et al., 1984). Interestingly, in both the rodent and cat all CCK-IR neurons are GABA or GAD immunoreactive, suggesting that non-GABA-containing CCK-IR terminals forming asymmetric synapses is a unique feature of primate cortical circuitry (Hendry et al., 1984; Kubota and Kawaguchi, 1997). Consistent with the idea of an intrinsic source of CCK-IR asymmetric terminals, 29% of CR-containing axon terminals form asymmetric synapses and 23% of CR-IR neurons do not contain GABA in the monkey DLPFC (Melchitzky et al., 2005). Thus, CCK asymmetric synapses could arise from non-GABA-containing CR-IR neurons. Alternatively, CCK-IR asymmetric synapses could arise from subcortical structures, such as the thalamus and/or amygdala. Projections from the mediodorsal thalamus terminate in layers deep 3 and 4, whereas projection neurons in the basolateral complex of the amygdala innervate layers 2-3s of the monkey DLPFC (Porrino et al., 1981; Amaral and Price, 1984; Giguere and Goldman-Rakic, 1988; McDonald, 1992; Erickson and Lewis, 2004). Although neurons in these structures express CCK mRNA (Schiffmann and Vanderhaeghen, 1991; Marsicano and Lutz, 1999), the lack of CCK immunoreactivity in projection neurons, even after injections of colchicine, excludes these sources (Oeth and Lewis, 1990; Mascagni and McDonald, 2003). Similarly, asymmetric synapses could arise from cortical pyramidal neurons known to express CCK mRNA in rat (Schiffmann and Vanderhaeghen, 1991) and human (Hashimoto et al., 2007) cortex; however, cortical pyramidal neurons are not observed to be immunoreactive for CCK and are therefore an unlikely source of CCK-IR asymmetric synapses. Thus, our data are consistent with the idea that CCK-IR asymmetric synapses in the monkey DLPFC arise from a subpopulation of non-GABA-containing CR-IR intrinsic interneurons.

3.5.2 Functional significance

The axon terminals that contain both CB1 and CCK are likely to represent basket neurons that innervate the cell bodies and proximal dendrites of pyramidal neurons, and thus are positioned to powerfully regulate pyramidal neuron output. Indeed, in rat neocortical slices CB1 receptor

activation reduces GABA$_A$ receptor-mediated inhibitory postsynaptic currents in pyramidal neurons by presynaptically inhibiting GABA release (Trettel et al., 2004; Galarreta et al., 2004; Bodor et al., 2005) and perisomatic inhibition is more susceptible to CB1 agonists than dendritic inhibition (Trettel et al., 2004). In addition, in rat hippocampal and neocortical slices, the transient suppression of GABA-mediated IPSCs and strength of perisomatic inhibition following pyramidal cell depolarization [i.e., depolarization induced-suppression of inhibition (DSI)] is meditated by CB1 receptor activation (Pitler and Alger, 1992; Trettel et al., 2004; Bodor et al., 2005).

This suggests a mechanism by which inhibition from CB1/CCK-containing neurons may serve to regulate network activity that is necessary during working memory tasks (Sawaguchi et al., 1988; Sawaguchi et al., 1989; Rao et al., 2000; Constantinidis et al., 2002). Indeed, in the rodent hippocampus and neocortex CB1/CCK-containing neurons are chemically and electrically coupled (Galarreta et al., 2004) and in the hippocampus entrain oscillatory patterns of rhythmic activity (Klausberger et al., 2005; Robbe et al., 2006). Furthermore, in rat hippocampal slices the application of CB1 agonists reduces the power of gamma oscillations by disinhibiting pyramidal neurons (Hajos et al., 2000b; Klausberger et al., 2005; Robbe et al., 2006). The ability of CB1 activation to disrupt gamma oscillations may be the underlying mechanism by which the systemic administration of cannabinoids disrupts the ability to perform working memory tasks in both humans and animals (Winsauer et al., 1999; Schneider and Koch, 2003; D'Souza et al., 2004).

In the monkey and human DLPFC, pyramidal neurons receive convergent perisomatic input from PV-containing basket and chandelier neurons and CB1/CCK-contaiing basket neurons. In the rodent these convergent sources of perisomatic inhibition have been shown to play specific roles in shaping network activity. For example, CB1/CCK-containing and PV-containing neurons fire at different phases of network oscillations (Klausberger et al., 2005), generate temporally distinct epoch of somatic inhibition (Glickfeld and Scanziani, 2006), and play complementary roles in regulating gamma band oscillations (Hajos et al., 2000b). In the monkey DLPFC, PV- and GABA transporter (GAT) 1-IR axon cartridges of chandelier neurons undergo considerable changes during postnatal development, with these changes particularly marked during adolescence (Condé et al., 1996; Erickson and Lewis, 2002; Cruz et al., 2003). These developmental changes in PV- and GAT-1 cartridges are thought to reflect the maturation

of chandelier neurons' regulation of pyramidal cell output. Because stimulation of the CB1 receptor strongly suppresses the GABA inputs to pyramidal neurons from CCK-containing basket neurons, cannabis use during adolescence may alter the balance between the CB1/CCK-containing and PV-containing inhibitory inputs to the perisomatic region of DLPFC pyramidal neurons; this imbalance during a sensitive period may disrupt the developmental trajectories of these GABA inputs (Chattopadhyaya et al., 2007), producing persistent circuitry alterations that impair the mechanisms of neural synchrony required for the maturation of working memory performance.

4.0   ALTERED CB1 RECEPTOR mRNA AND PROTEIN EXPRESSION IN SCHIZOPHRENIA: IMPLICATIONS FOR COGNITIVE DEFICITS

4.1   ABSTRACT

Cannabis use is associated with both impaired cognitive functions, including working memory, and an increased risk of schizophrenia. In addition, schizophrenia is characterized by impairments in working memory that are due, at least in part, to reduced GABA neurotransmission in the dorsolateral prefrontal cortex (DLPFC). The cannabinoid 1 (CB1) receptor is highly expressed in the DLPFC, is contained in the axon terminals of a subpopulation of perisomatic-targeting GABA neurons, and when activated, inhibits the release of GABA. In order to determine the potential relationship between CB1 receptor signaling and altered GABA neurotransmission in schizophrenia, we evaluated CB1 receptor mRNA and protein expression in the DLPFC from 23 matched pairs of schizophrenia and control subjects. CB1 mRNA levels, assessed by *in situ* hybridization, were significantly 15% lower in the subjects with schizophrenia. Similarly, CB1 protein, assessed by radioimmunocytochemistry and standard immunocytochemistry, was significantly decreased by 12% and 14%, respectively. CB1 mRNA expression was not changed in the DLPFC of monkeys chronically exposed to haloperidol or olanzapine, and neither CB1 mRNA or protein levels were affected by potential confounding factors in the subjects with schizophrenia. Finally, changes in CB1 mRNA levels were significantly correlated with changes in GAD_{67} mRNA levels in the same subjects with schizophrenia. Reduced CB1 mRNA and protein in schizophrenia may represent a compensatory mechanism to increase GABA transmission from perisomatic-targeting interneurons with impaired GABA synthesis. These findings suggest a novel drug target for the treatment of cognitive dysfunction in schizophrenia.

4.2   INTRODUCTION

The following convergent findings from epidemiological studies suggest that cannabis use represents an environmental risk factor for schizophrenia: 1) the association between cannabis use and schizophrenia is consistent across studies (replicated effect); 2) the association cannot be explained by other confounding factors (specificity of effect); 3) the degree of cannabis exposure is positively correlated with the risk of schizophrenia (dose-response effect); 4) the exposure to cannabis precedes the development of schizophrenia (temporal effect); and 5) cannabis use during early adolescence is associated with greater risk (developmental effect) (reviewed in Henquet et al., 2005b). In addition, chronic cannabis users exhibit marked disturbances in cognitive functions, such as working memory (Solowij et al., 2002), that are severe and persistent in schizophrenia (Elvevag and Goldberg, 2000).

Working memory processes are particularly dependent on the circuitry of the dorsolateral prefrontal cortex (DLPFC) and alterations in this brain region appear to contribute to working memory impairments in schizophrenia (Weinberger et al., 2001). In particular, GABA neurotransmission within the DLPFC is critical for normal working memory function (Sawaguchi et al., 1988; Rao et al., 2000) and reductions in markers of GABA neurotransmission have been consistently identified in the DLPFC of subjects with schizophrenia (Lewis et al., 2005). Interestingly, the CB1 cannabinoid receptor, the principal cannabinoid receptor in the brain, is highly expressed in the primate DLPFC and is contained in the axon terminals of a specific subpopulation of GABA interneurons that express the neuropeptide cholecystokinin (CCK) and that furnish perisomatic inputs to pyramidal neurons (Bodor et al., 2005; Eggan and Lewis, 2007). Activation of CB1 receptors inhibits the release of GABA and reduces inhibitory postsynaptic currents (Freund et al., 2003). Thus, CB1 receptors play an important role in regulating network activity patterns by controlling proximal inhibitory input to pyramidal neurons.

In concert, the evidence that cannabis use is a risk factor for schizophrenia, that cannabis use impairs working memory function, and that the CB1 receptor modulates GABA neurotransmission suggests that alterations in the expression of CB1 receptors in the DLPFC might be involved in the pathophysiology of working memory dysfunction in schizophrenia. In order to test this hypothesis, we used *in situ* hybridization and immunocytochemical techniques

89

to 1) assess the expression of CB1 receptor mRNA and protein in the DLPFC of subjects with schizophrenia, 2) determine the effects of potential confounds on measures of CB1 receptors, and 3) examine the relationship between these measures and markers of GABA neurotransmission in schizophrenia.

4.3   MATERIALS AND METHODS

4.3.1   Human subjects

Following informed consent for brain donation from the next-of-kin and using procedures approved by the University of Pittsburgh's Committee for Research Involving the Dead and Institutional Review Board for Biomedical Research, brain specimens from 23 normal control human subjects and 23 subjects with schizophrenia were obtained from autopsies conducted at the Allegheny County Medical Examiner's Office, Pittsburgh, PA. Each subject with schizophrenia was matched for sex, and as closely as possible for age and postmortem interval (PMI), with one control subject (**Table 6**). Subject groups (**see Table 6**) did not differ in mean age ($t_{(22)} = 0.16$; $p = 0.88$), PMI ($t_{(22)} = 0.22$; $p = 0.83$), RNA integrity number [RIN; assessed by Agilent Bioanalyzer ($t_{(22)} = 1.84$; $p = 0.08$)], or tissue storage time ($t_{(22)} = -0.96$; $p = 0.35$). Mean ± SD brain pH also did not differ ($t_{(22)} = 0.62$; $p = 0.54$), between schizophrenia (6.8 ± 0.30) and control (6.9 ± 0.20) subjects. Because our brain specimens were obtained from a community-based subject population, most subjects (21 control subjects and 18 subjects with schizophrenia) died suddenly outside of a hospital setting.

For each subject, consensus DSM-IV (*Diagnosis and Statistical Manual of Mental Disorders*, 1994) diagnoses were made by an independent committee of experienced research clinicians based on information obtained from clinical records and a structured interview conducted with a surviving relative. The diagnostic procedures revealed a history of post-traumatic stress disorder in one control subject (987) that was in remission at time of death. In the schizophrenia group, eight subjects met criteria for schizoaffective disorder, five subjects died by suicide, and fifteen subjects had a history of substance (including alcohol) abuse or dependence disorder, although only nine met criteria at time of death (**Table 6**). Seven subjects

90

with schizophrenia had a history of cannabis use (581, 587, 787, 829, 878, 722, and 930); three of these met criteria for abuse or dependence at time of death (787, 722, and 930) and one (829) had a history of abuse in remission at time of death. Toxicology revealed positive plasma alcohol levels (0.01 – 0.09%) in two control subjects (516 and 685) and one subject with schizophrenia (656). No other substances of abuse, including Δ^9-THC, were detected in any of the subjects. Four subjects with schizophrenia (537, 622, 829, and 621) were off antipsychotic medications for 9.6 months, 1.2 months, unknown, and 8.5 years prior to the time of death, respectively. The mean (± SD) age of illness onset in the schizophrenia group was 25.1 (± 8.1) years of age and the average duration of illness was 23.3 (± 13.3) years.

Neuropathological examinations revealed an acute infarction limited to the distribution of the inferior branch of the right middle cerebral artery in schizophrenia subject 622 and a previous infarction in the inferior aspect of the frontal lobe in schizophrenia subject 781. DLPFC area 9 appeared unaffected by these infarcts in both cases. Other brain disorders and abnormalities were excluded in each subject on the basis of both clinical and neuropathological criteria.

The 23 pairs of schizophrenia and matched control subjects used in this study (**Table 6**) were used in a previous study of GAD_{67} and CCK mRNA expression in DLPFC area 9 (Hashimoto et al., 2005; Hashimoto et al., 2007).

Table 6. Characteristics of subjects

Pair	Control Subjects							Schizophrenia Subjects								History of cannabis use
	Case	Sex/race	Age	PMI[a]	RIN	Storage Time[b]	Cause of death[c]	Case	DSM IV diagnosis	Sex/race	Age	PMI[a]	RIN	Storage time[b]	Cause of death[c]	
1*	592	M/B	41	22.1	9.0	120.3	ASCVD	533	Chronic undifferentiated schizophrenia	M/W	40	29.1	8.4	130.1	Accidental asphyxiation	None
2*	567	F/W	46	15.0	8.9	124.3	Mitral Valve prolapse	537	Schizoaffective disorder[d]	F/W	37	14.5	8.6	129.4	Suicide by hanging	None
3*	516	M/B	20	14.0	8.4	131.9	Homicide by gun shot	547	Schizoaffective disorder	M/B	27	16.5	7.4	128.0	Heat Stroke	None
4*	630	M/W	65	21.2	9.0	114.4	ASCVD	566	Chronic undifferentiated schizophrenia[e]	M/W	63	18.3	8.0	124.7	ASCVD	None
5*	604	M/W	39	19.3	8.6	118.0	Hypoplastic coronary artery	581	Chronic paranoid schizophrenia[e,f,g]	M/W	46	28.1	7.9	122.5	Accidental combined drug overdose	Use
6*	546	F/W	37	23.5	8.6	128.3	ASCVD	587	Chronic undifferentiated schizophrenia[e]	F/B	38	17.8	9.0	121.1	Myocardial hypertrophy	Use
7*	551	M/W	61	16.4	8.3	127.1	Cardiac Tamponade	625	Chronic disorganized schizophrenia[h]	M/B	49	23.5	7.6	115.0	ASCVD	None
8*	685	M/W	56	14.5	8.1	107.4	Hypoplastic coronary artery	622	Chronic undifferentiated schizophrenia[d]	M/W	58	18.9	7.4	115.2	Right MCA infarction	None
9*	681	M/W	51	11.6	8.9	108.0	Hypertrophic cardio-myopathy	640	Chronic paranoid schizophrenia	M/W	49	5.2	8.4	113.1	Pulmonary embolism	None
10	806	M/W	57	24.0	7.8	86.5	Pulmonary thromboembolism	665	Chronic paranoid schizophrenia[f]	M/B	59	28.1	9.2	110.6	Intestinal hemorrhage	None
11	822	M/B	28	25.3	8.5	83.9	ASCVD	787	Schizoaffective disorder[j]	M/B	27	19.2	8.4	90.1	Suicide by gun shot	Abuse & Dependence
12*	727	M/B	19	7.0	9.2	101.0	Trauma	829	Schizoaffective disorder[d,f,j]	M/W	25	5.0	9.3	81.8	Suicide by drug overdose	Abuse in remission
13	871	M/W	28	16.5	8.5	73.3	Trauma	878	Disorganized schizophrenia[f]	M/W	33	10.8	8.9	72.3	Myocardial fibrosis	Use
14*	575	F/B	55	11.3	9.6	123.0	ASCVD	517	Disorganized schizophrenia[f]	F/W	48	3.7	9.3	131.7	Intracerebral hemorrhage	None
15	700	M/W	42	26.1	8.7	105.1	ASCVD	539	Schizoaffective disorder[k]	M/W	50	40.5	8.1	129.2	Suicide by combined drug overdose	None
16	988	M/W	82	22.5	8.4	51.9	Trauma	621	Chronic undifferentiated schizophrenia[d]	M/W	83	16.0	8.7	115.5	Accidental asphyxiation	None
17	686	F/W	52	22.6	8.5	107.1	ASCVD	656	Schizoaffective disorder[f]	F/B	47	20.1	9.2	111.3	Suicide by gun shot	None
18	634	M/W	52	16.2	8.5	113.8	ASCVD	722	Chronic undifferentiated schizophrenia[j,l]	M/B	45	9.1	9.2	101.4	Upper GI bleeding	Abuse
19	852	M/W	54	8.0	9.1	76.3	Cardiac tamponade	781	Schizoaffective disorder[k]	M/B	52	8.0	7.7	91.3	Peritonitis	None
20*	987[m]	F/W	65	21.5	9.1	51.9	ASCVD	802	Schizoaffective disorder[f,l]	F/W	63	29.0	9.2	87.1	Right ventricular dysplasia	None
21	818	F/W	67	24.0	8.4	85.0	Anaphylactic reaction	917	Chronic undifferentiated schizophrenia	F/W	71	23.8	7.0	65.1	ASCVD	None
22	857	M/W	48	16.6	8.9	75.1	ASCVD	930	Disorganized schizophrenia[j,k]	M/W	47	15.3	8.2	61.7	ASCVD	Abuse
23	739	M/W	40	15.8	8.4	100.1	ASCVD	933	Disorganized schizophrenia	M/W	44	8.3	8.1	61.1	Myocarditis	None
	Mean		48.0	18.0	8.7	100.6					47.9	17.8	8.4	104.8		
	SD		15.5	5.5	0.4	23.5					14.1	9.3	0.7	23.6		

4.3.2 In situ hybridization

Tissue preparation. The right prefrontal cortex of each subject was blocked coronally, immediately frozen in isopentane on dry ice, and stored at -80°C. Serial tissue sections containing the superior frontal gyrus were cut on a cryostat at 20 µm, thaw mounted on Supra-frost slides (VWR Scientific, West Chester, PA, USA), and stored at -80°C until processed for *in situ* hybridization. Published cytoarchitectonic criteria (Rajkowska and Goldman-Rakic, 1995) were used to identify the location of DLPFC area 9 in Nissl-stained sections as previously described (Glantz et al., 2000; Volk et al., 2000). For each subject pair, three sections separated by at least 320 µm were chosen with the rostrocaudal locations matched. A total of six *in situ* hybridization runs were performed, with one section from a given pair processed side-by-side in a single run.

Generation of riboprobes. Templates for the synthesis of riboprobes against human CB1 receptor mRNA were generated by PCR. A 714 base pair fragment corresponding to bases 435-1148 of the human *CNR1* gene (Genbank accession number NM_033181) was amplified with specific primer sets. Nucleotide sequencing revealed 100% homology for the amplified fragment to a previously reported sequence. The fragment was subcloned into the plasmid pSTBlue-1 (Novagen, Madison, WI). Sense and antisense riboprobes were generated by *in vitro* transcription in the presence of ^{35}S-CTP using T7 or SP6 RNA polymerase, respectively, followed by digestion with DNaseI. The riboprobes were purified by centrifugation through RNeasy mini spin columns (Qiagen, Balencia, CA) and the length was reduced to approximately 100 bp by alkaline hydrolysis to increase the effectiveness of tissue penetration.

In situ hybridization. Hybridization procedures were performed as previously described (Hashimoto et al., 2003). Briefly, following fixation with 4% paraformaldehyde in 0.1 M phosphate buffered saline (PBS), sections were acetylated with 0.25% acetic anhydrate in 0.1 M triethanolamine/0.9% NaCl for 10 min, dehydrated through a graded ethanol series, and defatted in chloroform for 10 min. Sections were then hybridized with ^{35}S-labeled riboprobes (1 X 10^7 cpm/ml) in a standard hybridization buffer at 56°C for 16 hours. Sections were subsequently washed in a solution containing 0.3 M NaCl, 20 mM Tris-HCl, pH 8.0, 1 mM EDTA, pH 8.0, and 50% formamide at 63°C, treated with RNase A at 37°C, and washed in 0.1 x SSC at 66°C.

Sections were then dehydrated through a graded ethanol series, air-dried, and exposed to BioMax MR film (Eastman Kodak, Rochester, NY) for three days. After exposure to film, sections were coated with NTB2 emulsion (Eastman Kodak, Rochester, NY) using a mechanical dipper (Auto-dip Emulsion Coater, Ted Pella, Redding, CA), exposed for ~12 days at 4°C, developed with D-19 (Eastman Kodak, Rochester, NY), and counterstained with cresyl violet as previously described (Hashimoto et al., 2003).

Quantification of CB1 mRNA expression levels. CB1 mRNA expression levels were quantified using a Microcomputer Imaging Device (MCID) system (Imaging Research Inc, London, ON, Canada) without knowledge of diagnosis or subject number by random coding of film autoradiographs. Film autoradiographs were trans-illuminated on a light box, and images were captured by a video camera and digitized under precisely controlled conditions. Images of hybridized tissue sections were captured and superimposed on corresponding autoradiographic film images in order delineate the pial surface and gray and white matter borders. Contours in DLPFC area 9 were drawn around the full cortical thickness where the gray matter was cut perpendicular to the pial surface. Optical density (OD) was measured in those contours drawn and expressed as nanoCuries per gram tissue by reference to radioactive carbon-14 standards (American Radiolabeled Chemicals, St. Louis, MO) exposed on the same film. The mean ($\pm$ SD) total area sampled per subject was 385 ($\pm$ 140) mm^2 for control subjects and 354 ($\pm$ 112) mm^2 for subjects with schizophrenia.

To determine differences in CB1 mRNA expression across lamina, OD was measured in ~1-mm-wide cortical traverses extending from the pial surface to the white matter. Three cortical traverses per section (nine traverses per subject) were placed in locations where the tissue section was cut perpendicular to the pial surface as determined by the presence of pyramidal neurons with vertically oriented apical dendrites in adjacent Nissl-stained sections. Within each traverse, the OD in each layer was determined by dividing the total cortical thickness from the pial surface to white matter into zones of 1-10, 10-30, 30-50, 50-60, 60-80, and 80-100% approximating layers 1, 2-superficial 3 (3s), deep 3 (3d), 4, 5, and 6, respectively (Pierri et al., 1999). All cortical and laminar gray matter OD values were corrected by subtracting background OD values obtained from the white matter of each subject.

4.3.3 Radioimmunocytochemistry

Human fresh frozen tissue sections adjacent to those processed for *in situ* hybridization were processed for radioimmunocytochemistry (RICC). A total of 2 radioimmunocytochemistry runs were performed, with one section from a given pair processed side-by-side in a single run. Slides were immersed in 4% paraformaldehyde diluted in 0.1 M phosphate-buffered saline (PBS; pH 7.4) for 1 hour followed by three 10 minute washes in 0.01 M PBS. Following fixation, slides were incubated in a blocking solution containing 0.3% Triton-X, 4% normal donkey (NDS) and human (NHuS) sera (Jackson ImmunoResearch, West Grove, PA), and 1% bovine serum albumin (BSA; Jackson) in PBS for 1 hour to reduce non-specific binding. Slides were then placed in humidified boxes, and ~300 µl of blocking solution containing an affinity-purified polyclonal rabbit anti-CB1 antibody raised against the last 15 amino acids residues of the C-terminus of the rat CB1 receptor (anti-CB1-L15; diluted 1:5000; kindly provided by Dr. Ken Mackie, Indiana University, Bloomington, IN) was pipetted onto each section. The specificity of this antibody has been previously demonstrated by multiple lines of evidence including western blot analysis, preadsorption studies, and testing in knockout animals (see Eggan and Lewis, 2007). Sections were incubated for 48 hours at 4ºC. After 24 hours the primary antibody solution covering each section was removed and fresh primary antibody solution applied. Slides were then removed from the humidified boxes and rinsed three times for five minutes in PBS. Each section was subsequently covered with ~300 µl of secondary antibody solution containing a ^{35}S-labeled donkey anti-rabbit IgG secondary antibody (0.5 µCi/ml; GE Healthcare Bio-Sciences Corp, Piscataway, NJ), 0.3% Triton-X, and 4% NDS and NHuS in PBS and incubated for 2 hours at room temperature (RT) in humidified boxes. Slides were then washed three times for 15 minutes in PBS, rinsed with MilliQ H_2O to remove salt, air dried, and exposed to BioMax MR film (Eastman Kodak) for three days.

Quantification of CB1 radioimmunoreactivity levels. OD values of CB1 radioimmunoreactivity were measured as described above. Contours were drawn as close as possible to the same locations in DLPFC area 9 quantified for CB1 mRNA expression. The mean (± SD) total area sampled per subject was 70 (± 35) mm^2 for control subjects and 75 (± 32) mm^2 for subjects with schizophrenia. All cortical gray matter OD values were corrected by subtracting background OD values obtained from the white matter of each subject.

4.3.4   Immunocytochemistry

Tissue preparation. The fresh left hemisphere of 12 of the 23 subject pairs **(Table 6)** was cut into 1.0-cm thick coronal blocks and immersed in phosphate-buffered (0.1 M; pH 7.4) 4% paraformaldehyde for 48 hours at 4 ºC, cryoprotected and then stored in a solution containing glycerin and ethylene glycol in dilute phosphate buffer at -30ºC. Immunoreactivity for a number antigens has been demonstrated to be unaffected by this storage procedure (see Cruz et al., 2003). Coronal tissue blocks containing the DLPFC at the level of the superior frontal gyrus were serially sectioned at 40 µm on a cryostat. Every 10th section was stained for Nissl substance with thionin to identify DLPFC area 9 as described above. For each subject pair, two sections separated by at least 400 µm were chosen with the rostrocaudal locations matched as closely as possible. A total of four immunocytochemistry runs were performed, with one section from a given pair processed side-by-side in a single run.

 Immunocytochemistry. Free-floating tissue sections were processed for CB1 immunoreactivity using a previously described protocol (Eggan and Lewis, 2007). Briefly, tissue sections were pretreated with 1% hydrogen peroxide for 15 min to remove endogenous peroxidase activity, immersed in a blocking solution to reduce background, and subsequently incubated in a PBS solution containing 0.3% Triton-X, 3% NDS and NHuS, 0.05% BSA (Jackson), and the polyclonal rabbit anti-CB1-L15 antibody (diluted 1:6500) at 4ºC for 48 hours. Sections were then incubated in a biotinylated donkey anti-rabbit IgG secondary antibody (diluted 1:200; Jackson), processed with the avidin-biotin-peroxidase method (Hsu et al., 1981) using the Vectastain Avidin-Biotin Elite Kit (Vector Laboratories, Burlingame, CA) and the immunoperoxidase reaction was visualized using 3,3'-diaminobenzidine (DAB; 0.005%; Sigma, St. Louis, MO). Sections were subsequently mounted on gel-coated slides, air dried, and immersed serially in osmium tetroxide (0.005%) and thiocarbohydrazide (0.5%) to stabilize the DAB reaction product (Lewis et al., 1986).

 Quantification of CB1 immunoreactivity. Levels of CB1 immunoreactivity in DLPFC area 9 of subject pairs was assessed using a MCID system and were expressed as relative optical density. Slid-mounted sections were illuminated on a microscope (Leitz Diaplan, Germany) and images were captured at a magnification of 2.6X by a video camera under precisely controlled conditions and digitized. This method produced higher magnification and better image resolution

97

than the light box method utilized for film autoradiograms described above. Relative OD values of CB1 immunoreactivity were measured within three cortical traverses per section (six traverses per subject) as described above. Relative OD values for the entire cortex of each subject were calculated by averaging the OD values of the six traverses. The OD in each cortical layer was determined as described above with a modification. The highest density of CB1-IR axons precisely marks the cytoarchitectonic boundaries between layers 2-4 and 4-6 (Eggan and Lewis, 2007). Therefore, for every traverse, the data were aligned so that the peak OD value of each traverse corresponded to the zone representing the middle of layer 4. The mean ($\pm$ SD) total area sampled per subject was 15 ($\pm$ 1) mm^2 for control subjects and 15 ($\pm$ 1) mm^2 for subjects with schizophrenia. All cortical and laminar gray matter OD values were corrected by subtracting background OD values obtained from the white matter of each subject.

4.3.5 Antipsychotic-exposed monkeys

In order to evaluate the potential effects of long-term exposure to antipsychotic medications on CB1 mRNA expression levels, 18 experimentally naïve, young adult (4.5-5.3 years of age), male, long-tailed macaque monkeys (*Macaca fascicularis*) were arbitrarily divided into three groups and trained to take pellets containing either haloperidol, olanzapine, or sham orally twice daily (Dorph-Petersen et al., 2005). The total daily dose of haloperidol (38-32 mg) and olanzapine (11.0-13.2 mg) per animal was titrated to achieve trough plasma drug levels equivalent to the therapeutic range (~1.5 ng/ml for haloperidol and ~15 ng/ml for olanzapine) for the treatment of schizophrenia in humans (Nyberg et al., 1995; Kapur et al., 1997; Kapur et al., 1998; Kapur et al., 1999). Following chronic drug exposure for 17-27 months, animals were grouped into triads according to body weight and euthanized by an overdose of pentobarbital (50 mg/kg). Brains were immediately removed, and the right hemisphere was blocked into ~5 mm-thick coronal slabs and frozen, and then blocks containing the middle one-third of the principal sulcus were serially sectioned on a cryostat at 16 µm, thaw mounted on Supra-frost slides (VWR Scientific, West Chester, PA, USA), and stored at -80°C. For each triad, two sections from each animal spaced by 224 µm were processed for *in situ* hybridization as described above. A total of two *in situ* hybridization runs were performed, with one section from a given triad processed side-by-side in a single run. The OD of CB1 mRNA expression was assessed in contours

98

encompassing the gray matter between the cingulate and principal sulci, which includes DLPFC areas 9 and 46. The mean ($\pm$ SD) total area sampled per animal was 49 ($\pm$ 8) mm^2 for sham, 49 ($\pm$ 9) mm^2 for haloperidol, and 47 ($\pm$ 10) mm^2 for olanzapine exposed monkeys. All cortical gray matter OD values were corrected by subtracting background OD values obtained from the white matter of each animal. All housing and experimental procedures were conducted in accordance with USDA and NIH guidelines and with approval of the University of Pittsburgh's Institutional Animal Care and Use Committee.

4.3.6   Statistical analyses

Analysis of covariance (ANCOVA) models were performed to test the effect of diagnosis on each OD measure using averaged values across all sections from each subject. In the first ANCOVA model, OD was entered as the dependent variable and diagnostic group as the main effect. Subject pair was entered as a blocking effect to reflect the matching of individual subject pairs for sex, age, and PMI. In analyses of mRNA OD, RIN values and tissue storage time were entered as covariates because RIN reflects mRNA integrity (Stan et al., 2006) and storage time may affect mRNA preservation. In analyses of radioimmunoreactivity and immunoreactivity OD values, storage time was entered as a covariate because this variable has been reported to affect the density of CB1 radioligand binding (Mato and Pazos, 2004). Because using subject pair as a blocking effect may be considered an attempt to balance the two diagnostic groups with regard to the experimental factors instead of a true statistical paired design, a second ANCOVA model was performed to validate the first model. The second ANCOVA model used a main effect of diagnostic group and sex, age, PMI, RIN (in analyses of mRNA OD values only), and storage time as covariates. As a covariate, tissue storage time was never observed to have a significant effect and was therefore excluded in the reported analyses. Both ANCOVA models produced similar results for diagnostic group effect. We therefore report the results from the first model using pair as a blocking factor to reflect the matching of individual subject pairs for sex, age, and PMI in both cortical and laminar analyses.

The potential influence of confounding variables (sex, a diagnosis of schizoaffective disorder, suicide, use of antidepressant medication at time of death, a diagnosis of substance abuse/dependence at time of death, or a history of cannabis use/abuse) on the within-pair

differences in OD values were assessed by two-sample t-test analyses. A one-way analysis of variance (ANOVA) model with optical density as the dependent variable and drug group as the main effect was used for comparison of CB1 mRNA expression levels in the DLPFC of sham-, haloperidol-, and olanzapine- exposed monkeys. All statistics were performed using SPSS (SPSS Inc., Chicago, IL).

4.3.7 Photography

Darkfield and brightfield photomicrographs were obtained with a Zeiss Axiocam camera and the brightness and contrast were adjusted in Adobe Photoshop. Pseudocolor autoradiograms were generated using the MCID system. All photomicrographs and pseudocolor autoradiograms were assembled in Adobe Photoshop.

4.4   RESULTS

4.4.1   Analysis of CB1 mRNA expression by in situ hybridization

Specificity of riboprobe and expression pattern of CB1 mRNA in human DLPFC. The specificity of the riboprobe for CB1 mRNA was confirmed by several observations. First, in emulsion-dipped tissue sections, dense silver grain clusters were present over Nissl-stained neuronal nuclei of medium size, presumably inhibitory neurons, whereas very low levels of silver grains appeared over large, presumably pyramidal, neuronal nuclei as previously reported in rodent cortex (Marsicano and Lutz, 1999). Silver grain clusters were not present over glial cells identified by small, intensely Nissl-stained, nuclei **(Fig 24C)**. Second, the distribution of labeled neurons was consistent with previously reported laminar locations of CB1 mRNA-expressing cells in the human prefrontal cortex (Westlake et al., 1994; Wang et al., 2003) and of CB1-immunoreactive cell bodies in monkey and human DLPFC (Eggan and Lewis, 2007). Specifically, the density of CB1 mRNA-positive neurons was highest in layers 2-3s, lowest in deep layer 3, and intermediate in layers 4, 5, and 6 **(Fig 24B)**. Layer 1 did not exhibit CB1

mRNA-positive cell bodies. Third, specificity was confirmed by an absence of signal above background in tissue sections hybridized with the sense riboprobe for CB1 mRNA (data not shown).

Expression of CB1 mRNA in area 9 of subjects with schizophrenia and control subjects. In film autoradiograms, levels of CB1 mRNA expression appeared to be reduced in DLPFC area 9 of subjects with schizophrenia compared to matched control subjects **(Fig. 25)**. Indeed, quantitative measures made through the entire cortical gray matter revealed that the subject with schizophrenia had lower OD measures in 18 of the 23 pairs **(Fig. 26A)**. Comparison of film OD measures between the subject groups revealed that the mean (± SD) level of CB1 mRNA expression was significantly ($F_{(1,21)} = 8.9$; $p = 0.007$) reduced by 14.8% in subjects with schizophrenia (105.4 ± 24.3 nCi/g) compared to the matched control subjects (123.8 ± 17.2 nCi/g) **(Fig. 26A)**.

Laminar expression of CB1 mRNA in area 9 of subjects with schizophrenia and control subjects. In order to determine if the reduction in CB1 mRNA expression observed in subjects with schizophrenia was selective for specific layers, we evaluated the film OD for CB1 mRNA in each cortical layer **(Fig. 26B, C)**. The pattern of OD values across cortical layers was similar between the schizophrenia and control groups; however, the OD values for the schizophrenia group were lower in all layers compared to the control group **(Fig. 26B)**. Analysis of each layer revealed that CB1 mRNA expression was significantly reduced in the schizophrenia group by 15.9% ($F_{(1,21)} = 8.5$; $p = 0.008$) in layers 2-3s, 15.5% ($F_{(1,21)} = 10.2$; $p = 0.004$) in layer 5, and 17.7% ($F_{(1,21)} = 6.8$; $p = 0.017$) in layer 6 **(Fig. 26C)**.
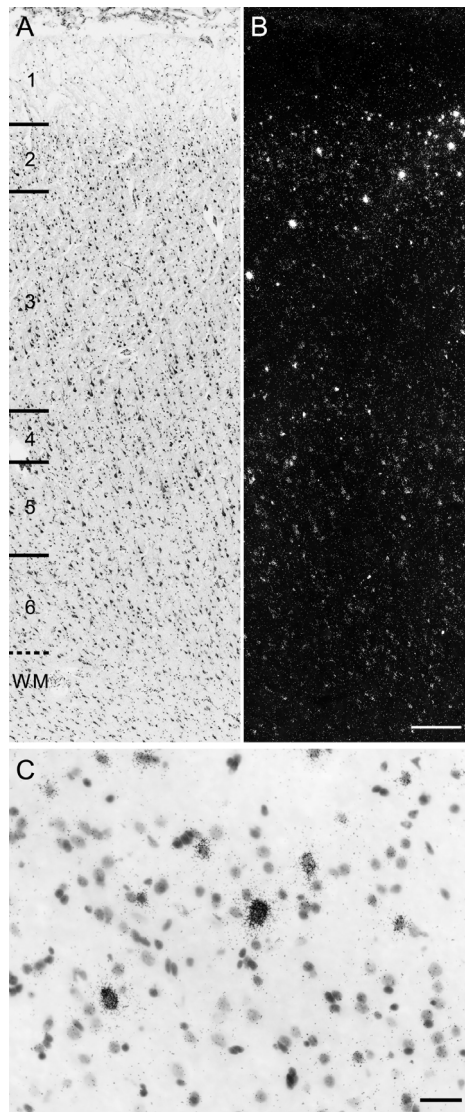
Figure 24. Distribution of silver grain clusters representing CB1 mRNA-positive neurons.
(A) Brightfield photomicrograph of a representative traverse from a Nissl-stained section of a control subject. **(B)** Darkfield photomicrograph of an adjacent emulsion-dipped section illustrating silver grain accumulation over neuronal nuclei of CB1 mRNA-positive neurons. Note that the density of CB1 mRNA-positive neurons appears greatest in layers 2-superficial 3 and that cells in these layers express very high levels of CB1 mRNA. **(C)** Representative high-power brightfield photomicrograph illustrating silver grain accumulation around neuronal nuclei. Numbers and hash marks in **A** indicate the relative positions of the cortical layers, and the dashed lines denote the layer 6-white matter (WM) border. Scale bar = 300 μm in **B** (applies to **A, B**) and 30 μm in **C**.

102
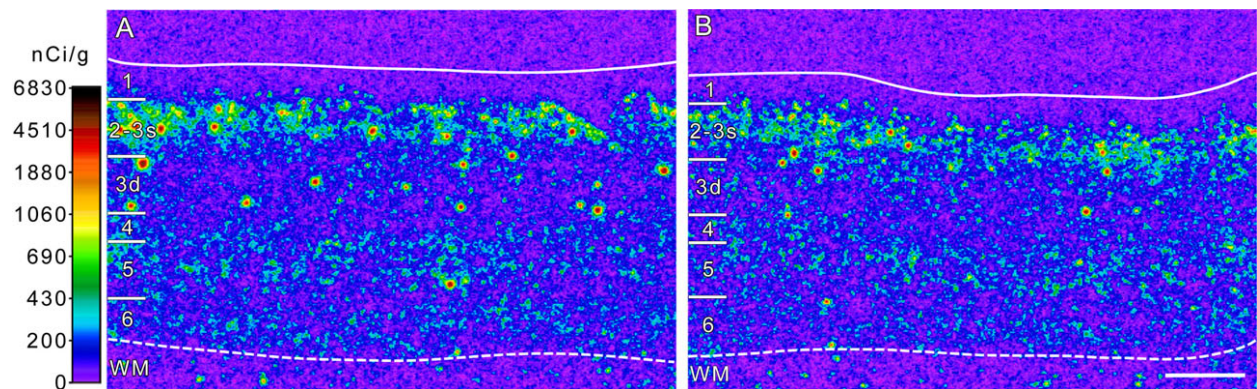
Figure 25. Representative film autoradiograms illustrating the expression of CB1 mRNA in DLPFC area 9 of a control subject (A) and a matched subject with schizophrenia (B) (pair 5; see Table 6). The density of hybridization signal is presented in pseudocolor according to the calibration bar to the left. CB1 receptor mRNA was expressed across layers 2-6, with the highest expression in layers 2 and superficial 3. Expression levels of CB1 mRNA in the schizophrenia subject **(B)** appear lower than in the matched control subject **(A)**. Solid and broken lines denote the pial surface and the gray matter-white matter (WM) border, respectively. Numbers and hash marks to the left indicate the relative positions of the cortical layers. Scale bar (1 mm) in **B** applies to both panels.
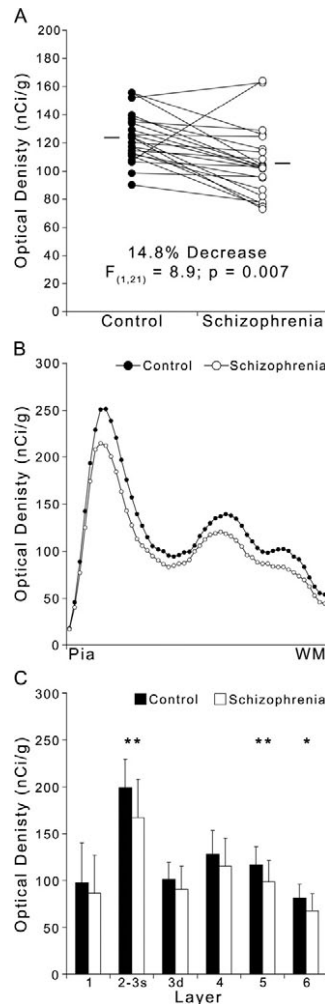
Figure 26. Lower CB1 mRNA expression in DLPFC area 9 of subjects with schizophrenia. (A) Comparison of the cortical expression levels of CB1 mRNA by film optical density in matched pairs of control subjects (filled circles) and subjects with schizophrenia (open circles). CB1 mRNA expression was lower in the subject with schizophrenia in 18 of the 23 pairs. Mean values for each subject group are indicated by horizontal bars. (B) Plot of mean CB1 mRNA optical density across cortical layers from the pial surface to the white matter border (WM) in control and schizophrenia groups. The distinctive laminar pattern of CB1 mRNA expression was similar between the schizophrenia and controls groups; however, the optical density values for the schizophrenia group were lower across all layers. (C) Comparison of mean ($\pm$ SD) film optical density for CB1 mRNA expression in each cortical layer between control and schizophrenia groups. **$p < 0.008$; *$p < 0.02$.

Analysis of potential confounding factors. The observed within-pair percent differences in CB1 mRNA in the subjects with schizophrenia compared to their matched controls did not differ as a function of sex, a diagnosis of schizoaffective disorder, suicide, use of antidepressant medication at time of death, a diagnosis of substance abuse/dependence at time of death, or a history of cannabis use/abuse (all $t_{(21)} < 1.70$; all $p > 0.105$; **Fig. 27**).

In order to test the potential effect of antipsychotic medications on the expression of CB1 mRNA, we evaluated film OD values in DLPFC areas 9 and 46 of monkeys chronically exposed to haloperidol, olanzapine, or sham **(Fig. 28)**. In these monkeys, the laminar distribution of CB1 mRNA expression in all three groups matched the pattern observed in humans **(Fig. 28A-C)**. Mean OD ($\pm$ SD) of CB1 mRNA did not differ ($F_{(2,15)} = p = 0.313$) between the haloperidol (184.6 $\pm$ 13.3 nCi/g), olanzapine (199.1 $\pm$ 16.0 nCi/g), and sham (192.1 $\pm$ 18.2 nCi/g) groups **(Fig. 28D)**.
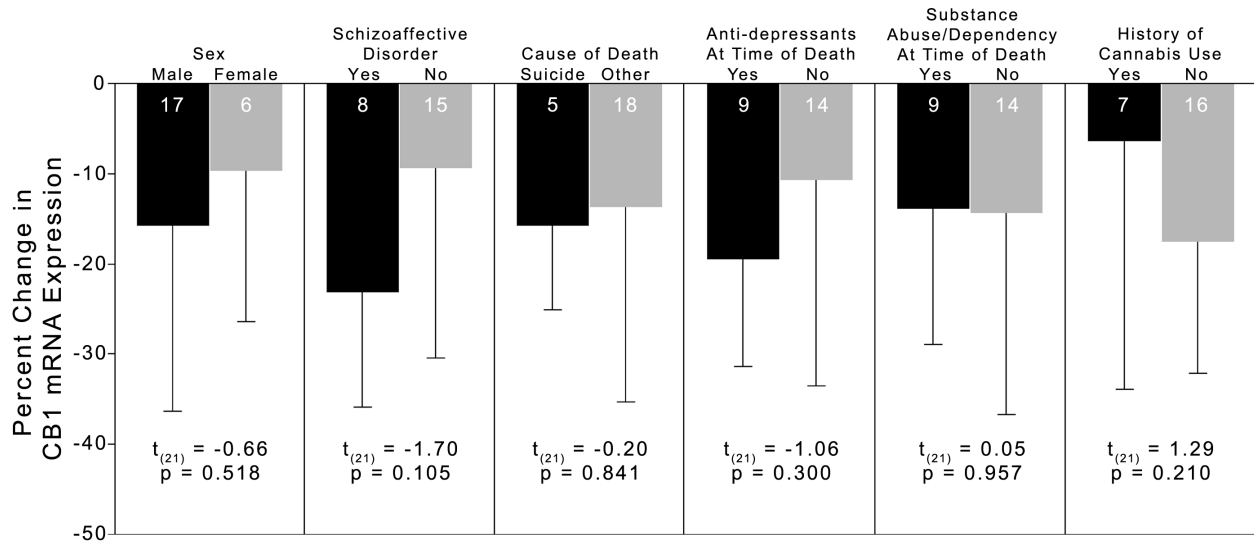
Figure 27. The effects of confounding factors on differences in CB1 mRNA expression in subjects with schizophrenia. Mean (± SD) percent difference from control subjects for CB1 mRNA expression within subject pairs grouped by potential confounding factors in the subjects with schizophrenia. Neither sex, a diagnosis of schizoaffective disorder, suicide, use of antidepressant medication at time of death, a diagnosis of substance abuse/dependence at time of death, nor a history of cannabis use/abuse significantly affected the expression changes in CB1 mRNA expression. Numbers in bars indicate the number of pairs for each category.
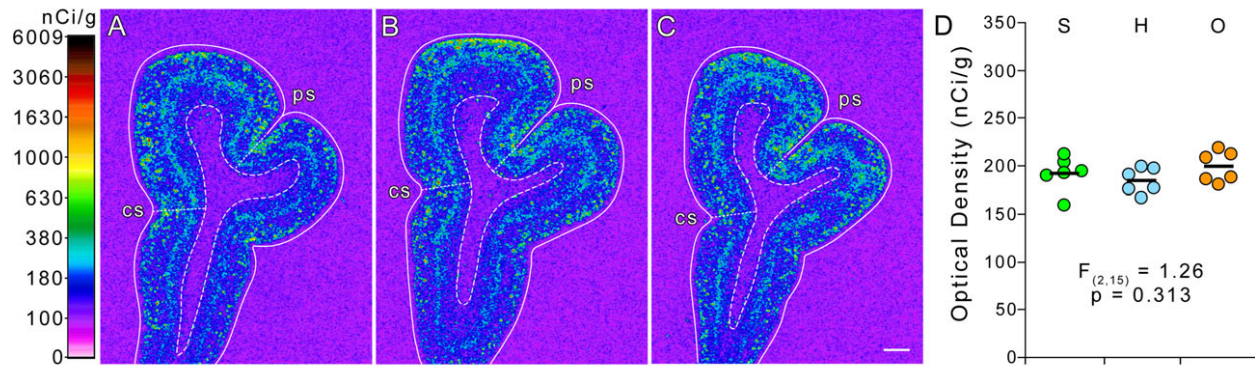
Figure 28. Representative film autoradiograms illustrating the expression of CB1 mRNA in the DLPFC of sham- (A), haloperidol- (B), and olanzapine- (C) exposed monkeys used to mimic the clinical treatment of individuals with schizophrenia. The density of hybridization signal is presented in pseudocolor according to the calibration bar to the left. CB1 mRNA expression was assessed between the cingulate sulcus (cs) and the principal sulcus (ps). Solid and broken lines denote the pial surface and the gray matter-white matter border, respectively. Scale bar (1 mm) in C applies to all panels. **(D)** Comparison of CB1 mRNA expression levels by film optical density in the DLPFC of sham- (S), haloperidol- (H), and olanzapine- (O) exposed monkeys. Hash bars equal group means.

4.4.2 Analysis of CB1 protein expression by radioimmunocytochemistry

Expression of CB1 radioimmunoreactivity in area 9 of subjects with schizophrenia and control subjects. Qualitative examination of film autoradiograms revealed a laminar pattern of CB1 radioimmunoreactivity identical to that of CB1-immunoreactive (IR) axons previously reported in human DLPFC (Eggan and Lewis, 2007). Specifically, the density of CB1 radioimmunoreactivity progressively increased across layers 2 and 3, and layer 4 contained a very dense band of radioimmunoreactivity. The lowest density of CB1 radioimmunoreactivity in layer 5 sharply demarcated the border with layer 4. Layer 6 contained a density of CB1 radioimmunoreactivity similar to that in layers 2-3s **(Fig. 29A)**.

Levels of CB1 radioimmunoreactivity appeared to be reduced in subjects with schizophrenia compared to matched control subjects **(Fig. 29)**. Indeed, quantitative measures made through the entire cortical gray matter revealed that the subject with schizophrenia had lower OD measures in 20 of 23 pairs **(Fig. 30A)**. The mean ($\pm$ SD) level of CB1 radioimmunoreactivity was significantly ($F_{(1,21)} = 8.8$; $p = 0.007$) 11.6% lower in subjects with schizophrenia (192.4 $\pm$ 57.4 nCi/g) compared to matched control subjects (217.6 $\pm$ 70.1 nCi/g) **(Fig. 30A)**. The within-pair percent change in CB1 radioimmunoreactivity in the subjects with schizophrenia strongly correlated with the within-pair percent change in CB1 mRNA expression **(Fig. 30B)**.

Analysis of potential confounding factors. The observed within-pair percent differences in CB1 radioimmunoreactivity did not differ as a function of sex, a diagnosis of schizoaffective disorder, suicide, use of antidepressant medication at time of death, a diagnosis of substance abuse/dependence at time of death (all $t_{(21)} < 1.57$; all $p > 0.131$), or a history of cannabis use/abuse ($t_{(7)} = 0.54$; $p = 0.605$) in the subjects with schizophrenia **(Fig. 31)**.
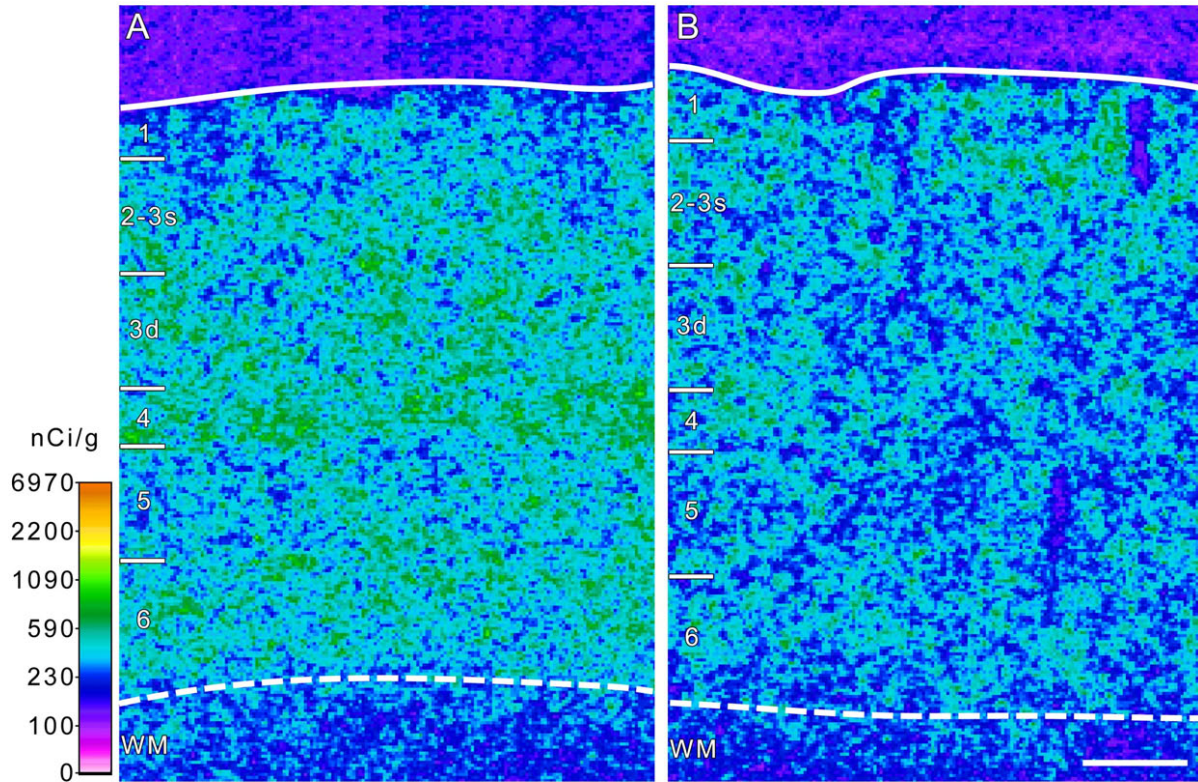
Figure 29. Representative film autoradiograms illustrating the expression of CB1 radioimmunoreactivity in DLPFC area 9 of a control subject (A) and a matched subject with schizophrenia (B) (pair 8; see Table 6). The density of radioimmunoreactivity signal is presented in pseudocolor according to the calibration bar to the left. CB1 radioimmunoreactivity was expressed across all layers, with the highest expression in layer 4. The level of CB1 radioimmunoreactivity in the schizophrenia subject **(B)** appeared lower than in the matched control subject **(A)**. Solid and broken lines denote the pial surface and the gray matter-white matter border, respectively. Numbers and hash marks to the left indicate the relative positions of the cortical layers. Scale bar (500 µm) in **B** applies to both panels.
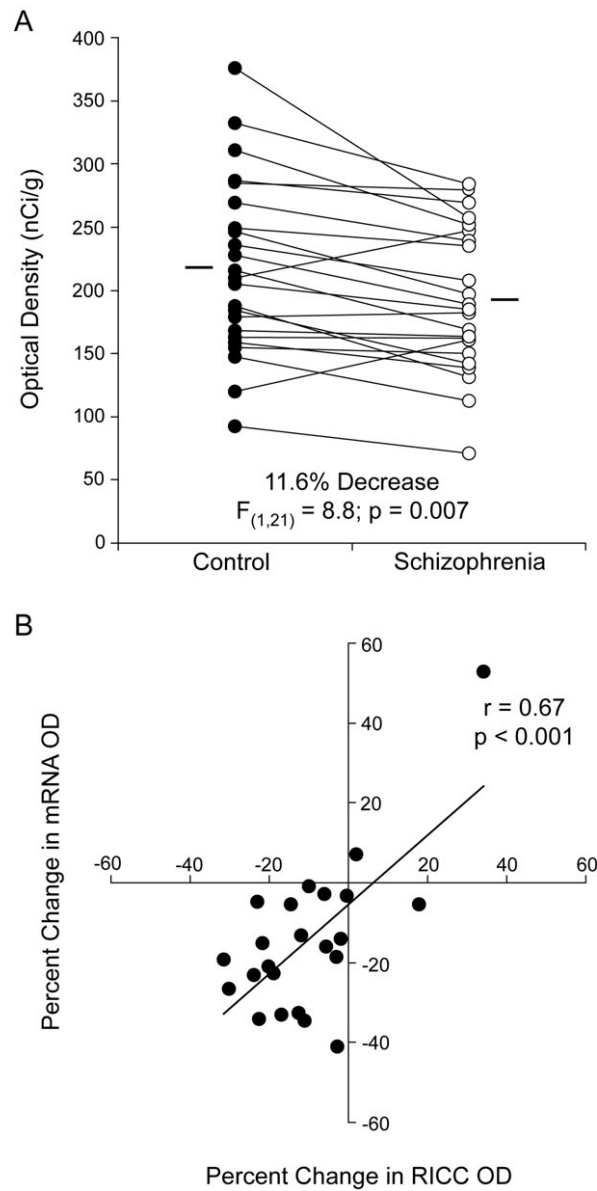
Figure 30. Reduced CB1 radioimmunoreactivity in DLPFC area 9 of subjects with schizophrenia. (A) Comparison of the cortical levels of CB1 radioimmunoreactivity by film optical density in matched pairs of control subjects (filled circles) and subjects with schizophrenia (open circles). CB1 radioimmunoreactivity was reduced in the subject with schizophrenia in 20 of the 23 pairs. Mean values for each subject group are indicated by horizontal bars. **(B)** The within-pair percent change in CB1 radioimmunoreactivity strongly correlated with the within-pair percent difference in CB1 mRNA expression.
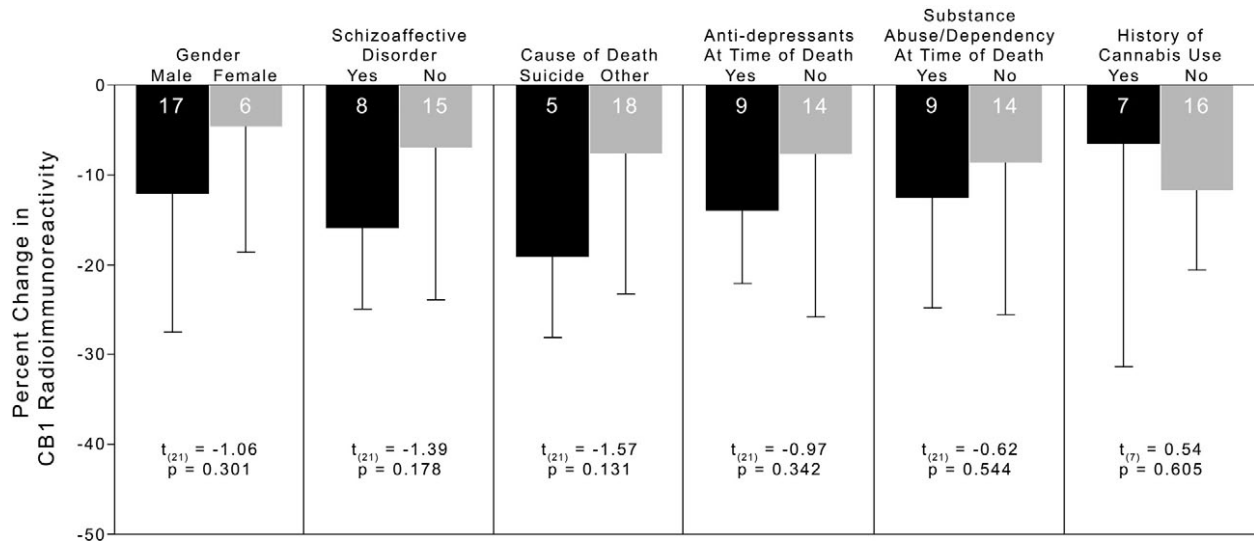
Figure 31. The effects of confounding factors on the changes in CB1 radioimmunoreactivity in subjects with schizophrenia. Mean (± SD) percent difference from control subjects for CB1 radioimmunoreactivity within subject pairs grouped by potential confounding factors in the subjects with schizophrenia. Neither sex, a diagnosis of schizoaffective disorder, suicide, use of antidepressant medication at time of death, a diagnosis of substance abuse/dependence at time of death, nor a history of cannabis use/abuse significantly affected the expression changes in CB1 radioimmunoreactivity. Numbers in bars indicate the number of pairs for each category.

4.4.3 Analysis of CB1 protein expression by immunocytochemistry

Expression of CB1 immunoreactivity in area 9 of subjects with schizophrenia and control subjects. In order to confirm the observed decrease in CB1 protein by radioimmunocytochemistry and to assess the potential affect of laterality, we performed standard immunocytochemistry in the fixed left hemisphere of 12 of the 23 subject pairs. In both control subjects and subjects with schizophrenia, intense CB1 immunoreactivity was observed primarily in axons and boutons as previously described (Eggan and Lewis, 2007). The laminar pattern of CB1-immunoreactive (IR) axons was identical to the pattern of CB1 radioimmunoreactivity described above **(Fig. 32)**.

The overall density of CB1-IR axons appeared to be reduced in the subjects with schizophrenia compared to matched control subjects **(Fig. 32)**. Indeed, quantitative measures made through the entire cortical gray matter revealed that the subject with schizophrenia had lower OD measures in 10 of 12 pairs **(Fig. 33A)**. The mean OD ($\pm$ SD) level of CB1 immunoreactivity was significantly ($F_{(1,11)} = 6.6$; $p = 0.026$) reduced by 13.9% in subjects with schizophrenia (0.230 $\pm$ 0.045) compared with matched control subjects (0.198 $\pm$ 0.023; **Fig. 33A**).

Laminar density of CB1-IR axons in area 9 of subjects with schizophrenia and control subjects. In order to determine if the reduction in CB1 immunocytochemistry observed in subjects with schizophrenia was selective for specific layers, we evaluated the relative OD of CB1 immunoreactivity in each cortical layer **(Fig. 33B, C)**. Laminar analysis was performed in tissue processed for standard immunocytochemistry because this method preserves axon morphology and produced better resolution of cytoarchitectonically-defined laminar boundaries. The pattern of OD values across cortical layers was similar between the schizophrenia and control groups; however, the OD values for the schizophrenia group were lower across all layers compared to the control group **(Fig. 33B)**. Analysis of each layer revealed that CB1 immunoreactivity was significantly reduced in the schizophrenia group by 15.2% ($F_{(1,11)} = 6.7$; $p = 0.026$) in layer 3d, 16.9% ($F_{(1,11)} = 6.8$; $p = 0.025$) in layer 4, and 17.5% ($F_{(1,11)} = 12.4$; $p = 0.005$) in layer 6 **(Fig. 33C)**.

Analysis of potential confounding factors. The observed within-pair percent differences in CB1 immunoreactivity in the subjects with schizophrenia compared to their matched controls did not differ as a function of sex, a diagnosis of schizoaffective disorder, suicide, use of antidepressant medication at time of death, a diagnosis of substance abuse/dependence at time of death (all $t_{(11)} < 1.27$; all $p > 0.232$), or a history of cannabis use/abuse ($t_{(8)} = -0.06$; $p = 0.957$) (data not shown).
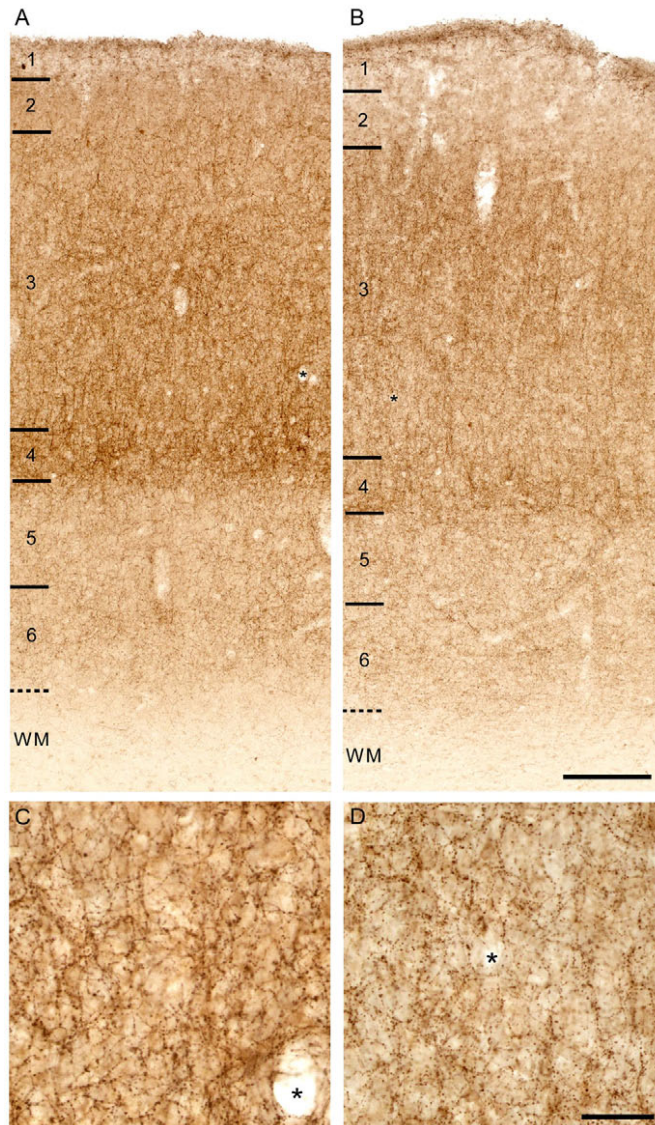
Figure 32. Brightfield photomicrographs demonstrating the density and laminar pattern of CB1 immunoreactivity in DLPFC area 9 of a control subject (A) and a matched subject with schizophrenia (B) (pair 4; see Table 6). Intense CB1 immunoreactivity was observed primarily in axons and boutons **(C, D)**. The density of CB1-IR axons and varicosities appeared to be decreased in the subject with schizophrenia **(B, D)** compared to the matched control **(A, C)**. Numbers and hash marks to the left indicate the relative positions of the cortical layers, and the dashed lines denote the layer 6-white matter (WM) border. Asterisk denote the same blood vessel in **A, C** and **B, D**. Scale bars = 300 μm in **B** (applies to **A, B**) and 50 μm in **D** (applies to **C, D**).
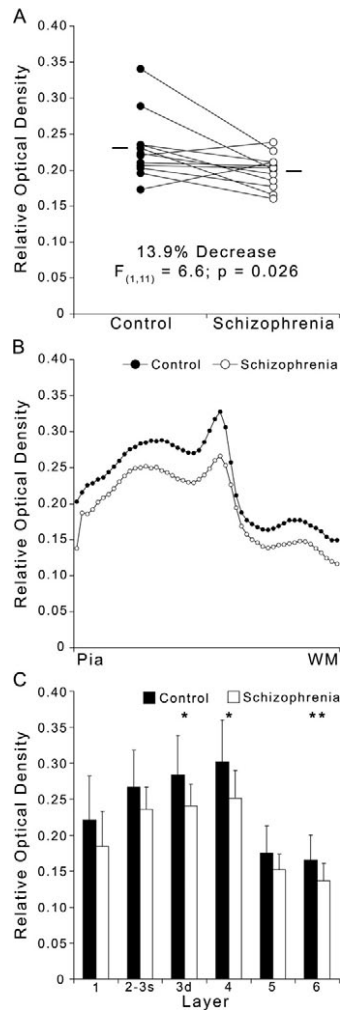
Figure 33. Reduced CB1 immunoreactivity in DLPFC area 9 of subjects with schizophrenia. (A) Comparison of the cortical relative optical density levels of CB1 immunoreactivity in matched pairs of control subjects (filled circles) and subjects with schizophrenia (open circles). Mean values for each subject group are indicated by horizontal bars. (B) Plot of the relative optical density of CB1 immunoreactivity across cortical layers from the pial surface to the white matter border (WM) in control (filled circles) and schizophrenia (open circles) groups. The distinctive laminar pattern of CB1 immunoreactivity was similar between the schizophrenia and control groups; however, the relative optical density levels of CB1 immunoreactivity for the schizophrenia group were reduced across all layers compared to the control group. (C) Comparison of mean (± SD) relative optical density of CB1 immunoreactivity in each cortical layer between control (closed bars) and schizophrenia (open bars) groups. **$p = 0.005$; *$p < 0.03$.

115

4.4.4 Correlation of altered CB1 mRNA expression with changes in other GABA related transcripts

In a previous study, we found that the expression of GAD_{67} and CCK mRNAs were significantly reduced in DLPFC area 9 in the same cohort of subjects used in this study (Hashimoto et al., 2007). In addition, the within-pair percent changes in GAD_{67} and CCK mRNAs in the subjects with schizophrenia were significantly correlated ($r = 0.81$; $p < 0.001$) suggesting that CCK-containing neurons exhibit a deficit in GABA synthesis (Hashimoto et al., 2007). Given that CB1 mRNA is highly expressed by CCK interneurons in the neocortex, the observed changes in CB1 mRNA were hypothesized to be associated with changes in these GABA-related mRNA levels; consistent with this prediction the within-pair percent change in CB1 mRNA expression was significantly correlated with the within-pair percent changes in GAD_{67} mRNA ($r = 0.64$, $p = 0.001$) and CCK mRNA ($r = 0.68$; $p < 0.001$) expression levels (**Fig. 34**).
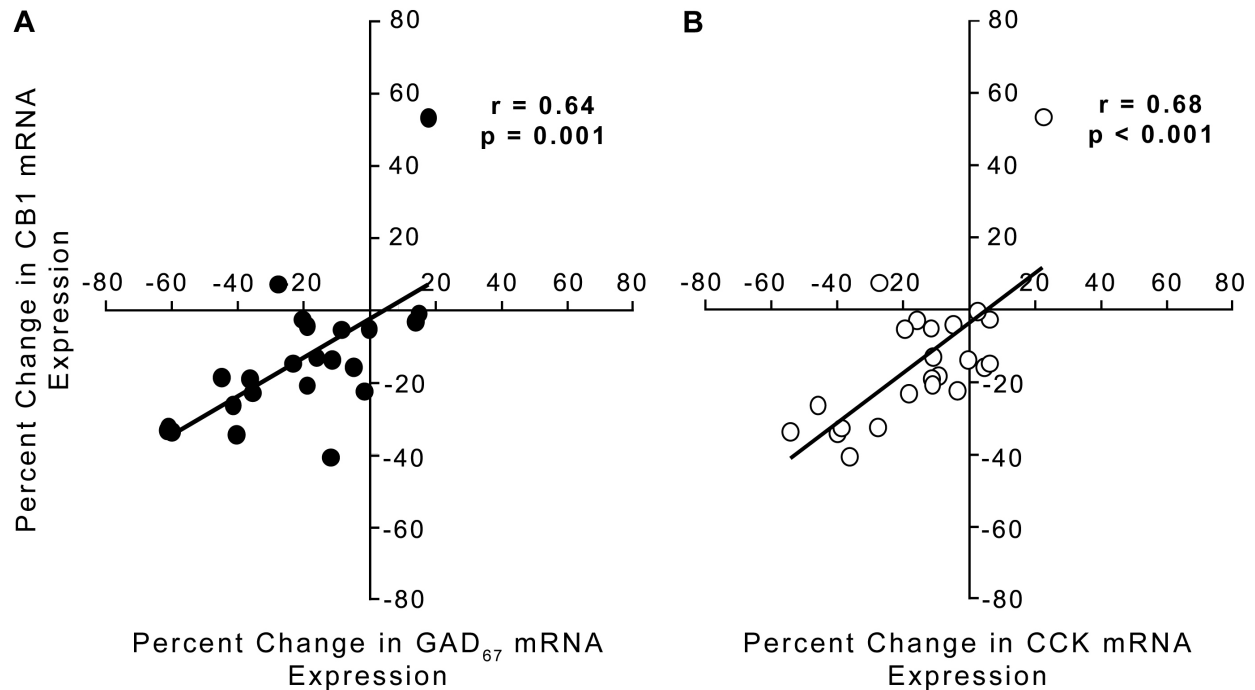
Figure 34. Correlation analyses between the differences in CB1 mRNA and GAD$_{67}$ or CCK mRNA expression across subject pairs. The within-pair percent difference in CB1 mRNA expression is plotted against those for GAD$_{67}$ **(A)** or CCK **(B)** mRNA expression (from Hashimoto et al., 2007) for the 23 subject pairs. Changes in CB1 mRNA expression significantly correlated with changes in GAD$_{67}$ and CCK mRNA expression across the 23 subject pairs.

4.5   DISCUSSION

In order to explore the potential role of the CB1 receptor in DLPFC dysfunction in schizophrenia, we examined the expression of CB1 receptor mRNA and protein. We found that 1) the levels of CB1 receptor mRNA and protein are significantly reduced in the DLPFC of subjects with schizophrenia; 2) these reductions cannot be explained by potential confounding factors, suggesting that a reduction in CB1 receptors is intrinsic to the disease process of schizophrenia; and 3) the observed changes in CB1 receptor mRNA expression correlated with expression changes in GAD_{67} and CCK mRNA in the same subjects with schizophrenia, suggesting that downregulation of the CB1 receptor may be a compensatory response to impaired GABA neurotransmission in CCK-containing neurons.

Several lines of evidence indicate that the observed reductions in CB1 mRNA and protein expression were not a consequence of factors frequently associated with schizophrenia. First, CB1 mRNA expression was not altered in the DLPFC of monkeys chronically exposed to typical or atypical antipsychotics in a manner that mimics the clinical treatment of schizophrenia (**Fig. 28**). Consistent with these observations, the four subjects with schizophrenia (537, 622, 829, and 621) who were not receiving antipsychotic medications at the time of death showed decreased expression of CB1 mRNA or protein compared to their matched controls.

Second, it is unlikely that comorbid substance use contributed to the reductions in CB1 mRNA and protein. Neither a diagnosis of substance abuse and/or dependence present at the time of death, nor a history of cannabis use, accounted for the group differences in CB1 mRNA or protein expression (**Figs. 27, 31**). In addition, the two control subjects (516 and 685) who had positive plasma alcohol levels at the time of death had higher expression levels of both CB1 mRNA and protein than their matched controls. Consistent with these observations, rodent studies demonstrated that substances of abuse do not affect CB1 mRNA expression or CB1 binding in the neocortex [with the exception of cocaine, which only affected CB1 mRNA levels (Gonzalez et al., 2002; Ortiz et al., 2004)] and that chronic exposure to CB1 agonists does not alter CB1 mRNA expression (Romero et al., 1998; Garcia-Gil et al., 1999).

Third, the observed reductions in CB1 mRNA and protein expression did not appear to be associated with the use of antidepressant medication at the time of death, death by suicide, or a diagnosis of schizoaffective disorder **(Fig. 27, 31)**.

Finally, the levels of some mRNA species may be affected by premortem agonal state events associated with hypoxia and acidosis (Stan et al., 2006). An accurate indicator of mRNA quality is the RIN value: RIN values >7.0 represent high RNA quality and all subjects had a RIN value greater than 7.0. Furthermore, the RIN values did not differ between the subject groups. In addition, in the same subjects used in this study the expression of other transcripts was not altered in schizophrenia (Hashimoto et al., 2003; Hashimoto et al., 2005; Hashimoto et al., 2007), confirming that the observed reductions in CB1 mRNA are not attributable to a general deterioration of mRNA integrity in the subjects with schizophrenia.

In contrast to our findings of reduced levels of CB1 receptor mRNA and protein increased binding of the CB1 agonist [^{3}H]CP-55940 was reported in the DLPFC (Dean et al., 2001) and posterior cingulate cortex (Newell et al., 2006) of subjects with schizophrenia. Increased binding of the CB1 receptor antagonist [^{3}H]SR141716 was also reported in the anterior cingulate cortex of subjects with schizophrenia (Zavitsanou et al., 2004). The apparent discrepancy between these findings and those of the present study may be due to the fact that the radioligands used in these studies bind receptors other than CB1. CP-55940 is known to be a non-specific CB1 agonist, and SR141716 has functional effects in CB1 knockout mice suggesting that it binds receptors other than the CB1 receptor (Breivogel et al., 2001; Hajos et al., 2001). Therefore, the increased binding of radioligands in subjects with schizophrenia in these studies may represent binding to receptors other than CB1. This argument is strengthened by the fact that the laminar patterns of radioligand binding described in these studies did not match the laminar distribution of CB1-IR axons and varicosities in the same regions of monkey and human brains (Eggan and Lewis, 2007).

Disturbances in inhibitory neurotransmission appear to play a prominent role in the dysfunction of the DLPFC of subjects with schizophrenia (Lewis et al., 2005). Indeed, in postmortem studies one of the most consistent findings is a ~25-35% reduction in the expression of GAD_{67} mRNA, across layers 2-5 in the DLPFC of subjects with schizophrenia (Akbarian et al., 1995; Guidotti et al., 2000; Volk et al., 2000; Straub et al., 2007). Parvalbumin-containing interneurons appear to account for the decreased GAD_{67} mRNA expression in layers 3 and 4

119

(Hashimoto et al., 2003), and the results of the present study suggest that CB1/CCK containing neurons may contribute to the GAD_{67} mRNA deficit in layers 2-superficial 3. Specifically, in the primate DLPFC, the highest densities of both CB1- and CCK-positive neurons are found in these layers and both CB1- and CCK-positive axon terminals densely innervate layer 4 (Oeth and Lewis, 1990; Eggan et al., 2007). In addition, these two proteins are colocalized in terminals that furnish perisomatic inputs to pyramidal neurons (Marsicano and Lutz, 1999; Galarreta et al., 2004; Bodor et al., 2005). Thus, the finding in the present study of reduced CB1 mRNA in layers 2-superfical 3, reduced CB1 immunoreactivity in layer 4, and correlated changes in CB1, CCK and GAD_{67} mRNAs in schizophrenia converge on the interpretation that GABA neurotransmission is altered in the subset of CB1/CCK-containing GABA neurons that project from the superficial to middle cortical layers.

How might these disturbances be related to the working memory impairments associated with DLPFC dysfunction in schizophrenia? In the human DLPFC, the power of gamma band oscillations (30-80 HZ) increases specifically with, and in proportion to, working memory load (Howard et al., 2003), and impairments in cognitive control and working memory in individuals with schizophrenia are associated with reduced frontal lobe gamma band power (Cho et al., 2006). GABA neurotransmission in the DLPFC is essential for both working memory performance (Sawaguchi et al., 1988; Rao et al., 2000) and oscillatory activity (Glickfeld and Scanziani, 2006). Interestingly, in line with the anatomical localization of CB1 receptors to CCK-containing neuron axon terminals, activation of CB1 receptors inhibits GABA release from these terminals and strongly suppresses $GABA_A$ receptor-mediated inhibitory postsynaptic currents in pyramidal neurons (Trettel et al., 2004; Galarreta et al., 2004; Bacci et al., 2004; Bodor et al., 2005). Indeed, the acute activation of CB1 receptors with exogenous cannabinoids decreases the power of gamma oscillations presumably by disrupting the synchronous firing of pyramidal neurons (Hajos et al., 2000b; Robbe et al., 2006). Thus, the disruption of gamma oscillations by CB1 receptor activation may explain the impairments in working memory performance in both humans and animals following systemic administration of cannabinoids (Winsauer et al., 1999; Schneider and Koch, 2003; D'Souza et al., 2004).

Based on these observations, the down regulation of CB1 receptor mRNA and protein in schizophrenia may be considered a compensatory response to a deficit of GABA synthesis in CCK-containing neurons. That is, a lower density of CB1 receptors could, by reducing the

endocannabinoid-mediated block of GABA release from the perisomatic inhibitory terminals of CB1/CCK containing interneurons, contribute to a partial normalization of gamma band power and working memory function. This interpretation implies that cannabis exposure in vulnerable individuals would impair this compensatory response, providing a potential mechanism linking cannabis exposure with an increased risk for the cognitive impairments of schizophrenia.

This interpretation also suggests possible novel molecular targets for treating the cognitive deficits in schizophrenia. For instance, CB1 receptor antagonists would be predicted to augment the intrinsic compensatory down-regulation of CB1 receptor expression, further limit the endocannabinoid-mediated suppression of GABA release from CB1/CCK containing terminals, and enhance the ability of CCK basket neurons to synchronize pyramidal neurons in gamma oscillations. In addition, at least in the hippocampus, $GABA_A$ receptors containing the α2 subunit are selectively located on pyramidal cell bodies post-synaptic to CB1/CCK-containing terminals (Nyiri et al., 2001). Thus, positive allosteric modulators of the benzodiazepine binding site with selectivity for $GABA_A$ receptors containing the α2 subunit would be predicted to increase the efficacy of GABA released from CB1/CCK-containing terminals, and might be synergistic with the proposed effects of such agents at augmenting the input from parvalbumin-containing chandelier neurons to the axon initial segment of pyramidal neurons (Lewis et al., 2004b; Volk and Lewis, 2005). Together, such agents might enhance the synchronization of pyramidal neuron activity by restoring normal levels of perisomatic GABA input to pyramidal neurons.

5.0   GENERAL DISCUSSION

In this dissertation, we were drawn to the potential relationship between the endocannabinoid system and schizophrenia on the basis of epidemiological evidence indicating that exposure to cannabis represents a significant risk factor for the development of the illness. Furthermore, data in the rodent demonstrated that the CB1 receptor is expressed by CCK basket neurons, that activation of this receptor strongly modulates GABA neurotransmission, and that the CB1 receptor mediates network activity that is necessary for working memory, all of which are known to be dysfunctional in subjects with schizophrenia. The main conclusion was that correlated changes in CB1, CCK and GAD_{67} mRNAs suggest that GABA neurotransmission is altered in the subset of CB1/CCK-containing GABA neurons within the DLPFC of subjects with schizophrenia **(Fig. 35)**. We posited that the CB1/CCK-containing GABA neurons may account for the GABA neurons in layers 2-superficial 3 that exhibit reduced GAD_{67} mRNA expression **(see chapter 1.2.3)**. We interpret the data to indicate that, in schizophrenia, a down regulation of CB1 receptor mRNA and protein may be a compensatory response to a deficit in GABA synthesis in order to increase GABA release from the perisomatic inhibitory terminals of CB1/CCK containing interneurons. Furthermore, since CB1/CCK-containing basket neurons appear to play a critical role in regulating the synchronization of pyramidal neuron firing during working memory, these findings suggest that the alterations in CB1/CCK-containing basket neurons in schizophrenia represent a neuropathological entity that gives rise to the pathophysiology of altered gamma oscillations and the clinical feature of impaired working memory.

Previous postmortem investigations indicate that the chandelier class of GABA neurons exhibit reduced GABA synthesis and down regulate PV and GAT1 and upregulate the $GABA_A$ α_2 subunit as compensatory responses (Lewis et al., 2005) **(chapter 1.2.3; Fig. 35)**. Together, these data and the data of this dissertation suggest that pyramidal neurons that receive convergent

perisomatic input from PV-containing chandelier neurons and CB1/CCK-containg basket neurons are likely to be severely dysregulated in subjects with schizophrenia (**Fig. 35)**.

In the following discussion, I will address some caveats and confounds not addressed in individual data chapters. I will explore the role of cannabis use and reductions in CB1 receptor expression in the disease process of schizophrenia by constructing a cascade of events model that incorporates previous findings in the illness and the findings of this dissertation **(Fig. 36)**. Finally, I will present a proposal for a therapeutic intervention strategy, and end with a brief discussion of important future directions.
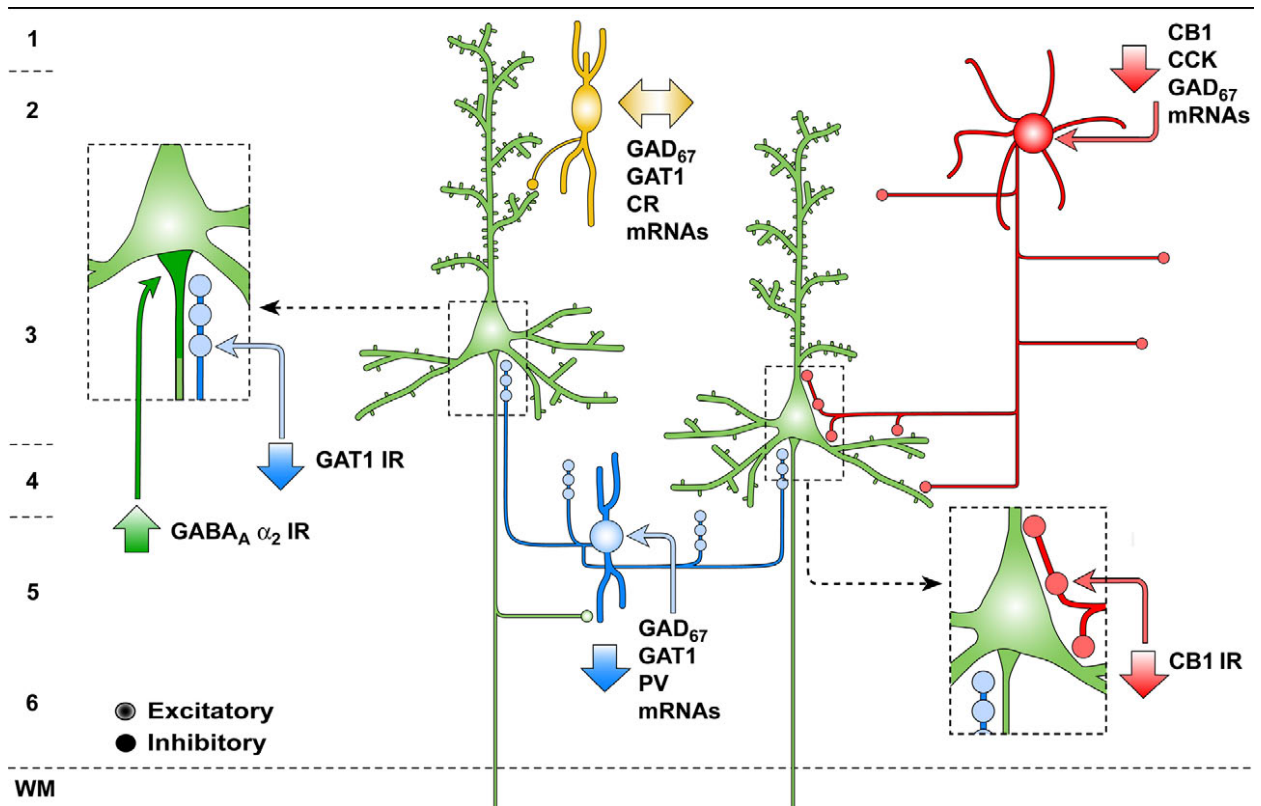
Figure 35. Schematic summary of alterations in perisomatic GABA circuitry in the dorsolateral prefrontal cortex of individuals with schizophrenia. CCK-containing large basket neurons (red) represent a separate, but convergent, source of perisomatic inhibition from PV-containing neurons. CCK-containing basket neurons exhibit reduced levels of CB1, CCK, and GAD_{67} mRNAs and these reduced levels of gene expression are associated with a decrease in CB1 immunoreactivity. Reduced levels of gene expression in chandelier neurons (blue) are associated with a decrease in immunoreactivity for GABA (γ-aminobutyric acid) transporter 1 (GAT1) in the axon cartridges of these neurons and an upregulation of $GABA_A$ receptor α_2 subunit immunoreactivity in the postsynaptic axon initial segment of pyramidal neurons (green). Gene expression in the calretinin (CR)-expressing subpopulation of GABA neurons (yellow) does not seem to be altered. CB1, cannabinoid 1 receptor; CCK, cholecystokinin; GAD_{67}, 67 kD isoform of glutamic acid decarboxylase; PV, parvalbumin; 1-6, layers of dorsolateral prefrontal cortex.

5.1 CAVEATS AND CONFOUNDS

In **chapters 2 and 3** we demonstrated that CB1 immunoreactivity is extensively found in a subset of CCK-containing neurons and axons and that CB1-IR axon terminals exclusively form symmetric synapses. These findings are consistent with previous immunocytochemical experiments (Katona et al., 1999; Katona et al., 2000; Hajos et al., 2000a; Bodor et al., 2005) and the known physiological effects of CB1 receptors on GABA release and participation in DSI in the neocortex (Trettel et al., 2004; Bodor et al., 2005). However, in contrast to our findings, several studies suggest that CB1 receptors might be located presynaptically in pyramidal cell axon terminals in the neocortex where they could modulate excitatory transmission (Auclair et al., 2000; Hajos et al., 2001). For instance, the application of CB1 receptor agonists has been shown to reduce the amplitude of excitatory postsynaptic potentials and endogenous cannabinoids have been reported to mediate depolarization-induced suppression of excitation (DSE) (reviewed in Chevaleyre et al., 2006). In addition, low levels of CB1 mRNA expression have been observed in pyramidal neurons (Marsicano and Lutz, 1999; **chapter 4** of this dissertation). Until recently, the physiological effects of CB1 receptor activation on glutamate transmission and mRNA findings were unsubstantiated by anatomical investigations utilizing immunocytochemistry. However, two recent studies using a well characterized and specific rabbit anti-CB1 antibody raised against the C-terminus (amino acid residues 443-473) of the rat CB1 receptor reported asymmetric synapses formed by CB1-IR axon terminals in the rat hippocampus, suggesting that CB1 receptors are located in excitatory terminals that release glutamate (Kawamura et al., 2006; Katona et al., 2006). This discrepancy is not likely to be due to antibody specificity because the anti-CB1 antibodies utilized in the experiments of this dissertation were shown to meet the "gold standards" of antibody specificity in **chapter 2**, (Saper and Sawchenko, 2003; Saper, 2005). In addition to the arguments presented in **chapter 2.5.1**, the apparent discrepancy between these findings and those of **chapter 3** may be due to the fact that pyramidal neurons selectively express a CB1 receptor-interacting protein (CRIP1B), which putatively binds to the last nine amino acids of CB1 receptor C-terminus (Niehaus et al., 2004). This CB1 receptor-interacting protein may mask the epitope of the CB1 receptor that the rabbit

anti-CB1-L14 antibody recognizes and may have rendered CB1 receptors in asymmetric synapses nonimmunoreactive to the antibody used in our studies. However, the rabbit anti-CB1-CT antibody recognizes the entire C-terminus of the CB1 receptor and was not found to label asymmetric synapses in chapter 2 or in other reports in rodent (Hajos et al., 2000b; Katona et al., 2001; Bodor et al., 2005). A more likely explanation is that the expression of CB1 receptors in excitatory terminals is below the threshold of immunocytochemical detection with the rabbit anti-CB1-L14 antibody. Consistent with this idea, Kawamura and colleagues (2006) using semi-quantitative immunogold electron microscopy, found that in the hippocampus and cerebellum, the density of CB1 receptors in inhibitory synapses was 20- to 30-fold higher in inhibitory terminals than in excitatory terminals. Furthermore, electrophysiological studies have revealed a substantial difference in the sensitivity of CB1 receptors in inhibiting the release of neurotransmitter from inhibitory verses excitatory terminals; i.e. the concentration of CB1 receptor agonist necessary for 50% suppression of neurotransmitter release from excitatory terminals is on the order of 30 times higher than the concentration necessary to affect release from inhibitory terminals (Ohno-Shosaku et al., 2002).

In **chapter 3**, several factors may have contributed to an underestimation of the number of immunoreactive profiles. First, the fixatives used during animal perfusion are necessary for ultrastructural preservation may reduce immunoreactivity. This was apparent in tissue processed for CB1 immunoperoxidase labeling, where the density of labeled axons was noticeably reduced compared to tissue prepared for light microscopy. The procedure of processing tissue for electron microscopy investigation requires a low concentration of detergent in order to maintain membrane integrity, which may reduce antibody penetration into the tissue. Decreased penetration of primary and secondary antibodies may result in an increase in false negatives in labeled tissue. However, although these issues may decrease the incidence of labeled structures it should not affect the proportional frequency of labeled terminals.

In **chapter 4**, we argued that the subset of CB1/CCK-containing GABA neurons is altered in schizophrenia and that these neurons account for the observed reduced expression of CB1 mRNA and protein in the DLPFC of subjects with the illness. One caveat to this interpretation is that the reduction in CB1 mRNA expression could be partially due to reductions in pyramidal neurons. In **chapter 4** we used riboprobes because they are more specific than oligonucleotide probes. However, use of riboprobes requires treatment with RNase, which

reduces cellular morphology in cresyl violet counterstaining precluding the definitive identification of interneurons and pyramidal neurons. However, we found that changes in CB1 mRNA expression correlated with changes in CB1 radioimmunoreactivity (**Fig. 30; chapter 4.4.2**). As described above, given that our antibody appears to selectively label CB1 receptors in inhibitory axons, these data suggest that the reductions in CB1 radioimmunoreactivity and immunoreactivity in subjects with schizophrenia reported in **chapter 4** are likely to reflect specific decreases in the expression of CB1 receptor protein in inhibitory neurons and axons terminals rather than in pyramidal neurons and axons. Given the high correlation of changes in CB1 mRNA with changes in GAD_{67} and CCK mRNAs, the observed changes in CB1 are unlikely due to decreased CB1 mRNA in pyramidal cells, although this possibility cannot be completely ruled out.

5.2   UNDERSTANDING THE DISEASE PROCESS OF SCHIZOPHRENIA: AN UPDATE

Once neuropathological entities in schizophrenia have been identified it must be determined how those alterations fit in to the cascade of the disease process. That is, is an alteration a potential causal factor, a deleterious consequence of an upstream factor, or a compensatory response? Understanding where observed abnormalities fit in to this cascade is important for the development of therapeutic interventions because those alterations that are most proximal to the pathophysiology (reduced gamma oscillations; see **chapter 1.2**) that give rise to the clinical symptoms are often the most effective targets for treating the illness.

In **chapter 1.2.3** I reviewed previous findings indicating that reductions in PV and GAT1 proteins in chandelier neuron cartridges and increases in the $GABA_A$ receptor α_2 at the axon initial segment represent neuropathological entities in the DLPFC of subjects with schizophrenia. In this dissertation, we identified reductions in the expression of the CB1 receptor mRNA and protein in CCK neurons as a novel neuropathological entity in the DLPFC of individuals with schizophrenia. We have argued that these alterations represent a compensatory response to reduced GAD_{67} mRNA expression. Here, I will provide evidence for these interpretations by constructing a cascade of events model incorporating the alterations observed in PV-containing

chandelier and CB1/CCK-containing neurons into the cascade of the disease process (**Fig. 36**). I will show that these two separate disease process pathways converge on a common pathophysiology that gives rise to working memory impairments, a core clinical feature of schizophrenia (**Fig. 36**).

5.2.1 Etiopathogenetic mechanisms underlying reduced GAD$_{67}$

The importance of the observed changes in PV-containing chandelier and CB1/CCK-containing neurons and the validity of our interpretations would be strengthened by showing that they can be the consequence of upstream causal factors. Here, I will discuss a couple possibilities, although there are many plausible mechanisms.

5.2.1.1 Evidence for the involvement of reduced excitatory transmission in schizophrenia

Altered glutamate neurotransmission has been implicated in the pathophysiology of schizophrenia (reviewed in Moghaddam, 2003; Konradi and Heckers, 2003). Specifically, clinical observations suggest the involvement of a deficit in glutamate-meditated excitatory transmission via the NMDA receptor in the disorder (Moghaddam, 2003; Konradi and Heckers, 2003). For example, NMDA receptor antagonists such as the psychotomimetic drug phencyclidine (PCP) or ketamine produce schizophrenia-like symptoms in healthy individuals and exacerbate both positive and negative symptoms in individuals with schizophrenia (Moghaddam, 2003; Konradi and Heckers, 2003). Furthermore, subanesthetic doses of ketamine produce cognitive impairments in healthy individuals (Krystal et al., 1994), systemic administration of NMDA antagonists impairs working memory in rats (Verma and Moghaddam, 1996), and perfusion of an NMDA receptor blocker in the DLPFC disrupts working memory function in macaque monkeys (Dudkin et al., 2001). These data converge on the idea that NMDA receptor hypofunction could contribute to the pathophysiology of schizophrenia.

In addition to these clinical observations, postmortem studies have reported significant alterations in glutamate receptor binding, as well as changes in transcription and protein expression that result in alterations in the composition of NMDA receptor subunits across a number of brain regions in schizophrenia, including the DLPFC (Konradi and Heckers, 2003). These changes are modest in magnitude and not consistently replicated making it difficult to

128

draw conclusions about NMDA receptor hypofunction based on these data alone (Konradi and Heckers, 2003). However, NMDA receptor hypofunction does not necessarily have to result from reduced levels of NMDA receptors. For example, recently identified gene variants that have been associated with an increased risk for schizophrenia can influence the function of modulatory sites on the NMDA receptor or proteins that regulate NMDA intracellular signal transduction pathways (Moghaddam, 2003; Harrison and Weinberger, 2005). Consistent with this interpretation, variants in the gene for neuregulin 1 (*NRG1*) have been implicated as a susceptibility gene in schizophrenia (Stefansson et al., 2002) and can reduce NMDA receptor activation through interactions with erbB4 receptors in the DLPFC of subjects with schizophrenia (Hahn et al., 2006).

Reduced excitatory transmission can be an independent neuropathology in schizophrenia that underlies cognitive impairments in the illness (Moghaddam, 2003). However, reduced excitatory transmission can also be linked to the observed reductions in the expression of GABA-related markers discussed in **chapter 1.2.3** and **chapter 4**. For instance, the expression of GAD_{67} is activity dependent suggesting that the observed reductions in this transcript in schizophrenia could be secondary to reduced excitatory drive to GABA neurons in the DLPFC (Jones, 1997) **(Fig. 36)**. Consistent with this idea, neonatal lesions of the ventral hippocampus, which furnish excitatory inputs to the prefrontal cortex, produce deficits in GAD_{67} mRNA in the adult rat prefrontal cortex (Lipska et al., 2003). In addition, blockade of NMDA receptors with the antagonist MK-801 results in decreased mRNA expression levels of GAD_{67} in the cortex of rats (Paulson et al., 2003). Furthermore, monocular deprivation induced by intravitreal injections of tetrodotoxin produce reductions in GAD_{67} mRNA in the lateral geniculate nucleus and visual cortex of macaque monkeys (Huntsman et al., 1995). These data suggest that NMDA hypofunction could be a potential upstream *causal* factor of the observed reductions in the expression of GAD_{67} mRNA in subjects with schizophrenia **(Fig. 36)**.

Interestingly, excitatory transmission does not appear to affect all GABA neuron subtypes equally. For instance, several lines of evidence suggest that PV-containing GABA neurons are more sensitive to NMDA hypofunction than calretinin-containing GABA neurons. First, in both the rat hippocampus and monkey DLPFC, PV-containing GABA neurons receive a significantly greater number of excitatory inputs than calretinin-containing GABA neurons (Gulyas et al., 1999; Melchitzky and Lewis, 2003). Second, 50-90% of PV-containing GABA

neurons are immunoreactive for the NMDAR1 subunit, whereas <10% of calretinin-containing neurons express detectable levels of this subunit in the primate cortex (Huntley et al., 1994; Huntley et al., 1997). Third, chronic administration of PCP produced a 25% reduction in the level of PV mRNA expression per neuron, but did not change the density of PV mRNA positive neurons in the rat prefrontal cortex (Cochran et al., 2003). Interestingly, this finding is strikingly reminiscent of the pattern observed in the DLPFC of subjects with schizophrenia (described in **chapter 1.2.3**). Fourth, application of ketamine, at sublethal concentrations, induced a decrease in PV and GAD_{67} immunoreactivity in cultured PV-containing interneurons that was mediated by NR2A-containing receptors (Kinney et al., 2006). Together, these data converge on the idea that the observed reductions in GAD_{67} mRNA in PV-containing GABA neurons in subjects with schizophrenia could be a *consequence* of an upstream reduction in signaling through NMDA receptors **(Fig. 36)**.

It is less clear if the alterations observed in CB1/CCK GABA neurons in subjects with schizophrenia could result from NMDA hypofunction **(Fig. 36)**. However, several studies suggest that CB1/CCK-containing GABA neurons may be sensitive to reduced excitatory neurotransmission. For instance, although CCK-containing neurons receive less total synaptic input than PV-containing neurons, 64% of the synapses they receive are excitatory, suggesting that CCK-containing receive considerable excitatory drive (Matyas et al., 2004). In addition, the release of CCK-like immunoreactivity from rat cortical synaptosomes is elicited by NMDA and increases in a concentration-dependent manner (Paudice et al., 1998). In addition, injections of MK-801 produces significant reductions in CCK mRNA expression and peptide in the frontal cortex and hippocampus of rats (Arif et al., 2006). Unfortunately, the effect of NMDA antagonists on the expression of GAD_{67} and CB1 mRNA in CCK-containing neurons has not been investigated. However, these findings suggest that the observed reductions in the expression of GAD_{67} mRNA and CCK mRNA in subjects with schizophrenia could be a *consequence* of NMDA receptor hypofunction. Consistent with this interpretation, the density of GAD_{67} mRNA-containing neurons expressing the NR2A subunit of the NMDA receptor was reported to be significantly decreased in layer 2 of the anterior cingulate cortex in subjects with schizophrenia (Woo et al., 2004). Interestingly, layer 2 contains a high density of CCK and CB1 mRNA expressing neurons and CB1 mRNA was found to be significantly decreased in this layer **(chapter 4)**.

130

5.2.1.2 Evidence for the involvement of reduced neurotrophin signaling in schizophrenia

Reduced signaling through the tyrosine kinase TrkB receptor has also been implicated as an upstream causal factor of the observed reductions in the expression of GABA-related markers (Hashimoto et al., 2005; Lewis et al., 2005) **(Fig. 36)**. Signaling mediated by brain-derived neurotrophic factor (BDNF) and TrkB regulates the functional and morphological development of cultured hippocampal GABA neurons (Yamada et al., 2002; Kohara et al., 2003). In addition, BDNF-TrkB signaling induces the expression of GAD_{67}, GAT1, and PV mRNAs (Huang et al., 1999; Yamada et al., 2002). This neurotrophic signaling pathway may be selective for specific GABA neuron subtypes because TrkB is expressed in PV-containing GABA neurons, but not calretinin-containing GABA neurons (Cellerino et al., 1996; Gorba and Wahle, 1999). These data suggest that disturbances in BDNF-TrkB signaling might contribute to the observed alterations in GABA-related markers in the DLPFC of subjects with schizophrenia. Indeed, levels of both BDNF and TrkB mRNA expression are reduced in the DLPFC of subjects with schizophrenia (Weickert et al., 2003; Hashimoto et al., 2005).

A direct causal relationship between reduced BDNF-TrkB signaling and changes in GABA-related markers was demonstrated in a proof-of-principal experiment using genetically engineered mice (Hashimoto et al., 2005). Specifically, TrkB hypomorphic mice that exhibited a 42% decrease in TrkB mRNA expression demonstrated 25% and 40% reductions in GAD_{67} and PV mRNAs, respectively, and no change in the expression of calretinin mRNA in the prefrontal cortex (Hashimoto et al., 2005). In addition, the density of GAD_{67} neurons was reduced, but the expression level of GAD_{67} per neuron was unchanged (Hashimoto et al., 2005). These patterns replicate those observed in schizophrenia. Furthermore, BDNF knockout mice did not show alterations in GAD_{67} or PV mRNA expression. These data converge on the idea that a deficiency in TrkB signaling is a pathogenetic mechanism that can *cause* reduced GAD_{67} mRNA expression in the PV expressing GABA neurons **(Fig. 36)**.

Currently, there is no direct evidence indicating whether reductions in TrkB signaling might affect expression levels of CB1 or CCK mRNA. However, immature CB1/CCK-containing neurons from the fetal rat cortex express TrkB and signaling mediated by BDNF regulates the morphological development of these neurons (Berghuis et al., 2005; Berghuis et al., 2007). These data suggest that a reduction in TrkB could cause a reduction in GAD_{67} mRNA

expression and possibly reductions CCK and CB1 mRNAs **(Fig. 36)**. However, these cause-and-effect relationships remain to be tested.

5.2.1.3 Cannabis exposure during adolescence: Pushing the system over the edge?

Cannabis exposure is one environmental factor that has been implicated as a risk factor for the development of schizophrenia **(chapter 1.3)** (McDonald and Murray, 2000) **(Fig. 36)**. The use of cannabis is first initiated by most individuals during the adolescent ages of 12-17 (Gfroerer and Epstein, 1999), a time period during which the DLPFC undergoes significant refinements (Lewis et al., 2004a) and may be particularly vulnerable to environmental insults. Indeed, chronic administration of Δ^9-THC, the chief psychoactive cannabinoid in cannabis, to peripubertal but not adult rats produces long-lasting deficits in various memory tasks, even after sustained drug-free intervals (Schneider and Koch, 2003). In humans, cannabis use during adolescence is associated with more severe cognitive deficits compared to first use later in life (Ehrenreich et al., 1999; Pope, Jr. et al., 2003).

During adolescence, the development of perisomatic GABA inputs to DLPFC pyramidal cells appears to play an important role in the emergence of DLFPC circuitry in mediating working memory processes. For instance, GABA markers undergo considerable changes during postnatal development, with these changes particularly marked during adolescence (Condé et al., 1996; Erickson and Lewis, 2002; Cruz et al., 2003). In particular, during early postnatal development (birth to 3 months), chandelier cell axon cartridges immunoreactive for GAT1 or PV and AIS immunoreactive for the α_2 subunit of the GABA$_A$ receptor demonstrate distinct densities and trajectories of change (Cruz et al., 2003). However, these pre- and postsynaptic markers of GABA all exhibit similar significant declines in density from approximately 15 months to 42 months of age, the time period associated with adolescence in monkeys, before attaining adult levels (Cruz et al., 2003). The developmental changes in PV and GAT1 cartridges likely occur to allow chandelier neurons to maintain a proper regulatory role on pyramidal cell output. Indeed, this coordinated developmental change in GABA inputs to pyramidal cells in the DLPFC during adolescence correlates with increased involvement of the DLPFC in working memory tasks. Thus, developmental refinements of GABA markers during adolescence appear to be directly involved in the maturation of functional properties of the DLPFC that contribute to

working memory, such as gamma band synchrony (Yordanova et al., 2002; Vreugdenhil et al., 2003).

The development of GABA inhibitory circuitry is known to be shaped by neural activity (Chattopadhyaya et al., 2007). However, the maturation of perisomatic synapses during adolescence has recently been shown to require GABA signaling for shaping GABA circuits (Chattopadhyaya et al., 2007). Specifically, a reduction in GAD_{67}-mediated GABA synthesis and signaling during adolescence significantly reduced the maturation of perisomatic synapses in the visual cortex (Chattopadhyaya et al., 2007). In the monkey DLPFC, pyramidal neurons receive convergent perisomatic input from PV-containing basket and chandelier neurons and CB1/CCK-containg basket neurons **(chapter 3)**. These convergent sources of perisomatic inhibition have been shown to play specific roles in shaping network activity in the rodent. For example, CB1/CCK-containing and PV-containing neurons fire at different phases of network oscillations (Klausberger et al., 2005), generate temporally distinct epochs of somatic inhibition (Glickfeld and Scanziani, 2006), and play complementary roles in regulating gamma band oscillations (Hajos et al., 2000b). Thus, because stimulation of the CB1 receptor strongly suppresses the GABA inputs to pyramidal neurons from CCK-containing basket neurons, cannabis use during adolescence may alter the balance between the CB1/CCK-containing and PV-containing inhibitory inputs to the perisomatic region of DLPFC pyramidal neurons; this imbalance during a sensitive period may disrupt the developmental trajectories of these GABA inputs, producing persistent circuitry alterations that impair the mechanisms of neural synchrony required for the maturation of working memory performance.

5.2.2   Putting the pieces together: Convergent pathways onto a common pathophysiology

As summarized in **Figure 36**, the data reviewed above converge on the interpretation that different upstream *causes*, including genetic risk variants, NMDA receptor hypofunction, and reduced signaling through the TrkB receptors, converge through a variety of mechanisms to produce a functional decrease in the expression of GAD_{67} mRNA in PV- and CCK-containing GABA neurons. As a *consequence*, PV- and CCK-containing neurons exhibit deficient GABA synthesis. Thus, GABA signaling via $GABA_A$ α_2 receptors at pyramidal neuron axon initial

segments from PV-containing chandelier and at pyramidal neuron cell bodies from CCK-containing basket neurons is deficient. Cannabis use may precipitate the onset of schizophrenia by disrupting the developmental trajectories of PV-containing inhibitory inputs to the perisomatic region of DLPFC pyramidal neurons and/or compound the deficit in perisomatic GABA signaling by activating CB1 receptors on the terminals of CCK-containing basket neurons. Decreased GABA neurotransmission from these two separate neuron types converge to produce a reduction in gamma oscillations, which gives rise to impairments in working memory, despite apparent *compensatory* responses, which include a decrease in the levels of presynaptic GAT1 and PV, upregulation of postsynaptic $GABA_A$ α_2 at pyramidal cell AIS, and decreased CB1 receptors in the terminals of CCK-containing neurons.

It should be noted that other pathways might participate in the proposed cascade of events model. For instance, given the evidence that CB1 receptors are expressed by pyramidal neurons and have been shown to inhibit glutamate release (Marsicano and Lutz, 1999; Auclair et al., 2000; Hajos et al., 2001; Kawamura et al., 2006; Katona et al., 2006), a possible hypothesis is that cannabis exposure could directly produce a reduction in excitatory transmission **(Fig. 36)**. Interestingly, a recent study demonstrated that mice hypomorphic for the *Nrg1* gene were more susceptible to the effects of cannabis exposure than wild type mice in a number of behavioral tests (Boucher et al., 2007). These findings provide evidence for a possible gene x environment interaction. Although this interaction is possible, a reduction in excitatory drive via CB1 receptor activation on excitatory terminals would, in the proposed model, produce a downstream decrease in GAD_{67} mRNA expression **(Fig. 36)**. This interpretation suggests that cannabis exposure could produce a reduction in perisomatic inhibition from CB1/CCK-continaing neurons both directly by activating CB1 receptors and indirectly by producing a reduction in GAD_{67} mRNA expression through decreased excitatory transmission.

It could be argued that the reductions in CB1 mRNA and protein expression in subjects with schizophrenia might result directly from cannabis exposure. In rats, chronic exposure to CB1 agonists decreases CB1 radioligand binding in the cortex (Romero et al., 1998; Garcia-Gil et al., 1999). However, in these same studies CB1 mRNA expression was unaltered (Romero et al., 1998; Garcia-Gil et al., 1999). Consistent with these observations, in **chapter 4** the observed within-pair percent differences in CB1 mRNA expression in the subjects with schizophrenia did not differ as a function of a history of cannabis use/abuse **(Fig. 36)**. In addition, the within-pair

percent differences in CB1 radioimmunoreactivity and immunoreactivity did not differ between subjects with schizophrenia with or without a history of cannabis use **(Fig. 36)**. These data indicate that decreased mRNA expression levels are unlikely to result directly from cannabis exposure.
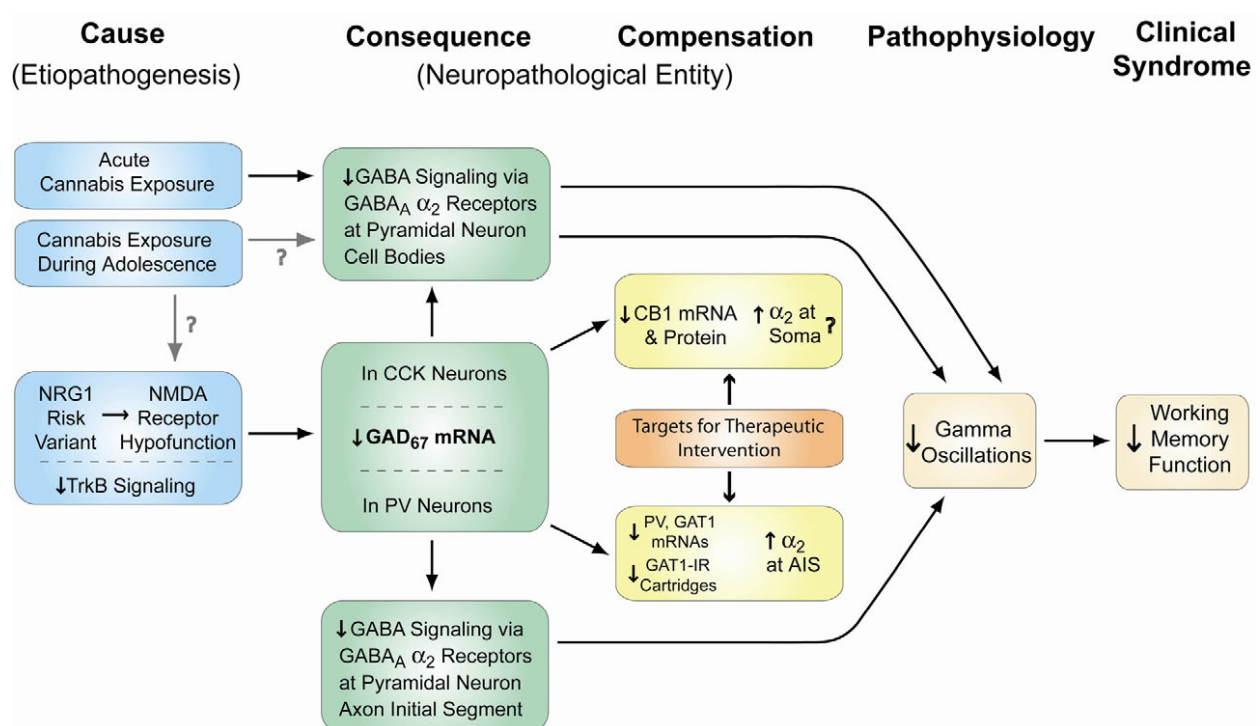
Figure 36. Hypothetical model illustrating potential cascade of events of the disease process in schizophrenia. According to this model, a set of genetic liabilities and environmental risk factors produce reduced GABA signaling from two distinct subclasses of GABA neurons. Despite apparent compensatory responses, deficient perisomatic GABA transmission from these two neuron types to pyramidal cells converge to produce a reduction in gamma oscillations, which gives rise to impairments in working memory.

5.3   A NOVEL TREATMENT INTERVENTION FOR COGNITIVE DYSFUNCTION IN SCHIZOPHRENIA

Developing more effective pharmacological treatments for schizophrenia requires a better knowledge and understanding of the underlying disease process(es) of the illness. Specifically, development of new therapeutic interventions in schizophrenia requires the identification of neuropathological entities that alter the brain's normal circuitry giving rise to a pathophysiology that emerges as a clinical feature in the illness **(chapter 1.2)**. The findings discussed above indicate that GABA transmission from PV-containing and CB1/CCK-containing neurons is deficient in subjects with schizophrenia. Therefore, augmenting GABA transmission from these neurons would be an effective treatment intervention. As suggested in **Figures 36 and 37** the CB1 receptor and the GABA$_A$ α_2 subunit are two potential molecular targets for treating cognitive deficits associated with schizophrenia. Specifically, drugs that have antagonistic activity on CB1 receptors could block the activation of CB1 receptors and limit the endocannabinoid-mediated suppression of GABA release from CB1/CCK containing terminals **(Fig. 37)**. As a result, GABA release from CB1/CCK-containing terminals would be enhanced, but only when CB1/CCK-containing neurons are active. In addition, at least in the hippocampus, GABA$_A$ receptors containing the α_2 subunit are selectively located on pyramidal cell bodies post-synaptic to CB1/CCK-containing terminals (Nyiri et al., 2001) **(Fig. 37)**. Thus, positive allosteric modulators of the benzodiazepine binding site with selectivity for GABA$_A$ receptors containing the α_2 subunit would be predicted to increase the efficacy of GABA released from CB1/CCK-containing terminals. GABA$_A$ receptors containing the α_2 subunit are also heavily expressed on the AIS of pyramidal neurons opposed to the terminals of PV-containing chandelier neurons **(Fig. 37)**. These data suggest that a GABA$_A$ α_2 agonist would also increase the efficacy of GABA released from PV-containing chandelier neurons at the AIS (Lewis et al., 2004b; Volk and Lewis, 2005) **(Fig. 37)**. Together, such agents might enhance the synchronization of pyramidal neuron activity by restoring normal levels of perisomatic GABA input to pyramidal neurons.

To date, only one clinical trial has examined the efficacy of the CB1 receptor antagonist Rimonabant in the treatment of subjects with schizophrenia (Meltzer et al., 2004). The results of this study did not show any significant improvement in the psychotic symptoms of subjects with schizophrenia who received the drug (Meltzer et al., 2004). However, the dose of the CB1 antagonist was not titrated in this study. Furthermore, the efficacy of Rimonabant on specific cognitive measures, such was working memory tests, were not assessed. However, the negative effect may emphasize the need to use a drug cocktail in order to significantly improve the functioning of individuals with schizophrenia.
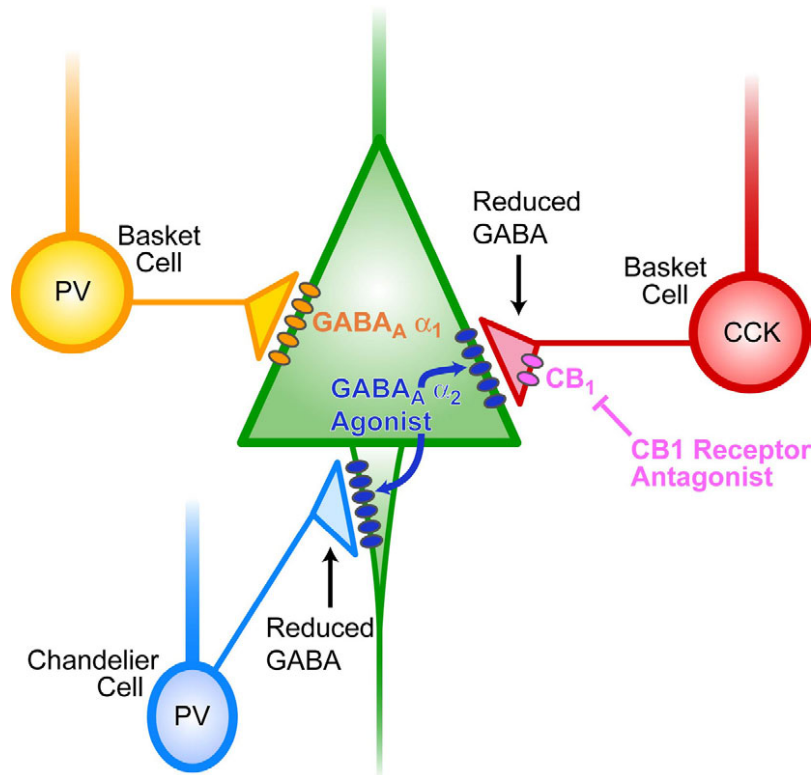
Figure 37. A novel pathophysiologically based intervention for the treatment of schizophrenia. A CB1 receptor antagonist would augment the intrinsic compensatory down-regulation of CB1 receptor expression, further limit the endocannabinoid-mediated suppression of GABA release from CB1/CCK containing terminals, and enhance the ability of CCK basket neurons (red) to synchronize pyramidal neurons (green) in gamma oscillations. In addition, positive allosteric modulators of the benzodiazepine binding site with selectivity for $GABA_A$ receptors containing the α_2 subunit would increase the efficacy of GABA released from CB1/CCK-containing terminals, and would act synergistically at inputs from PV-containing chandelier neurons (blue) to the axon initial segment of pyramidal neurons. Together, this drug cocktail might enhance the synchronization of pyramidal neuron activity by restoring normal levels of perisomatic GABA input to pyramidal neurons. PV-containing basket neurons (orange) would not be affected by these agents because these neurons do not contain CB1 receptors and $GABA_A$ receptors containing the α_1 subunit are selectively located on pyramidal cell bodies postsynaptic to these neurons.

5.4   FUTURE DIRECTIONS

5.4.1   Extending CB1 studies in schizophrenia

5.4.1.1 Are changes in CB1 expression regionally and disease specific?

If an observed neuropathological entity is common to all psychiatric disorders, and not specific to the disease process of schizophrenia, then a drug targeting it may have limited efficacy at ameliorating a clinical symptom specific to schizophrenia. Therefore, knowing whether an observed neuropathological entity is specific to schizophrenia is important in the ability to evaluate its usefulness as a molecular target for therapeutic intervention. In this regard, we have initiated a project in which we will assess CB1 protein expression in subjects with schizophrenia individually matched to one normal control subject and one subject with major depressive disorder (MDD), in order to assess whether individuals with other psychiatric disorders show similar changes in CB1 protein. Increased CB1 radioligand binding and protein levels (assessed by Western blot) have been reported in the prefrontal cortex of alcoholic and depressed suicide victims, suggesting that the reduction in CB1 in schizophrenia could be specific to the disease process of schizophrenia (Hungund et al., 2004; Vinod et al., 2005).

In addition, it is important to know whether the observed decrease in CB1 receptor expression is restricted to the DLPFC, or if this disturbance is distributed across other cortical regions that have been implicated in other aspects schizophrenia. For example, reductions in GAD_{67} mRNA expression have been observed in the anterior cingulate cortex of subjects with schizophrenia (reviewed in Woo et al., 2004; Akbarian and Huang, 2006). In this regard, we plan to measure CB1 immunoreactivity in the anterior cingulate cortex of subjects with schizophrenia in the same study in which we will address disease specificity.

5.4.2 Beyond CB1: Investigating other components of the endocannabinoid system in Schizophrenia

This dissertation focused on the role of the CB1 receptor in primate DLFC circuitry and schizophrenia. There are many other components of the endocannabinoid system that may be altered in the illness and additional experiments may be performed to further elucidate the role the endogenous cannabinoid system may play in the pathophysiology of schizophrenia **(Fig. 38)**. It could be hypothesized that other components of the endocannabinoid system could be altered to limit the endocannabinoid-mediated suppression of GABA in schizophrenia to compensate for a deficit in GABA synthesis. For instance, in the cascade of endocannabinoid signaling **(Fig. 38)**, a number of molecules could be downregulated in order to limit the production of the endocannabinoid 2-AG. Attractive candidates include phospholipase C beta (PLβ; isoform 1) and diacylglycerol lipase (DAGL) **(Fig. 38)**. Additionally, monoglyceride lipase (MGLL), the enzyme that metabolizes 2-AG (Dinh et al., 2002), could be selectively upregulated to decrease the amount of available 2-AG that could bind to and activate CB1 receptors **(Fig. 38)**. Studies assessing whether the mRNA and protein expression of these molecules would aid our understanding of how the endocannabinoid system may be altered in schizophrenia.
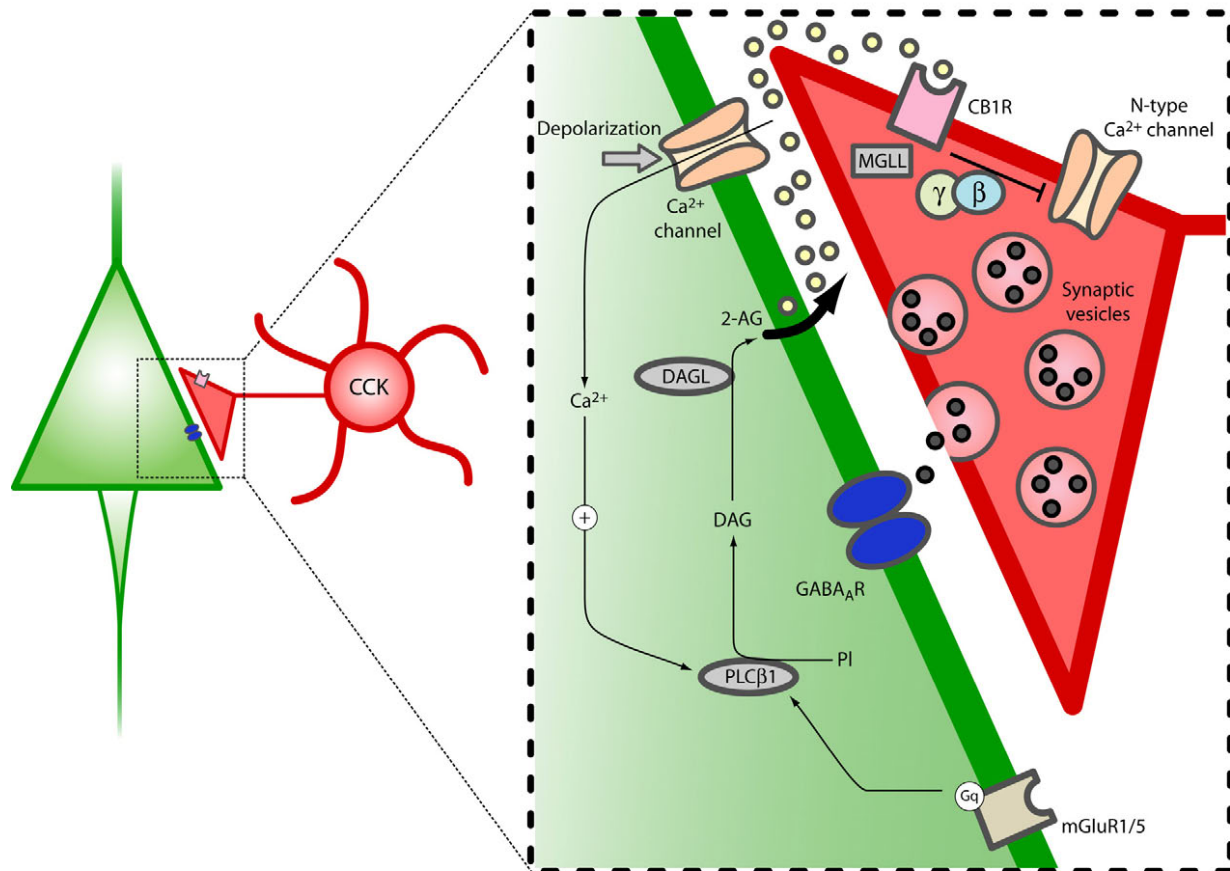
Figure 38. The endocannabinoid system. In addition to depolarization through Ca^{2+} channels, the synthesis of 2-AG is regulated by activation of group I metabotropic receptors (mGluR 1 and 5). Activation of mGluR1/5 increases the activity of PLCβ1, which synthesizes diacylglycerol (DAG). DAG is subsequently converted to 2-AG by DAGL. Presynaptically, 2-AG is metabolized by MGLL. These markers of endocannabinoid signaling could be altered in schizophrenia to limit endocannabinoid-mediated inhibition of GABA release.

142

5.4.3 Proof of principle experiments

5.4.3.1 The effects of CB1 agonists on monkey DLPFC activity

In this dissertation, we have argued that, within the context of DLPFC circuitry, CB1 receptors play an important role in regulating DLPFC activity and, consequently working memory, by controlling proximal inhibitory input to pyramidal neurons. It is known that systemic administration of cannabinoids causes deficits in working memory (Winsauer et al., 1999; Schneider and Koch, 2003; D'Souza et al., 2004); however, little is known about the direct influence of the CB1 receptor activation on prefrontal function. It has been suggested that the delay activity of DLPFC neurons during a memory task is the neural correlate of working memory. Furthermore, inhibitory activity has been shown to be necessary for the spatial tuning of neuronal responses spatial tuning of neurons during a delay task. The effects of CB1 ligands on neuronal delay activity and spatial tuning have not yet been investigated. Therefore, experiments designed to determine the physiological effects of CB1 receptors on neural activity in the DLPFC of awake behaving monkeys performing a working memory task would greatly advance our understanding of the critical physiological role that the CB1 receptor play in mediating working memory.

5.4.3.2 Determining a cause-and-effect relationships

In this dissertation we interpreted a reduction in CB1 mRNA expression to be a compensatory response to an upstream reduction in GAD_{67} mRNA. This interpretation was supported by correlation analysis; however, correlation analyses do not show a causal relationship. Therefore, our interpretation would be greatly strengthened by showing that reduced GAD_{67} mRNA expression could directly cause a reduction in CB1 mRNA expression. Genetically engineered mice and/or *in vivo* viral vector-mediated RNA silencing techniques are powerful tools that could be used to address whether an upstream reduction in GAD_{67} mRNA could cause reduced CB1 mRNA expression. These tools could also be used to address relationships between CB1 expression and the pathways discussed in **chapter 5.2**.

5.5 CONCLUSIONS

In the 1950's, the serendipitous discovery of the antipsychotic effects of chlorpromazine (Thorazine) revolutionized the treatment of schizophrenia (Lopez-Munoz et al., 2005). Since then, new antipsychotic medications with improved efficacy and reduced side-effects have been introduced. However, the development of new drugs that significantly improve cognitive performance has been lacking (Lewis and Gonzalez-Burgos, 2006). The research in this dissertation has identified the CB1 receptor as a potential therapeutic target for improving cognitive functions. It was proposed that a combination of a CB1 antagonist and a $GABA_A$ α_2 agonist might significantly improve perisomatic inhibitory input to DLPFC pyramidal neurons thereby improving DLPFC function and ameliorating working memory impairments in individuals with schizophrenia. If the proposed therapeutic intervention proves effective, the quality of life of many individuals with schizophrenia could improve significantly. However, there is much research to be performed and many questions to be answered concerning the relationship between the endocannabinoid system and schizophrenia. The future is exciting.

In brief summary, the main findings from each chapter of this dissertation were:

- **Chapter 2:** The results of this study demonstrate that 1) the distribution of CB1-IR axons is heterogeneous across neocortical regions of the macaque monkey with regions associated with higher cognitive functions, such as the prefrontal cortex, containing higher densities of CB1-IR axons than primary motor and sensory cortices; 2) different neocortical regions exhibit distinctive laminar distributions of CB1-IR axons, which precisely mark the cytoarchitectonic boundaries between many regions; 3) the density and distribution of CB1-IR axons also differ substantially across other regions of the primate brain; 4) the regional and laminar distributions of CB1-IR axons in the human neocortex are quite similar to those in monkey, although the morphology of labeled axons is altered by postmortem delay and; 5) in the monkey neocortex CB1 immunoreactivity is primarily contained in cells and axon terminals that have the morphologic features characteristic of GABA neurons.

- **Chapter 3:** The results of this study demonstrate that in the macaque monkey DLPFC 1) the laminar distributions of CB1- and CCK-IR neurons and axons are very similar; 2)

CB1 and CCK immunoreactivities are colocalized in neurons, axons, and axon terminals although structures single-labeled for each protein are also present; 3) CB1-IR axon terminals exclusively form symmetric synapses, whereas CCK-IR axon terminals form both symmetric and asymmetric synapses; 4) the majority of both CB1- and CCK-IR axon terminals forming symmetric synapses contact dendritic shafts; and 5) the synaptic targets of CB1- and CCK-IR axon terminals are similar in layer 4 but different in layers 2-3s, where CCK-IR terminals are more likely to contact cell bodies and less likely to contact spines than are CB1-IR terminals.

- **Chapter 4:** In order to explore the potential role of the CB1 receptor in DLPFC dysfunction in schizophrenia, we examined the expression of CB1 receptor mRNA and protein. We found that 1) the levels of CB1 receptor mRNA and protein are significantly reduced in the DLPFC of subjects with schizophrenia; 2) these reductions cannot be explained by potential confounding factors, suggesting that a reduction in CB1 receptors is intrinsic to the disease process of schizophrenia; and 3) the observed changes in CB1 receptor mRNA expression correlated with expression changes in GAD_{67} and CCK mRNA in the same subjects with schizophrenia, suggesting that downregulation of the CB1 receptor may be a compensatory response to impaired GABA neurotransmission in CCK-containing neurons.

BIBLIOGRAPHY

Akbarian S and Huang HS (2006) Molecular and cellular mechanisms of altered GAD1/GAD67 expression in schizophrenia and related disorders. Brain Res Rev 52:293-304.

Akbarian S, Kim JJ, Potkin SG, Hagman JO, Tafazzoli A, Bunney JrWE, and Jones EG (1995) Gene expression for glutamic acid decarboxylase is reduced without loss of neurons in prefrontal cortex of schizophrenics. Arch Gen Psychiatry 52:258-266.

Alonso JR and Amaral DG (1995) Cholinergic innervation of the primate hippocampal formation. I. Distribution of choline acetyltransferase immunoreactivity in the Macaca fascicularis and Macaca mulatta monkeys. J Comp Neurol 355:135-170.

Amaral DG and Bassett JL (1989) Cholinergic innervation of the monkey amygdala: an immunohistochemical analysis with antisera to choline acetyltransferase. J Comp Neurol 281:337-361.

Amaral DG, Insausti R, and Cowan WM (1987) The entorhinal cortex of the monkey: I. Cytoarchitectonic organization. J Comp Neurol 264:326-355.

Amaral DG and Price JL (1984) Amygdalo-cortical projections in the monkey (*Macaca fascicularis*). J Comp Neurol 230:465-496.

Ameri A (1999) The effects of cannabinoids on the brain. Prog Neurobiol 58:315-348.

American Psychiatric Association (1994) DSM-IV. Diagnostic and Statistical Manual of Mental Disorders. Fourth EditionWashington, D.C.: American Psychiatric Association.

Andreasen NC (1995) Symptoms, signs, and diagnosis of schizophrenia. Lancet 346:477-481.

Andreasson S, Allebeck P, Engstrom A, and Rydberg U (1987) Cannabis and schizophrenia. A longitudinal study of Swedish conscripts. Lancet 2:1483-1486.

Aoki C, Venkatesan C, Go C-G, Forman R, and Kurose H (1998) Cellular and subcellular sites for noradrenergic action in the monkey dorsolateral prefrontal cortex as revealed by the immunocytochemical localization of noradrenergic receptors and axons. Cereb Cortex 8:269-277.

Arendt M, Rosenberg R, Foldager L, Perto G, and Munk-Jorgensen P (2005) Cannabis-induced psychosis and subsequent schizophrenia-spectrum disorders: follow-up study of 535 incident cases. Br J Psychiatry 187:510-515.

Arif M, Ahmed MM, Kumabe Y, Hoshino H, Chikuma T, and Kato T (2006) Clozapine but not haloperidol suppresses the changes in the levels of neuropeptides in MK-801-treated rat brain regions. Neurochem Int 49:304-311.

Arseneault L, Cannon M, Poulton R, Murray R, Caspi A, and Moffitt TE (2002) Cannabis use in adolescence and risk for adult psychosis: longitudinal prospective study. BMJ 325:1212-1213.

Arseneault L, Cannon M, Witton J, and Murray RM (2004) Causal association between cannabis and psychosis: examination of the evidence. Br J Psychiatry 184:110-117.

Auclair N, Otani S, Soubrie P, and Crepel F (2000) Cannabinoids modulate synaptic strength and plasticity at glutamatergic synapses of rat prefrontal cortex pyramidal neurons. J Neurophysiol 83:3287-3293.

Bacci A, Huguenard JR, and Prince DA (2004) Long-lasting self-inhibition of neocortical interneurons mediated by endocannabinoids. Nature 431:312-316.

Barbas H and Pandya DN (1989) Architecture and intrinsic connections of the prefrontal cortex in the rhesus monkey. J Comp Neurol 286:353-375.

Barnes TR, Mutsatsa SH, Hutton SB, Watt HC, and Joyce EM (2006) Comorbid substance use and age at onset of schizophrenia. Br J Psychiatry 188:237-242.

Bayer TA, Falkai P, and Maier W (1999) Genetic and non-genetic vulnerability factors in schizophrenia: the basis of the "two hit hypothesis". J Psychiatr Res 33:543-548.

Begg M, Pacher P, Batkai S, Osei-Hyiaman D, Offertaler L, Mo FM, Liu J, and Kunos G (2005) Evidence for novel cannabinoid receptors. Pharmacol Ther 106:133-145.

Berghuis P, Dobszay MB, Wang X, Spano S, Ledda F, Sousa KM, Schulte G, Ernfors P, Mackie K, Paratcha G, Hurd YL, and Harkany T (2005) Endocannabinoids regulate interneuron migration and morphogenesis by transactivating the TrkB receptor. Proc Natl Acad Sci U S A 102:19115-19120.

Berghuis P, Rajnicek AM, Morozov YM, Ross RA, Mulder J, Urban GM, Monory K, Marsicano G, Matteoli M, Canty A, Irving AJ, Katona I, Yanagawa Y, Rakic P, Lutz B, Mackie K, and Harkany T (2007) Hardwiring the brain: endocannabinoids shape neuronal connectivity. Science 316:1212-1216.

Biegon A and Kerman IA (2001) Autoradiographic study of pre- and postnatal distribution of cannabinoid receptors in human brain. Neuroimage 14:1463-1468.

147

Block RI, O'Leary DS, Hichwa RD, Augustinack JC, Boles Ponto LL, Ghoneim MM, Arndt S, Hurtig RR, Watkins GL, Hall JA, Nathan PE, and Andreasen NC (2002) Effects of frequent marijuana use on memory-related regional cerebral blood flow. Pharmacol Biochem Behav 72:237-250.

Bodor AL, Katona I, Nyiri G, Mackie K, Ledent C, Hajos N, and Freund TF (2005) Endocannabinoid signaling in rat somatosensory cortex: laminar differences and involvement of specific interneuron types. J Neurosci 25:6845-6856.

Boucher AA, Arnold JC, Duffy L, Schofield PR, Micheau J, and Karl T (2007) Heterozygous neuregulin 1 mice are more sensitive to the behavioural effects of Delta(9)-tetrahydrocannabinol. Psychopharmacology (Berl) 192:325-336.

Boussaoud D, Ungerleider LG, and Desimone R (1990) Pathways for motion analysis: cortical connections of the medial superior temporal and fundus of the superior temporal visual areas in the macaque. J Comp Neurol 296:462-495.

Braak H (1976) On the striate area of the human isocortex. A Golgi- and pigmentarchitectonic study. J Comp Neurol 166:341-364.

Breier A, Schreiber JL, Dyer J, and Pickar D (1991) National Institute of Mental Health longitudinal study of chronic schizophrenia. Prognosis and predictors of outcome. Arch Gen Psychiatry 48:239-246.

Breivogel CS, Griffin G, Di M, V, and Martin BR (2001) Evidence for a new G protein-coupled cannabinoid receptor in mouse brain. Mol Pharmacol 60:155-163.

Bromet EJ and Fennig S (1999) Epidemiology and natural history of schizophrenia. Biol Psychiatry 46:871-881.

Brown S, Birtwistle J, Roe L, and Thompson C (1999) The unhealthy lifestyle of people with schizophrenia. Psychol Med 29:697-701.

Burton H, Fabri M, and Alloway K (1995) Cortical areas within the lateral sulcus connected to cutaneous representations in areas 3b and 1: a revised interpretation of the second somatosensory area in macaque monkeys. J Comp Neurol 355:539-562.

Callicott JH, Bertolino A, Mattay VS, Langheim FJP, Duyn J, Coppola R, Goldberg TE, and Weinberger DR (2000) Physiological dysfunction of the dorsolateral prefrontal cortex in schizophrenia revisited. Cereb Cortex 10:1078-1092.

Callicott JH, Mattay VS, Verchinski BA, Marenco S, Egan MF, and Weinberger DR (2003) Complexity of prefrontal cortical dysfunction in schizophrenia: more than up or down. Am J Psychiatry 160:2209-2215.

Carmichael ST and Price JL (1994) Architectonic subdivision of the orbital and medial prefrontal cortex in the macaque monkey. J Comp Neurol 346:366-402.

Carpenter WT, Jr. and Buchanan RW (1994) Schizophrenia. N Engl J Med 330:681-690.

Carr DB and Sesack SR (2000) GABA-containing neurons in the rat ventral tegmental area project to the prefrontal cortex. Synapse 38:114-123.

Cavada C and Goldman-Rakic PS (1989) Posterior parietal cortex in rhesus monkey: I. Parcellation of areas based on distinctive limbic and sensory corticocortical connections. J Comp Neurol 287:393-421.

Celio MR, Baier W, Schärer L, de Viragh PA, and Gerday Ch (1988) Monoclonal antibodies directed against the calcium binding protein parvalbumin. Cell Calcium 9:81-86.

Cellerino A, Maffei L, and Domenici L (1996) The distribution of brain-derived neurotrophic factor and its receptor trkB in parvalbumin-containing neurons of the rat visual cortex. Eur J Neurosci 8:1190-1197.

Chattopadhyaya B, Di Cristo G, Wu CZ, Knott G, Kuhlman S, Fu Y, Palmiter RD, and Huang ZJ (2007) GAD67-Mediated GABA Synthesis and Signaling Regulate Inhibitory Synaptic Innervation in the Visual Cortex. Neuron 54:889-903.

Chevaleyre V, Takahashi KA, and Castillo PE (2006) Endocannabinoid-mediated synaptic plasticity in the CNS. Annu Rev Neurosci 29:37-76.

Childers SR and Breivogel CS (1998) Cannabis and endogenous cannabinoid systems. Drug Alcohol Depend 51:173-187.

Cho RY, Konecky RO, and Carter CS (2006) Impairments in frontal cortical gamma synchrony and cognitive control in schizophrenia. Proc Natl Acad Sci U S A 103:19878-19883.

Chopra GS and Smith JW (1974) Psychotic reactions following cannabis use in East Indians. Arch Gen Psychiatry 30:24-27.

Cipolloni PB and Pandya DN (1999) Cortical connections of the frontoparietal opercular areas in the rhesus monkey. J Comp Neurol 403:431-458.

Cochran SM, Kennedy M, McKerchar CE, Steward LJ, Pratt JA, and Morris BJ (2003) Induction of metabolic hypofunction and neurochemical deficits after chronic intermittent exposure to phencyclidine: differential modulation by antipsychotic drugs. Neuropsychopharm 28:265-275.

Colby CL and Goldberg ME (1999) Space and attention in parietal cortex. Annu Rev Neurosci 22:319-349.

Condé F, Lund JS, and Lewis DA (1996) The hierarchical development of monkey visual cortical regions as revealed by the maturation of parvalbumin-immunoreactive neurons. Dev Brain Res 96:261-276.

Connors BW and Long MA (2004) Electrical synapses in the mammalian brain. Annu Rev Neurosci 27:393-418.

Constantinidis C, Williams GV, and Goldman-Rakic PS (2002) A role for inhibition in shaping the temporal flow of information in prefrontal cortex. Nat Neurosci 5:175-180.

Cruz DA, Eggan SM, and Lewis DA (2003) Postnatal development of pre- and post-synaptic GABA markers at chandelier cell inputs to pyramidal neurons in monkey prefrontal cortex. J Comp Neurol 465:385-400.

D'Souza DC, Abi-Saab WM, Madonick S, Forselius-Bielen K, Doersch A, Braley G, Gueorguieva R, Cooper TB, and Krystal JH (2005) Delta-9-tetrahydrocannabinol effects in schizophrenia: implications for cognition, psychosis, and addiction. Biol Psychiatry 57:594-608.

D'Souza DC, Perry E, MacDougall L, Ammerman Y, Cooper T, Wu YT, Braley G, Gueorguieva R, and Krystal JH (2004) The psychotomimetic effects of intravenous delta-9-tetrahydrocannabinol in healthy individuals: implications for psychosis. Neuropsychopharm 29:1558-1572.

Davidson M, Reichenberg A, Rabinowitz J, Weiser M, Kaplan Z, and Mark M (1999) Behavioral and intellectual markers for schizophrenia in apparently healthy male adolescents. Am J Psychiatry 156:1328-1335.

Dean B, Sundram S, Bradbury R, Scarr E, and Copolov D (2001) Studies on [3H]CP-55940 binding in the human central nervous system: regional specific changes in density of cannabinoid-1 receptors associated with schizophrenia and cannabis use. Neuroscience 103:9-15.

DeFelipe J, González-Albo MC, del Río MR, and Elston GN (1999) Distribution and patterns of connectivity of interneurons containing calbindin, calretinin, and parvalbumin in visual areas of the occipital and temporal lobes of the macaque monkey. J Comp Neurol 412:515-526.

DeFelipe J, Hendry SHC, and Jones EG (1989) Visualization of chandelier cell axons by parvalbumin immunoreactivity in monkey cerebral cortex. Proc Natl Acad Sci USA 86:2093-2097.

Devane WA, Dysarz FA, III, Johnson MR, Melvin LS, and Howlett AC (1988) Determination and characterization of a cannabinoid receptor in rat brain. Mol Pharmacol 34:605-613.

Devane WA, Hanus L, Breuer A, Pertwee RG, Stevenson LA, Griffin G, Gibson D, Mandelbaum A, Etinger A, and Mechoulam R (1992) Isolation and Structure of A Brain Constituent That Binds to the Cannabinoid Receptor. Science 258:1946-1949.

Dinh TP, Carpenter D, Leslie FM, Freund TF, Katona I, Sensi SL, Kathuria S, and Piomelli D (2002) Brain monoglyceride lipase participating in endocannabinoid inactivation. Proc Natl Acad Sci U S A 99:10819-10824.

Dorph-Petersen K-A, Pierri JN, Perel JM, Sun Z, Sampson AR, and Lewis DA (2005) The influence of chronic exposure to antipsychotic medications on brain size before and after tissue fixation: A comparison of haloperidol and olanzapine in macaque monkeys. Neuropsychopharm 30:1649-1661.

Dudkin KN, Kruchinin VK, and Chueva IV (2001) Neurophysiological correlates of delayed visual differentiation tasks in monkeys: the effects of the site of intracortical blockade of NMDA receptors. Neurosci Behav Physiol 31:207-218.

Egan MF, Goldberg TE, Gscheidle T, Weirich M, Rawlings R, Hyde TM, Bigelow L, and Weinberger DR (2001) Relative risk for cognitive impairments in siblings of patients with schizophrenia. Biol Psychiatry 50:98-107.

Egertová M and Elphick MR (2000) Localisation of cannabinoid receptors in the rat brain using antibodies to the intracellular C-terminal tail of CB. J Comp Neurol 422:159-171.

Eggan SM, Hashimoto T, and Lewis DA (2007) Alterations in CB1 receptor MRNA and protein expression in the DLPFC of subjects with schizophrenia: Implications for cognitive deficits. Schizophr Bull 33:259.

Eggan SM and Lewis DA (2007) Immunocytochemical distribution of the cannabinoid CB1 receptor in the primate neocortex: a regional and laminar analysis. Cereb Cortex 17:175-191.

Ehrenreich H, Rinn T, Kunert HJ, Moeller MR, Poser W, Schilling L, Gigerenzer G, and Hoehe MR (1999) Specific attentional dysfunction in adults following early start of cannabis use. Psychopharmacology (Berl) 142:295-301.

Elvevag B and Goldberg TE (2000) Cognitive impairment in schizophrenia is the core of the disorder. Crit Rev Neurobiol 14:1-21.

Erickson SL and Lewis DA (2004) Cortical connections of the lateral mediodorsal thalamus in cynomolgus monkeys. J Comp Neurol 473:107-127.

Erickson SL and Lewis DA (2002) Postnatal development of parvalbumin- and GABA transporter-immunoreactive axon terminals in monkey prefrontal cortex. J Comp Neurol 448:186-202.

Erlenmeyer-Kimling L, Rock D, Roberts SA, Janal M, Kestenbaum C, Cornblatt B, Adamo UH, and Gottesman II (2000) Attention, memory, and motor skills as childhood predictors of schizophrenia-related psychoses: the New York High-Risk Project. Am J Psychiatry 157:1416-1422.

Fergusson DM, Horwood LJ, and Swain-Campbell NR (2003) Cannabis dependence and psychotic symptoms in young people. Psychol Med 33:15-21.

Fergusson DM, Poulton R, Smith PF, and Boden JM (2006) Cannabis and psychosis. BMJ 332:172-175.

Fitzpatrick D, Lund JS, and Blasdel GG (1985) Intrinsic connections of macaque striate cortex: afferent and efferent connections of lamina 4C. J Neurosci 5:3329-3349.

Freund TF (2003) Interneuron Diversity series: Rhythm and mood in perisomatic inhibition. Trends Neurosci 26:489-495.

Freund TF, Katona I, and Piomelli D (2003) Role of endogenous cannabinoids in synaptic signaling. Physiol Rev 83:1017-1066.

Funahashi S, Bruce CJ, and Goldman-Rakic PS (1989) Mnemonic coding of visual space in the monkey's dorsolateral prefrontal cortex. J Neurophysiol 61:331-349.

Funahashi S, Chafee MV, and Goldman-Rakic PS (1993) Prefrontal neuronal activity in rhesus monkeys performing a delayed anti-saccade task. Nature 365:753-756.

Fuster JM (2001) The prefrontal cortex - an update: Time is of the essence. Neuron 30:319-333.

Galaburda AM and Pandya DN (1983) The intrinsic architectonic and connectional organization of the superior temporal region of the rhesus monkey. J Comp Neurol 221:169-184.

Galarreta M, Erdelyi F, Szabo G, and Hestrin S (2004) Electrical coupling among irregular-spiking GABAergic interneurons expressing cannabinoid receptors. J Neurosci 24:9770-9778.

Garcia-Gil L, Romero J, Ramos JA, and Fernandez-Ruiz JJ (1999) Cannabinoid receptor binding and mRNA levels in several brain regions of adult male and female rats perinatally exposed to delta9-tetrahydrocannabinol. Drug Alcohol Depend 55:127-136.

Gaspar P, Berger B, Fabvret A, Vigny A, and Henry JP (1989) Catecholamine innervation of the human cerebral cortex as revealed by comparative immunohistochemistry of tyrosine hydroxylase and dopamine-beta-hydroxylase. J Comp Neurol 279:249-271.

Geola FL, Hershman JM, Warwick R, Reeve JR, Walsh JH, and Tourtellotte WW (1981) Regional distribution of cholecystokinin-like immunoreactivity in the human brain. J Clin Endocrinol Metab 53:270-275.

Gfroerer JC and Epstein JF (1999) Marijuana initiates and their impact on future drug abuse treatment need. Drug Alcohol Depend 54:229-237.

Giguere M and Goldman-Rakic PS (1988) Mediodorsal nucleus: Areal, laminar, and tangential distribution of afferents and efferents in the frontal lobe of rhesus monkeys. J Comp Neurol 277:195-213.

Glantz LA, Austin MC, and Lewis DA (2000) Normal cellular levels of synaptophysin mRNA expression in the prefrontal cortex of subjects with schizophrenia. Biol Psychiatry 48:389-397.

Glass M, Dragunow M, and Faull RLM (1997) Cannabinoid receptors in the human brain: A detailed anatomical and quantitative autoradiographic study in the fetal, neonatal and adult human brain. Neuroscience 77:299-318.

Glickfeld LL and Scanziani M (2006) Distinct timing in the activity of cannabinoid-sensitive and cannabinoid-insensitive basket cells. Nat Neurosci 9:807-815.

Goldman-Rakic PS (1988) Topography of cognition: Parallel distributed networks in primate association cortex. Ann Rev Neurosci 11:137-156.

Goldman-Rakic PS (1995) Cellular basis of working memory. Neuron 14:477-485.

Gonzalez S, Fernandez-Ruiz J, Sparpaglione V, Parolaro D, and Ramos JA (2002) Chronic exposure to morphine, cocaine or ethanol in rats produced different effects in brain cannabinoid CB(1) receptor binding and mRNA levels. Drug Alcohol Depend 66:77-84.

Gorba T and Wahle P (1999) Expression of trkB and trkC but not BDNF mRNA in neurochemically identified interneurons in rat visual cortex *in vivo* and in organotypic cultures. Eur J Neurosci 11:1179-1190.

Grech A, van Os J, Jones PB, Lewis SW, and Murray RM (2005) Cannabis use and outcome of recent onset psychosis. Eur Psychiatry 20:349-353.

Green MF (1996) What are the functional consequences of neurocognitive deficits in schizophrenia? Am J Psychiatry 153:321-330.

Guidotti A, Auta J, Davis JM, Gerevini VD, Dwivedi Y, Grayson DR, Impagnatiello F, Pandey G, Pesold C, Sharma R, Uzunov D, and Costa E (2000) Decrease in reelin and glutamic acid decarboxylase$_{67}$ (GAD$_{67}$) expression in schizophrenia and bipolar disorder. Arch Gen Psychiatry 57:1061-1069.

Gulyas AI, Megias M, Emri Z, and Freund TF (1999) Total number and ratio of excitatory and inhibitory synapses converging onto single interneurons of different types in the CA1 area of the rat hippocampus. J Neurosci 19:10082-10097.

Guo J and Ikeda SR (2004) Endocannabinoids modulate N-type calcium channels and G-protein-coupled inwardly rectifying potassium channels via CB1 cannabinoid receptors heterologously expressed in mammalian neurons. Molecular Pharmacology 65:665-674.

Hackett TA, Stepniewska I, and Kaas JH (1998) Subdivisions of auditory cortex and ipsilateral cortical connections of the parabelt auditory cortex in macaque monkeys. J Comp Neurol 394:475-495.

Hahn CG, Wang HY, Cho DS, Talbot K, Gur RE, Berrettini WH, Bakshi K, Kamins J, Borgmann-Winter KE, Siegel SJ, Gallop RJ, and Arnold SE (2006) Altered neuregulin 1-erbB4 signaling contributes to NMDA receptor hypofunction in schizophrenia. Nat Med 12:734-735.

Hajos N, Katona I, Mackie K, and Freund TF (2000a) Presynaptic CB1 cannabinoid receptors modulate hippocampal GABAergic transmission. Journal of Physiology-London 526:17S.

Hajos N, Katona I, Naiem SS, Mackie K, Ledent C, Mody I, and Freund TF (2000b) Cannabinoids inhibit hippocampal GABAergic transmission and network oscillations. Eur J Neurosci 12:3239-3249.

Hajos N, Ledent C, and Freund TF (2001) Novel cannabinoid-sensitive receptor mediates inhibition of glutamatergic synaptic transmission in the hippocampus. Neuroscience 106:1-4.

Harrison PJ and Weinberger DR (2005) Schizophrenia genes, gene expression, and neuropathology: on the matter of their convergence. Mol Psychiatry 10:40-68.

Hashimoto T, Arion D, Unger T, Maldonado-Aviles JG, Morris HM, Volk DW, Mirnics K, and Lewis DA (2007) Alterations in GABA-related transcriptome in the dorsolateral prefrontal cortex of subjects with schizophrenia. Mol Psychiatry.

Hashimoto T, Bergen SE, Nguyen QL, Xu B, Monteggia LM, Pierri JN, Sun Z, Sampson AR, and Lewis DA (2005) Relationship of brain-derived neurotrophic factor and its receptor TrkB to altered inhibitory prefrontal circuitry in schizophrenia. J Neurosci 25:372-383.

Hashimoto T, Volk DW, Eggan SM, Mirnics K, Pierri JN, Sun Z, Sampson AR, and Lewis DA (2003) Gene expression deficits in a subclass of GABA neurons in the prefrontal cortex of subjects with schizophrenia. J Neurosci 23:6315-6326.

Heaton R, Paulsen JS, McAdams LA, Kuck J, Zisook S, Braff D, Harris J, and Jeste DV (1994) Neuropsychological deficits in schizophrenics. Relationship to age, chronicity, and dementia. Arch Gen Psychiatry 51:469-476.

Hefft S and Jonas P (2005) Asynchronous GABA release generates long-lasting inhibition at a hippocampal interneuron-principal neuron synapse. Nat Neurosci 8:1319-1328.

Hendry SHC, Jones EG, DeFelipe J, Schmechel D, Brandon C, and Emson PC (1984) Neuropeptide-containing neurons of the cerebral cortex are also GABAergic. Proc Natl Acad Sci USA 81:6526-6530.

Henquet C, Krabbendam L, Spauwen J, Kaplan C, Lieb R, Wittchen HU, and van Os J (2005a) Prospective cohort study of cannabis use, predisposition for psychosis, and psychotic symptoms in young people. BMJ 330:11-16.

Henquet C, Murray R, Linszen D, and van Os J (2005b) The environment and schizophrenia: the role of cannabis use. Schizophr Bull 31:608-612.

Herkenham M, Lynn AB, Johnson MR, Melvin LS, De Costa BR, and Rice KC (1991) Characterization and localization of cannabinoid receptors in rat brain: a quantitative in vitro autoradiographic study. J Neurosci 11:563-583.

Herkenham M, Lynn AB, Little MD, Johnson MR, Melvin LS, De Costa BR, and Rice KC (1990) Cannabinoid receptor localization in brain. Proc Natl Acad Sci U S A 87:1932-1936.

Howard MW, Rizzuto DS, Caplan JB, Madsen JR, Lisman J, Aschenbrenner-Scheibe R, Schulze-Bonhage A, and Kahana MJ (2003) Gamma oscillations correlate with working memory load in humans. Cereb Cortex 13:1369-1374.

Hsieh C, Brown S, Derleth C, and Mackie K (1999) Internalization and recycling of the CB1 cannabinoid receptor. J Neurochem 73:493-501.

Hsu S-M, Raine L, and Fanger H (1981) Use of avidin-biotin-peroxidase complex (ABC) in immunoperoxidase techniques: A comparison between ABC and unlabeled antibody (PAP) procedures. J Histochem Cytochem 29:577-580.

Huang ZJ, Kirkwood A, Pizzorusso T, Porciatti V, Morales B, Bear MF, Maffei L, and Tonegawa S (1999) BDNF regulates the maturation of inhibition and the critical period of plasticity in mouse visual cortex. Cell 98:739-755.

Hungund BL, Vinod KY, Kassir SA, Basavarajappa BS, Yalamanchili R, Cooper TB, Mann JJ, and Arango V (2004) Upregulation of CB1 receptors and agonist-stimulated [35S]GTPgammaS binding in the prefrontal cortex of depressed suicide victims. Mol Psychiatry 9:184-190.

Huntley GW, Vickers JC, Janssen W, Brose N, Heinemann SF, and Morrison JH (1994) Distribution and synaptic localization of immunocytochemically identified NMDA receptor subunit proteins in sensory-motor and visual cortices of monkey and human. J Neurosci 14:3603-3619.

Huntley GW, Vickers JC, and Morrison JH (1997) Quantitative localization of NMDAR1 receptor subunit immunoreactivity in inferotemporal and prefrontal association cortices of monkey and human. Brain Res 749:245-262.

Huntsman MM, Wood TM, and Jones EG (1995) Laminar patterns of expression of GABA$_A$ receptor subunit mRNAs in monkey sensory motor cortex. J Comp Neurol 362:565-582.

Hyman SE and Fenton WS (2003) Medicine. What are the right targets for psychopharmacology? Science 299:350-351.

Ilan AB, Smith ME, and Gevins A (2004) Effects of marijuana on neurophysiological signals of working and episodic memory. Psychopharmacology (Berl) 176:214-222.

Jones EG (1997) Cortical development and thalamic pathology in schizophrenia. Schizophr Bull 23:483-501.

Jongen-Relo AL, Pitkanen A, and Amaral DG (1999) Distribution of GABAergic cells and fibers in the hippocampal formation of the macaque monkey: an immunohistochemical and in situ hybridization study. J Comp Neurol 408:237-271.

Kanayama G, Rogowska J, Pope HG, Gruber SA, and Yurgelun-Todd DA (2004) Spatial working memory in heavy cannabis users: a functional magnetic resonance imaging study. Psychopharmacology (Berl) 176:239-247.

Kapur S, Zipursky R, Roy P, Jones C, Remington G, Reed K, and Houle S (1997) The relationship between D_2 receptor occupancy and plasma levels on low dose oral haloperidol: A PET study. Psychopharmacology (Berl) 131:148-152.

Kapur S, Zipursky RB, and Remington G (1999) Clinical and theoretical implications of 5-HT_2 and D_2 receptor occupancy of clozapine, risperidone, and olanzapine in schizophrenia. Am J Psychiatry 156:286-293.

Kapur S, Zipursky RB, Remington G, Jones C, DaSilva J, WIlson AA, and Houle S (1998) 5-HT_2 and D_2 receptor occupancy of olanzapine in schizophrenia: A PET investigation. Am J Psychiatry 155:921-928.

Katona I, Rancz EA, Acsady L, Ledent C, Mackie K, Hajos N, and Freund TF (2001) Distribution of CB1 cannabinoid receptors in the amygdala and their role in the control of GABAergic transmission. J Neurosci 21:9506-9518.

Katona I, Sperlagh B, Magloczky Z, Santha E, Kofalvi A, Czirjak S, Mackie K, Vizi ES, and Freund TF (2000) GABAergic interneurons are the targets of cannabinoid actions in the human hippocampus. Neuroscience 100:797-804.

Katona I, Sperlagh B, Sik A, Kafalvi A, Vizi ES, Mackie K, and Freund TF (1999) Presynaptically located CB1 cannabinoid receptors regulate GABA release from axon terminals of specific hippocampal interneurons. J Neurosci 19:4544-4558.

Katona I, Urban GM, Wallace M, Ledent C, Jung KM, Piomelli D, Mackie K, and Freund TF (2006) Molecular composition of the endocannabinoid system at glutamatergic synapses. J Neurosci 26:5628-5637.

Kawaguchi Y and Kondo S (2002) Parvalbumin, somatostatin and cholecystokinin as chemical markers for specific GABAergic interneuron types in the rat frontal cortex. J Neurocytol 31:277-287.

Kawaguchi Y and Kubota Y (1997) GABAergic cell subtypes and their synaptic connections in rat frontal cortex. Cereb Cortex 7:476-486.

Kawamura Y, Fukaya M, Maejima T, Yoshida T, Miura E, Watanabe M, Ohno-Shosaku T, and Kano M (2006) The CB1 cannabinoid receptor is the major cannabinoid receptor at excitatory presynaptic sites in the hippocampus and cerebellum. J Neurosci 26:2991-3001.

Keefe RS, Eesley CE, and Poe MP (2005) Defining a cognitive function decrement in schizophrenia. Biol Psychiatry 57:688-691.

Kendler KS (1983) Overview: a current perspective on twin studies of schizophrenia. Am J Psychiatry 140:1413-1425.

Kinney JW, Davis CN, Tabarean I, Conti B, Bartfai T, and Behrens MM (2006) A specific role for NR2A-containing NMDA receptors in the maintenance of parvalbumin and GAD67 immunoreactivity in cultured interneurons. J Neurosci 26:1604-1615.

Klausberger T, Marton LF, O'Neill J, Huck JH, Dalezios Y, Fuentealba P, Suen WY, Papp E, Kaneko T, Watanabe M, Csicsvari J, and Somogyi P (2005) Complementary roles of cholecystokinin- and parvalbumin-expressing GABAergic neurons in hippocampal network oscillations. J Neurosci 25:9782-9793.

Kohara K, Kitamura A, Adachi N, Nishida M, Itami C, Nakamura S, and Tsumoto T (2003) Inhibitory but not excitatory cortical neurons require presynaptic brain-derived neurotrophic factor for dendritic development, as revealed by chimera cell culture. J Neurosci 23:6123-6131.

Konradi C and Heckers S (2003) Molecular aspects of glutamate dysregulation: implications for schizophrenia and its treatment. Pharmacol Ther 97:153-179.

Kovacs TO, Walsh JH, Maxwell V, Wong HC, Azuma T, and Katt E (1989) Gastrin is a major mediator of the gastric phase of acid secretion in dogs: proof by monoclonal antibody neutralization. Gastroenterology 97:1406-1413.

Krystal JH, Karper LP, Seibyl JP, Freeman GK, Delaney R, Bremner JD, Heninger GR, Bowers MB, Jr., and Charney DS (1994) Subanesthetic effects of the noncompetitive NMDA antagonist, ketamine, in humans. Psychotomimetic, perceptual, cognitive, and neuroendocrine responses. Arch Gen Psychiatry 51:199-214.

Kubota Y and Kawaguchi Y (1997) Two distinct subgroups of cholecystokinin-immunoreactive cortical interneurons. Brain Res 752:175-183.

Kupfer DJ, Detre T, Koral J, and Fajans P (1973) A comment on the "amotivational syndrome" in marijuana smokers. Am J Psychiatry 130:1319-1322.

Lane SD, Cherek DR, Lieving LM, and Tcheremissine OV (2005) Marijuana effects on human forgetting functions. J Exp Anal Behav 83:67-83.

Leweke FM, Gerth CW, and Klosterkotter J (2004) Cannabis-associated psychosis: current status of research. CNS Drugs 18:895-910.

Lewis DA (2000) Is there a neuropathology of schizophrenia? Recent findings converge on altered thalamic-prefrontal cortical connectivity. The Neuroscientist 6:208-218.

Lewis DA and Anderson SA (1995) The Functional Architecture of the Prefrontal Cortex and Schizophrenia. Psychological Medicine 25:887-894.

Lewis DA, Campbell MJ, and Morrison JH (1986) An immunohistochemical characterization of somatostatin-28 and somatostatin-28 (1-12) in monkey prefrontal cortex. J Comp Neurol 248:1-18.

Lewis DA, Cruz D, Eggan S, and Erickson S (2004a) Postnatal development of prefrontal inhibitory circuits and the pathophysiology of cognitive dysfunction in schizophrenia. Adolescent Brain Development: Vulnerabilities and Opportunities 1021:64-76.

Lewis DA and Gonzalez-Burgos G (2006) Pathophysiologically based treatment interventions in schizophrenia. Nat Med 12:1016-1022.

Lewis DA, Hashimoto T, and Volk DW (2005) Cortical inhibitory neurons and schizophrenia. Nat Rev Neurosci 6:312-324.

Lewis DA and Lieberman JA (2000) Catching up on schizophrenia: Natural history and neurobiology. Neuron 28:325-334.

Lewis DA and Lund JS (1990) Heterogeneity of chandelier neurons in monkey neocortex: Corticotropin-releasing factor and parvalbumin immunoreactive populations. J Comp Neurol 293:599-615.

Lewis DA and Morrison JH (1989) The noradrenergic innervation of monkey prefrontal cortex: A dopamine-beta-hydroxylase immunohistochemical study. J Comp Neurol 282:317-330.

Lewis DA, Volk DW, and Hashimoto T (2004b) Selective alterations in prefrontal cortical GABA neurotransmission in schizophrenia: A novel target for the treatment of working memory dysfunction. Psychopharmacology 174:143-150.

Lewis JW and Van Essen DC (2000) Mapping of architectonic subdivisions in the macaque monkey, with emphasis on parieto-occipital cortex. J Comp Neurol 428:79-111.

Lichtman AH, Varvel SA, and Martin BR (2002) Endocannabinoids in cognition and dependence. Prostaglandins Leukot Essent Fatty Acids 66:269-285.

Lipska BK, Lerman DN, Khaing ZZ, Weickert CS, and Weinberger DR (2003) Gene expression in dopamine and GABA systems in an animal model of schizophrenia: Effects of antipsychotic drugs. Eur J Neurosci 18:391-402.

Lopez-Munoz F, Alamo C, Cuenca E, Shen WW, Clervoy P, and Rubio G (2005) History of the discovery and clinical introduction of chlorpromazine. Ann Clin Psychiatry 17:113-135.

Loup F, Weinmann O, Yonekawa Y, Aguzzi A, Wieser H-G, and Fritschy J-M (1998) A highly sensitive immunofluorescence procedure for analyzing the subcellular distribution of GABA$_A$ receptor subunits in the human brain. J Histochem Cytochem 46:1129-1139.

Lu XR, Ong WY, and Mackie K (1999) A light and electron microscopic study of the CB1 cannabinoid receptor in monkey basal forebrain. J Neurocytol 28:1045-1051.

Lund JS and Lewis DA (1993) Local circuit neurons of developing and mature macaque prefrontal cortex: Golgi and immunocytochemical characteristics. J Comp Neurol 328:282-312.

Lundqvist T, Jonsson S, and Warkentin S (2001) Frontal lobe dysfunction in long-term cannabis users. Neurotoxicol Teratol 23:437-443.

Mackie K, Lai Y, Westenbroek R, and Mitchell R (1995) Cannabinoids activate an inwardly rectifying potassium conductance and inhibit Q-type calcium currents in AtT20 cells transfected with rat brain cannabinoid receptor. J Neurosci 15:6552-6561.

Madigan JC, Jr. and Carpenter MB (1971) Cerebellum of the Rhesus Monkey: Atlas of Lobules, Laminae, and Folia in SectionsBaltimore: University Park Press.

Markram H, Toledo-Rodriguez M, Wang Y, Gupta A, Silberberg G, and Wu C (2004) Interneurons of the neocortical inhibitory system. Nat Rev Neurosci 5:793-807.

Marsicano G and Lutz B (1999) Expression of the cannabinoid receptor CB1 in distinct neuronal subpopulations in the adult mouse forebrain. Eur J Neurosci 11:4213-4225.

Mascagni F and McDonald AJ (2003) Immunohistochemical characterization of cholecystokinin containing neurons in the rat basolateral amygdala. Brain Res 976:171-184.

Mato S and Pazos A (2004) Influence of age, postmortem delay and freezing storage period on cannabinoid receptor density and functionality in human brain. Neuropharmacology 46:716-726.

Matsuda LA, Bonner TI, and Lolait SJ (1993) Localization of cannabinoid receptor mRNA in rat brain. J Comp Neurol 327:535-550.

Matsuda LA, Lolait SJ, Brownstein MJ, Young AC, and Bonner TI (1990) Structure of a cannabinoid receptor and functional expression of the cloned cDNA. Nature 346:561-564.

Matyas F, Freund TF, and Gulyas AI (2004) Convergence of excitatory and inhibitory inputs onto CCK-containing basket cells in the CA1 area of the rat hippocampus. Eur J Neurosci 19:1243-1256.

Maynard TM, Sikich L, Lieberman JA, and LaMantia AS (2001) Neural development, cell-cell signaling, and the "two-hit" hypothesis of schizophrenia. Schizophr Bull 27:457-476.

McBain CJ and Fisahn A (2001) Interneurons unbound. Nat Rev Neurosci 2:11-23.

McDonald AJ (1992) Projection neurons of the basolateral maygdala: A correlative Golgi and retrograde tract tracing study. Brain Res Bull 28:179-185.

McDonald C and Murray RM (2000) Early and late environmental risk factors for schizophrenia. Brain Res Brain Res Rev 31:130-137.

McGlashan TH (1996) Early detection and intervention in schizophrenia research. Schizophr Bull 22:327-345.

McGuire BA, Gilbert CD, Rivlin PK, and Wiesel TN (1991) Targets of horizontal connections in macaque primary visual cortex. J Comp Neurol 305:370-392.

Mechoulam R, Ben Shabat S, Hanus L, Ligumsky M, Kaminski NE, Schatz AR, Gopher A, Almog S, Martin BR, Compton DR, and . (1995) Identification of an endogenous 2-monoglyceride, present in canine gut, that binds to cannabinoid receptors. Biochem Pharmacol 50:83-90.

Melchitzky DS, Eggan SM, and Lewis DA (2005) Synaptic targets of calretinin-containing axon terminals in macaque monkey prefrontal cortex. Neuroscience 130:185-195.

Melchitzky DS and Lewis DA (2003) Pyramidal neuron local axon terminals in monkey prefrontal cortex: Differential targeting of subclasses of GABA neurons. Cereb Cortex 13:452-460.

Melchitzky DS, Sesack SR, and Lewis DA (1999) Parvalbumin-immunoreactive axon terminals in macaque monkey and human prefrontal cortex: Laminar, regional and target specificity of Type I and Type II synapses. J Comp Neurol 408:11-22.

Melchitzky DS, Sesack SR, Pucak ML, and Lewis DA (1998) Synaptic targets of pyramidal neurons providing intrinsic horizontal connections in monkey prefrontal cortex. J Comp Neurol 390:211-224.

Meltzer HY, Arvanitis L, Bauer D, and Rein W (2004) Placebo-controlled evaluation of four novel compounds for the treatment of schizophrenia and schizoaffective disorder. Am J Psychiatry 161:975-984.

Mesulam MM and Mufson EJ (1982) Insula of the old world monkey. I. Architectonics in the insulo-orbito-temporal component of the paralimbic brain. J Comp Neurol 212:1-22.

Miller EK and Cohen JD (2001) An integrative theory of prefrontal cortex function. Annu Rev Neurosci 24:167-202.

Mirnics K and Lewis DA (2001) Genes and subtypes of schizophrenia. Trends in Molecular Medicine 7:281-283.

Moghaddam B (2003) Bringing order to the glutamate chaos in schizophrenia. Neuron 40:881-884.

Morecraft RJ, Cipolloni PB, Stilwell-Morecraft KS, Gedney MT, and Pandya DN (2004) Cytoarchitecture and cortical connections of the posterior cingulate and adjacent somatosensory fields in the rhesus monkey. J Comp Neurol 469:37-69.

Munro S, Thomas KL, and Abu-Shaar M (1993) Molecular characterization of a peripheral receptor for cannabinoids. Nature 365:61-65.

Negrete JC, Knapp WP, Douglas DE, and Smith WB (1986) Cannabis affects the severity of schizophrenic symptoms: results of a clinical survey. Psychol Med 16:515-520.

Newell KA, Deng C, and Huang XF (2006) Increased cannabinoid receptor density in the posterior cingulate cortex in schizophrenia. Exp Brain Res 172:556-560.

Niehaus JL, Wallis KT, Elphick MR, and Lewis DL. CRIP1B a novel CB1 cannabinoid receptor interaction protein, interacts with CB1 at the distal C-terminal tail. Soc Neurosci Abstr 30, 623.19. 2004.

Nusser Z, Sieghart W, Benke D, Fritschy J-M, and Somogyi P (1996) Differential synaptic localization of two major γ-aminobutyric acid type A receptor α subunits on hippocampal pyramidal cells. Proc Natl Acad Sci USA 93:11939-11944.

Nyberg S, Farde L, Halldin C, Dahl ML, and Bertilsson L (1995) D_2 dopamine receptor occupancy during low-dose treatment with haloperidol decanoate. Am J Psychiatry 152:173-178.

Nyiri G, Freund TF, and Somogyi P (2001) Input-dependent synaptic targeting of alpha(2)-subunit-containing GABA(A) receptors in synapses of hippocampal pyramidal cells of the rat. Eur J Neurosci 13:428-442.

Oeth KM and Lewis DA (1990) Cholecystokinin innervation of monkey prefrontal cortex: An immunohistochemical study. J Comp Neurol 301:123-137.

Oeth KM and Lewis DA (1992) Cholecystokinin- and dopamine- containing mesencephalic neurons provide distinct projections to monkey prefrontal cortex. Neurosci Lett 145:87-92.

Oeth KM and Lewis DA (1993) Postnatal development of the cholecystokinin innervation of monkey prefrontal cortex. J Comp Neurol 336:400-418.

Ohno-Shosaku T, Tsubokawa H, Mizushima I, Yoneda N, Zimmer A, and Kano M (2002) Presynaptic cannabinoid sensitivity is a major determinant of depolarization-induced retrograde suppression at hippocampal synapses. J Neurosci 22:3864-3872.

Ong WY and Mackie K (1999) A light and electron microscopic study of the CB1 cannabinoid receptor in primate brain. Neuroscience 92:1177-1191.

Oropeza VC, Mackie K, and Van Bockstaele EJ (2007) Cannabinoid receptors are localized to noradrenergic axon terminals in the rat frontal cortex. Brain Res 1127:36-44.

Ortiz S, Oliva JM, Perez-Rial S, Palomo T, and Manzanares J (2004) Chronic ethanol consumption regulates cannabinoid CB1 receptor gene expression in selected regions of rat brain. Alcohol Alcohol 39:88-92.

Owen MJ, Williams NM, and O'Donovan MC (2004) The molecular genetics of schizophrenia: findings promise new insights. Molecular Psychiatry 9:14-27.

Pandya DN and Seltzer B (1982) Intrinsic connections and architectonics of posterior parietal cortex in the rhesus monkey. J Comp Neurol 204:196-210.

Paudice P, Gemignani A, and Raiteri M (1998) Evidence for functional native NMDA receptors activated by glycine or D-serine alone in the absence of glutamatergic coagonist. Eur J Neurosci 10:2934-2944.

Paulson L, Martin P, Persson A, Nilsson CL, Ljung E, Westman-Brinkmalm A, Eriksson PS, Blennow K, and Davidsson P (2003) Comparative genome- and proteome analysis of cerebral cortex from MK-801-treated rats. J Neurosci Res 71:526-533.

Paxinos G, Huang X-F, and Toga AW (2000) The Rhesus Monkey Brain in Stereotaxic CoordinatesSan Diego: Academic Press.

Pencer A, Addington J, and Addington D (2005) Outcome of a first episode of psychosis in adolescence: a 2-year follow-up. Psychiatry Res 133:35-43.

Perlstein WM, Carter CS, Noll DC, and Cohen JD (2001) Relation of prefrontal cortex dysfunction to working memory and symptoms in schizophrenia. Am J Psychiatry 158:1105-1113.

Peters A, Palay SL, and Webster DF (1991) The Fine Structure of The Nervous System.New York: Oxford University Press.

Pierri JN, Chaudry AS, Woo T-U, and Lewis DA (1999) Alterations in chandelier neuron axon terminals in the prefrontal cortex of schizophrenic subjects. Am J Psychiatry 156:1709-1719.

Piomelli D (2003) The molecular logic of endocannabinoid signalling. Nat Rev Neurosci 4:873-884.

Pistis M, Ferraro L, Pira L, Flore G, Tanganelli S, Gessa GL, and Devoto P (2002) Delta(9)-tetrahydrocannabinol decreases extracellular GABA and increases extracellular glutamate and dopamine levels in the rat prefrontal cortex: an in vivo microdialysis study. Brain Res 948:155-158.

Pitkanen A and Amaral DG (1998) Organization of the intrinsic connections of the monkey amygdaloid complex: projections originating in the lateral nucleus. J Comp Neurol 398:431-458.

Pitler TA and Alger BE (1992) Postsynaptic spike firing reduces synaptic GABAA responses in hippocampal pyramidal cells. J Neurosci 12:4122-4132.

Pope HG, Jr., Gruber AJ, Hudson JI, Cohane G, Huestis MA, and Yurgelun-Todd D (2003) Early-onset cannabis use and cognitive deficits: what is the nature of the association? Drug Alcohol Depend 69:303-310.

162

Pope HG, Jr. and Yurgelun-Todd D (1996) The residual cognitive effects of heavy marijuana use in college students. JAMA 275:521-527.

Porrino LJ, Crane AM, and Goldman-Rakic PS (1981) Direct and indirect pathways from the amygdala to the frontal lobe in rhesus monkeys. J Comp Neurol 198:121-136.

Pulver AE (2000) Search for schizophrenia susceptibility genes. Biol Psychiatry 47:221-230.

Rajkowska G and Goldman-Rakic PS (1995) Cytoarchitectonic definition of prefrontal areas in the normal human cortex: I. Remapping of areas 9 and 46 using quantitative criteria. Cereb Cortex 5:307-322.

Rao SG, Williams GV, and Goldman-Rakic PS (1999) Isodirectional tuning of adjacent interneurons and pyramidal cells during working memory: Evidence for microcolumnar organization in PFC. J Neurophysiol 81:1903-1916.

Rao SG, Williams GV, and Goldman-Rakic PS (2000) Destruction and creation of spatial tuning by disinhibition: $GABA_A$ blockade of prefrontal cortical neurons engaged by working memory. J Neurosci 20:485-494.

Rehfeld JF (1978) Localisation of gastrins to neuro- and adenohypophysis. Nature 271:771-773.

Rinaldi-Carmona M, Barth F, Heaulme M, Shire D, Calandra B, Congy C, Martinez S, Maruani J, Neliat G, Caput D, and et al. (1994) SR141716A, a potent and selective antagonist of the brain cannabinoid receptor. FEBS Lett 350:240-244.

Rinaldi-Carmona M, Barth F, Millan J, Derocq JM, Casellas P, Congy C, Oustric D, Sarran M, Bouaboula M, Calandra B, Portier M, Shire D, Breliere JC, and Le Fur GL (1998) SR 144528, the first potent and selective antagonist of the CB2 cannabinoid receptor. J Pharmacol Exp Ther 284:644-650.

Robbe D, Montgomery SM, Thome A, Rueda-Orozco PE, McNaughton BL, and Buzsaki G (2006) Cannabinoids reveal importance of spike timing coordination in hippocampal function. Nat Neurosci 9:1526-1533.

Romero J, Berrendero F, Manzanares J, Perez A, Corchero J, Fuentes JA, Fernandez-Ruiz JJ, and Ramos JA (1998) Time-course of the cannabinoid receptor down-regulation in the adult rat brain caused by repeated exposure to delta9-tetrahydrocannabinol. Synapse 30:298-308.

Rupp A and Keith SJ (1993) The Costs of Schizophrenia - Assessing the Burden. Psychiatric Clinics of North America 16:413-423.

Saper CB (2005) An open letter to our readers on the use of antibodies. J Comp Neurol 493:477-478.

Saper CB and Sawchenko PE (2003) Magic peptides, magic antibodies: guidelines for appropriate controls for immunohistochemistry. J Comp Neurol 465:161-163.

Sawaguchi T, Matsumura M, and Kubota K (1988) Delayed response deficit in monkeys by locally disturbed prefrontal neuronal activity by bicuculline. Behavioural Brain Research 31:193-198.

Sawaguchi T, Matsumura M, and Kubota K (1989) Delayed response deficits produced by local injection of bicuculline into the dorsolateral prefrontal cortex in Japanese macaque monkeys. Exp Brain Res 75:457-469.

Saykin AJ, Shtasel DL, Gur RE, Kester DB, Mozley LH, Stafiniak P, and Gur RC (1994) Neuropsychological deficits in neuroleptic naive patients with first-episode schizophrenia. Arch Gen Psychiatry 51:124-131.

Schiffmann SN and Vanderhaeghen JJ (1991) Distribution of cells containing mRNA encoding cholecystokinin in the rat central nervous system. J Comp Neurol 304:219-233.

Schneider M and Koch M (2003) Chronic pubertal, but not adult chronic cannabinoid treatment impairs sensorimotor gating, recognition memory, and the performance in a progressive ratio task in adult rats. Neuropsychopharm 28:1760-1769.

Seltzer B and Pandya DN (1989) Intrinsic connections and architectonics of the superior temporal sulcus in the rhesus monkey. J Comp Neurol 290:451-471.

Sesack SR, Bressler CN, and Lewis DA (1995a) Ultrastructural associations between dopamine terminals and local circuit neurons in the monkey prefrontal cortex: A study of calretinin-immunoreactive cells. Neurosci Lett 200:9-12.

Sesack SR, Hawrylak VA, Matus C, Guido MA, and Levey AI (1998) Dopamine axon varicosities in the prelimbic division of the rat prefrontal cortex exhibit sparse immunoreactivity for the dopamine transporter. J Neurosci 18:2697-2708.

Sesack SR, Snyder CL, and Lewis DA (1995b) Axon Terminals Immunolabeled for Dopamine Or Tyrosine-Hydroxylase Synapse on Gaba-Immunoreactive Dendrites in Rat and Monkey Cortex. Journal of Comparative Neurology 363:264-280.

Shire D, Carillon C, Kaghad M, Calandra B, Rinaldi-Carmona M, Le Fur G, Caput D, and Ferrara P (1995) An amino-terminal variant of the central cannabinoid receptor resulting from alternative splicing. J Biol Chem 270:3726-3731.

Sitskoorn MM, Aleman A, Ebisch SJ, Appels MC, and Kahn RS (2004) Cognitive deficits in relatives of patients with schizophrenia: A meta-analysis. Schizophr Res 71:285-295.

Smiley JF and Goldman-Rakic PS (1993) Heterogeneous targets of dopamine synapses in monkey prefrontal cortex demonstrated by serial section electron microscopy: A laminar analysis using the silver-enhanced diaminobenzidine sulfide (SEDS) immunolabeling technique. Cereb Cortex 3:223-238.

Smit F, Bolier L, and Cuijpers P (2004) Cannabis use and the risk of later schizophrenia: a review. Addiction 99:425-430.

Solowij N, Stephens RS, Roffman RA, Babor T, Kadden R, Miller M, Christiansen K, McRee B, and Vendetti J (2002) Cognitive functioning of long-term heavy cannabis users seeking treatment. JAMA 287:1123-1131.

Spencer KM, Nestor PG, Salisbury DF, Shenton ME, and McCarley RW (2003) Abnormal neural synchrony in schizophrenia. J Neurosci 23:7407-7411.

Stan AD, Ghose S, Gao XM, Roberts RC, Lewis-Amezcua K, Hatanpaa KJ, and Tamminga CA (2006) Human postmortem tissue: What quality markers matter? Brain Res 1123:1-11.

Stefanis NC, Delespaul P, Henquet C, Bakoula C, Stefanis CN, and van Os J (2004) Early adolescent cannabis exposure and positive and negative dimensions of psychosis. Addiction 99:1333-1341.

Stefansson H, Sigurdsson E, Steinthorsdottir V, Bjornsdottir S, Sigmundsson T, Ghosh S, Brynjolfsson J, Gunnarsdottir S, Ivarsson O, Chou TT, Hjaltason O, Birgisdottir B, Jonsson H, Gudnadottir VG, Gudmundsdottir E, Bjornsson A, Ingvarsson B, Ingason A, Sigfusson S, Hardardottir H, Harvey RP, Lai D, Zhou M, Brunner D, Mutel V, Gonzalo A, Lemke G, Sainz J, Johannesson G, Andresson T, Gudbjartsson D, Manolescu A, Frigge ML, Gurney ME, Kong A, Gulcher JR, Petursson H, and Stefansson K (2002) *Neuregulin 1* and susceptibility to schizophrenia. Am J Hum Genet 71:877-892.

Straub RE, Lipska BK, Egan MF, Goldberg TE, Callicot JH, Mayhew MB, Vakkalanka RK, Kolachana BS, Kleinman JE, and Weinberger DR. Allelic variation in GAD1 (GAD67) is associated with schizophrenia and influences cortical function and gene expression. Molecular Psychiatry Epub ahead of print. 2007.

Tallon-Baudry C, Bertrand O, Peronnet F, and Pernier J (1998) Induced gamma-band activity during the delay of a visual short-term memory task in humans. J Neurosci 18:4244-4254.

Tamas G, Buhl EH, and Somogyi P (1997) Fast IPSPs elicited via multiple synaptic release sites by different types of GABAergic neurone in the cat visual cortex. J Physiol 500 (Pt 3):715-738.

Thomson AM, West DC, and Deuchars J (1995) Properties of single axon excitatory postsynaptic potentials elicited in spiny interneurons by action potentials in pyramidal neurons in slices of rat neocortex. Neuroscience 69:727-738.

Thomson AM, West DC, Hahn J, and Deuchars J (1996) Single axon IPSPs elicited in pyramidal cells by three classes of interneurons in slices of rat neocortex. Journal of Physiology 496:81-102.

Trettel J, Fortin DA, and Levine ES (2004) Endocannabinoid signalling selectively targets perisomatic inhibitory inputs to pyramidal neurones in juvenile mouse neocortex. J Physiol 556:95-107.

Tsou K, Brown S, Sanudo-Pena MC, Mackie K, and Walker JM (1998) Immunohistochemical distribution of cannabinoid CB1 receptors in the rat central nervous system. Neuroscience 83:393-411.

Tsuang M (2000) Schizophrenia: genes and environment. Biol Psychiatry 47:210-220.

Twitchell W, Brown S, and Mackie K (1997) Cannabinoids inhibit N- and P/Q-type calcium channels in cultured rat hippocampal neurons. J Neurophysiol 78:43-50.

Ujike H and Morita Y (2004) New perspectives in the studies on endocannabinoid and cannabis: cannabinoid receptors and schizophrenia. J Pharmacol Sci 96:376-381.

van Os J, Bak M, Hanssen M, Bijl RV, de Graaf R, and Verdoux H (2002) Cannabis use and psychosis: a longitudinal population-based study. Am J Epidemiol 156:319-327.

Veen ND, Selten JP, van dT, I, Feller WG, Hoek HW, and Kahn RS (2004) Cannabis use and age at onset of schizophrenia. Am J Psychiatry 161:501-506.

Verma A and Moghaddam B (1996) NMDA receptor antagonists impair prefrontal cortex function as assessed via spatial delayed alternation performance in rats: modulation by dopamine. J Neurosci 16:373-379.

Vinod KY, Arango V, Xie S, Kassir SA, Mann JJ, Cooper TB, and Hungund BL (2005) Elevated levels of endocannabinoids and CB1 receptor-mediated G-protein signaling in the prefrontal cortex of alcoholic suicide victims. Biol Psychiatry 57:480-486.

Vogt BA, Pandya DN, and Rosene DL (1987) Cingulate cortex of the rhesus monkey: I. Cytoarchitecture and thalamic afferents. J Comp Neurol 262:256-270.

Volk DW, Austin MC, Pierri JN, Sampson AR, and Lewis DA (2000) Decreased glutamic acid decarboxylase67 messenger RNA expression in a subset of prefrontal cortical gamma-aminobutyric acid neurons in subjects with schizophrenia. Arch Gen Psychiatry 57:237-245.

Volk DW, Austin MC, Pierri JN, Sampson AR, and Lewis DA (2001) GABA transporter-1 mRNA in the prefrontal cortex in schizophrenia: Decreased expression in a subset of neurons. Am J Psychiatry 158:256-265.

Volk DW and Lewis DA (2005) GABA targets for the treatment of cognitive dysfunction in schizophrenia. Current Neuropharmacology 3:45-62.

Volk DW, Pierri JN, Fritschy J-M, Auh S, Sampson AR, and Lewis DA (2002) Reciprocal alterations in pre- and postsynaptic inhibitory markers at chandelier cell inputs to pyramidal neurons in schizophrenia. Cereb Cortex 12:1063-1070.

Vreugdenhil M, Jefferys JG, Celio MR, and Schwaller B (2003) Parvalbumin-deficiency facilitates repetitive IPSCs and gamma oscillations in the hippocampus. J Neurophysiol 89:1414-1422.

Wang X, Dow-Edwards D, Keller E, and Hurd YL (2003) Preferential limbic expression of the cannabinoid receptor mRNA in the human fetal brain. Neuroscience 118:681-694.

Watson SJ, Benson JA, Jr., and Joy JE (2000) Marijuana and medicine: assessing the science base: a summary of the 1999 Institute of Medicine report. Arch Gen Psychiatry 57:547-552.

Weickert CS, Hyde TM, Lipska BK, Herman MM, Weinberger DR, and Kleinman JE (2003) Reduced brain-derived neurotrophic factor in prefrontal cortex of patients with schizophrenia. Mol Psychiatry 8:592-610.

Weinberger DR, Berman KF, and Zec RF (1986) Physiologic dysfunction of dorsolateral prefrontal cortex in schizophrenia. I. Regional cerebral blood flow evidence. Arch Gen Psychiatry 43:114-124.

Weinberger DR, Egan MF, Bertolino A, Callicott JH, Mattay VS, Lipska BK, Berman KF, and Goldberg TE (2001) Prefrontal neurons and the genetics of schizophrenia. Biol Psychiatry 50:825-844.

Westlake TM, Howlett AC, Bonner TI, Matsuda LA, and Herkenham M (1994) Cannabinoid receptor binding and messenger RNA expression in human brain: an in vitro receptor autoradiography and in situ hybridization histochemistry study of normal aged and Alzheimer's brains. Neuroscience 63:637-652.

Wilson RI, Kunos G, and Nicoll RA (2001) Presynaptic specificity of endocannabinoid signaling in the hippocampus. Neuron 31:453-462.

Wilson RI and Nicoll RA (2002) Endocannabinoid signaling in the brain. Science 296:678-682.

Winsauer PJ, Lambert P, and Moerschbaecher JM (1999) Cannabinoid ligands and their effects on learning and performance in rhesus monkeys. Behav Pharmacol 10:497-511.

Woo T-U, Walsh JP, and Benes FM (2004) Density of glutamic acid decarboxylase 67 messenger RNA-containing neurons that express the N-methyl-D-aspartate receptor subunit NR2A in the anterior cingulate cortex in schizophrenia and bipolar disorder. Arch Gen Psychiatry 61:649-657.

Woo T-U, Whitehead RE, Melchitzky DS, and Lewis DA (1998) A subclass of prefrontal gamma-aminobutyric acid axon terminals are selectively altered in schizophrenia. Proc Natl Acad Sci U S A 95:5341-5346.

Xiang Z, Huguenard JR, and Prince DA (2002) Synaptic inhibition of pyramidal cells evoked by different interneuronal subtypes in layer v of rat visual cortex. J Neurophysiol 88:740-750.

Yamada MK, Nakanishi K, Ohba S, Nakamura T, Ikegaya Y, Nishiyama N, and Matsuki N (2002) Brain-derived neurotrophic factor promotes the maturation of GABAergic mechanisms in cultured hippocampal neurons. J Neurosci 22:7580-7585.

Yordanova J, Kolev V, Heinrich H, Woerner W, Banaschewski T, and Rothenberger A (2002) Developmental event-related gamma oscillations: effects of auditory attention. Eur J Neurosci 16:2214-2224.

Yung AR and McGorry PD (1996) The prodromal phase of first-episode psychosis: past and current conceptualizations. Schizophr Bull 22:353-370.

Zammit S, Allebeck P, Andreasson S, Lundberg I, and Lewis G (2002) Self reported cannabis use as a risk factor for schizophrenia in Swedish conscripts of 1969: historical cohort study. BMJ 325:1199.

Zavitsanou K, Garrick T, and Huang XF (2004) Selective antagonist [3H]SR141716A binding to cannabinoid CB1 receptors is increased in the anterior cingulate cortex in schizophrenia. Prog Neuropsychopharmacol Biol Psychiatry 28:355-360.

Zimmer A, Zimmer AM, Hohmann AG, Herkenham M, and Bonner TI (1999) Increased mortality, hypoactivity, and hypoalgesia in cannabinoid CB1 receptor knockout mice. Proc Natl Acad Sci U S A 96:5780-5785.